

Wilfrid Laurier University

Scholars Commons @ Laurier

Theses and Dissertations (Comprehensive)

2015

Characterization of the Trans-plasma Membrane Electron Transport System in the Myelin Membrane

Afshan Sohail

Wilfrid Laurier University, soha1540@mylaurier.ca

Follow this and additional works at: <https://scholars.wlu.ca/etd>



Part of the [Biochemistry Commons](#), [Molecular and Cellular Neuroscience Commons](#), and the [Molecular Biology Commons](#)

Recommended Citation

Sohail, Afshan, "Characterization of the Trans-plasma Membrane Electron Transport System in the Myelin Membrane" (2015). *Theses and Dissertations (Comprehensive)*. 1694.

<https://scholars.wlu.ca/etd/1694>

This Thesis is brought to you for free and open access by Scholars Commons @ Laurier. It has been accepted for inclusion in Theses and Dissertations (Comprehensive) by an authorized administrator of Scholars Commons @ Laurier. For more information, please contact scholarscommons@wlu.ca.

Characterization of the Trans-plasma Membrane Electron Transport System in the Myelin Membrane

By

Afshan Sohail

THESIS

**Submitted to the Department of Chemistry
Faculty of Science
In partial fulfillment of the requirements for
Master of Science in Chemistry
Wilfrid Laurier University**

2014

© Afshan Sohail 2014

Abstract

Myelination is the key feature of evolution in the nervous system of vertebrates. Myelin is the protrusion of glial cells. More specifically, "oligodendrocytes" in the central nervous system (CNS), and "Schwann" cells in the peripheral nervous system (PNS) form myelin membranes. Myelin remarkably, enhances the propagation of nerve impulses. However, myelin restricts the access of extracellular metabolites to the axons. A pathology called "demyelination" is associated with myelin. The myelin sheath is not only an insulator, but it is itself metabolically active. In this study it is hypothesized that the ratio of $\text{NAD(P)}^+/\text{NAD(P)H}$ and the glycolytic pathway of the myelin sheath is maintained via trans-plasma membrane electron transport system (t-PMET).

The t-PMET contains various membrane associated oxidoreductases by which cells oxidize intracellular electron donors at the expense of the extracellular acceptors. In this research two members of the t-PMET system, cytochrome b5 reductase (CB5R) and NAD(P)H: quinone oxidoreductase (NQO1), were identified through enzymatic assays and immunodetection analysis.

The CB5R was detected in the myelin membrane via Western blotting as two bands, one at 35kDa and the other at 33kDa, potentially representing the myristoylated and non-myristoylated forms, respectively. The enzymatic activity was measured as an NADH: cytochrome c reductase activity and it was inhibited by the sulfhydryl agent p-hydroxymercuribenzoic acid.

The NQO1, an important antioxidant enzyme of t-PMET, was investigated in the myelin membrane through immunodetection and kinetic analysis. Western blot analysis

revealed a truncated form at ~13kDa in the myelin sheath. Furthermore, the associated activities of menadione-mediated cytochrome c reductase, water soluble tetrazolium 1 (WST-1) reductase and DCPIP reductase activity were found insensitive to the potent NQO1 inhibitor, dicoumarol.

Another facet of this research demonstrated the activity and enzyme expression level in the spontaneously demyelinating ND4 mouse model. The activity of CB5R was temporal; it increased with age, but fluctuated at earlier stages of life. Higher activity of NADH: cytochrome c reductase, and a higher rate of superoxide production were measured in the diseased myelin. The level of NQO1 also fluctuated over time. The fluctuation in the expression level may suggest its role in myelinogenesis, aging and disease. CB5R and NQO1, both, play important roles in decreasing oxidative stress by Coenzyme Q reduction, detoxification of quinones and xenobiotics, and through one and two electron reduction reactions.

Overall, this study reveals several putative components of t-PMET in the myelin membrane and provides a comprehensive insight into the activity of oxidoreductases catalyzing one and two electron transfer reduction reactions and their expression level in health and disease. The healthy and diseased myelin comparison will aid in deciphering the role of the identified proteins in the myelin energetics and the pathologies related to these enzymes.

Acknowledgements

In the name of Allah, Most Gracious, Most Merciful.

All Praises to Allah Almighty for giving me the ability and serenity to conduct this research, strength to persevere through hard times and for showering His countless blessings on me. Many people have been overwhelmingly supportive and encouraging of this work that surely my gratitude cannot be adequately expressed in just words here. Without the guidance, help, and support of those around me, completing this research would not have been possible.

First and foremost, I want to pay my gratitude to my advisor, Dr. Lillian DeBruin. Her guidance and input have been tremendously valuable and this research would not have been possible without her. I am thankful for the knowledge, depth and breadth of perspectives and diversity of ideas she brought to enrich my research enterprise. Her manner of mentoring and supervision are also paramount. Her leadership has greatly impacted my scientific thinking and developed my writing and analytical skills. She gave me the sense of professionalism. I must also mention the time she spared for me; the endless meetings especially during thesis writing. I would also like to thank her for providing generous financial support during my graduate studies. I consider it an honor for myself to be her student.

I would also like to thank my extraordinary dissertation committee, Dr. Allison McDonald and Dr. Masoud Jelokhani to take time out to be part of my thesis committee and guide me on this journey. Special thanks to Dr. Jelokhani for enhancing my interest in the field of kinetics. Thanks to Dr. Allison McDonald for maintain the quality of work without indulging into unnecessary complications, which kept me focused in achieving

my thesis objectives when it was easy to get lost during the exploration of interesting research ideas which popped every now and then. I am also thankful to Dr. Michael Suits, for serving as the external member of my thesis defence committee.

A big thank to Dr. Geoff Horsman, for his valuable discussion regarding kinetic analysis. I am grateful to Dr. Robin Slawson for allowing me to use the microscopic facility in her lab.

Thanks to my friends, colleagues and all lab mates for providing a friendly and creative atmosphere. Special thanks to Adrian Adamescu who helped in many academic and non-academic matters during my stay at campus. I met so many talented and wonderful individuals that are always ready to help.

Finally, I would like to express my deepest gratitude to my parents and my siblings for their prayers and encouragement, even from distance. I extend my sincerest gratitude to my husband Sohail, for his love, patience, sacrifices, support and encouragement which made it possible to complete this research. I must also mention my son Arham and daughters Manaal and Anaam, who bring so much joy to my life and remain a source of love, motivation and inspiration.

Declaration

I hereby declare that I am the sole author of this thesis. This is a true copy of the thesis, including any required final revisions, as accepted by my examiners. I understand that my thesis may be made electronically available to the public.

Table of Contents

List of Tables	ix
List of Figures	x
List of Abbreviations	xiii
Chapter 1 Introduction.....	1
1.1 The Central Nervous System	1
1.2 Myelin-Structure and Function:	3
1.2.1: Major Proteins in the Myelin Membrane:	4
1.2.2: Advantages and Disadvantages of Myelin:	4
1.3: CNS Energetic Theories	5
1.3.1: Neuron-Oligodendrocyte-Astrocyte (NOA) Interaction Theory	5
1.3.2: Nave Hypothetical Model.....	6
1.4: Proposed Alternative Model	7
1.5: Trans-plasma Membrane Electron Transport System (t-PMET)	9
1.5.1 Types and Components of t-PMET:	9
1.5.1. A: Electron Donors	10
1.5.1.B: Electron Acceptors.....	11
1.5.1 C: Intermediate Electron Carriers	11
1.5.1.D: Oxidoreductases in t-PMET:	12
1.5.2: Functions of t-PMET:	13
1.6 Thesis Organization	16
Chapter 2 Objectives, Approaches and General Methodologies.....	17
2.1 Objectives	17
2.2 Methods of Studying t-PMET.....	18
2.3 General Approaches to Measure Redox Activities	19
2.4 General Approach to Measure Superoxide Production	20
2.4.1 Enzyme Kinetics	21
2.5 General Methodologies	24
2.5.1 Isolation of Myelin	24
2.5.1(A) Myelin Detergent Fractionation	25
2.5.1(B) Myelin Delipidation	27

2.5.1 (C) Sodium Dodecyl Sulfate-Polyacrylamide Gel Electrophoresis and Western Blotting	28
2.5.1 (D) Immunohistochemistry	29
2.6 Research Significance	30
Chapter 3 Investigation of Cytochrome b₅ Reductase in the Myelin Membrane....	31
3.1 Introduction.....	31
3.2 Materials and Methods.....	35
3.2.1 Western Blot Analysis and Immunohistochemistry.....	35
3.2.2 NADH Dependent Cytochrome c Reductase Assay	36
3.2.3 Methodology of Detergent Fraction Assay	37
3.2.4 Kinetic and Statistical Analysis	38
3.3 Results and Discussion	38
3.2 Measurement of Cytochrome b ₅ Reductase Activity in Myelin Membrane.....	41
3.5.1 Enzyme Assay with Myelin Detergent Fractions.....	42
3.6 Conclusions.....	48
Chapter 4 Investigation of NAD(P)H: Oxidoreductase 1 (NQO1) in the Myelin Membrane	49
4.1 Introduction.....	49
4.2 Materials and Methods.....	53
4.2.1 Enzyme Activity Assays	53
(A) Menadione-Mediated Cytochrome c Reductase Activity	53
(B) PMS-Mediated WST-1 Reductase Activity.....	54
(C) DCPIP Reductase Activity.....	54
4.2.2 Measurement of Reductase Activity in Detergent Fractions	55
4.2.3 Western Blot Analysis and Immunohistology	55
4.2.4 Kinetic and Statistical Analysis	57
4.3 Results and Discussion	58
4.3.1 Immuno Detection of NQO1 in the Myelin Membrane.....	58
4.3.2 NQO1 Associated Activities in the Myelin Membrane	61
4.3.2 (A): Menadione -Mediated Cytochrome c Reductase Activity.....	62
Enzyme Assay with Myelin Detergent Fractions.....	63
4.3.2 (B): PMS-Mediated WST-1 Reductase Activity.....	67
4.3.2 (C): DCPIP Reductase Activity.....	68
4.4 Conclusions.....	80

Chapter 5 Comparison of Oxidoreductases in Healthy and Diseased Myelin.....	83
5.1 Introduction.....	83
5.1.1 Model of Demyelination	85
5.2 Material and Methods	86
5.2.1 Measurement of Superoxide Detection.....	86
5.3 Results and Discussion	87
5.3.1 Investigation of Cytochrome b5 Reductase Activities in Diseased and Healthy Myelin	87
5.3.2 Investigation of NQO1 in Healthy and Diseased Myelin	94
5.3.2.1 Immuno-Detection of NQO1 in Diseased and Healthy Myelin	94
5.3.2.2 Measurement of DCPIP Reductase Activity in Healthy and Diseased Myelin	98
5.5 Conclusions.....	99
Chapter 6 Summary, Conclusions and Future Directions.....	100
6.1 Summary and Conclusions	100
6.2 Future Directions	108
6.2.1 Bioanalytic Separation of Oxidoreductase Activities and the Proteomic Identification	108
References.....	110

List of Tables

Table 4.1	Chemical structures of used inhibitors	56
Table 5.1	Comparison of cytochrome c reductase activity with 20 μ g myelin with 100 μ M of cytochrome c in healthy and diseased samples	89
Table 5.2	Comparison of cytochrome c reductase activity with 10 μ g myelin with 500 μ M of cytochrome c in healthy and diseased samples	89
Table 6.1	Similarities and differences between CB5R and NQO1	100
Table 6.2	Specific activities of identified enzymes with various substrate	106

List of Figures

Figure 1.1	The wrapping of the oligodendrocytes around axon	3
Figure 1.2	Schematic overview of NOA theory	6
Figure 1.3	The hypothetical energy production model of myelinated axons by Nave	7
Figure 1.4	Possible redox activities in myelin t-PMET	8
Figure 1.5	Key Components of t-PMET	10
Figure 2.1	A typical Michaelis-Menten Kinetics representationCurve	22
Figure 2.2	Schematic of the myelin detergent fraction procedure	27
Figure 3.1.	Catalytic cycle of FAD in CB5R	32
Figure 3.2	Overall Structure of human CB5R	33
Figure 3.3	Reduction of hemoglobin by non-myristolated CB5R form	34
Figure 3.4	Immunodetection of CB5R in the myelin membrane	40
Figure 3.5	A typical graph depicting cytochrome c reductase activity	42
Figure 3.6	Comparison of myelin detergent fractions for NADH:cytochrome c reductase activity	42
Figure 3.7	NADH: cytochrome c reductase activity as a function of amount of myelin	43
Figure 3.8	NADH: cytochrome C reductase activity as a function of amount of substrate	44
Figure 3.9	Structure of pHMB	45
Figure 3.10	Inhibition of cytochrome c reductase activity by pHMB	46
Figure 3.11	Attempted inhibition of Cytochrome c reductase activity by KCN	47
Figure 4.1	Structure of human NQO1 enzyme	50

Figure 4.2	A proposed catalytic mechanism of human NQO1	51
Figure 4.3	Schematic of functions of NQO 1 enzyme	52
Figure 4.4	Immuno detection of NQO1	59
Figure 4.5	Structure of NQO1 mRNA and position of spliced exon 4	60
Figure 4.6	Typical reaction rate of menadione-mediated cytochrome c reduction by myelin	63
Figure 4.7	Comparison of myelin detergent fractions for menadione-mediated cytochrome c reductase activity	64
Figure 4.8	Cytochrome c reduction via menadione activity as a function of amount of myelin	65
Figure 4.9	Attempted inhibition of menadione-mediated cytochrome c reductase activity by inhibitors	66
Figure 4.10	Modified mechanism of reduction of WST-1 by intermediate electron carrier PMS	68
Figure 4.11	Attempted inhibition of WST-1 reductase activity by dicoumarol	68
Figure 4.12	Reduction of DCPIP by NQO1	69
Figure 4.13	Typical reaction rate of NADH-dependent reduction of DCPIP in the myelin	70
Figure 4.14	DCPIP reductase activity as a function of amount of myelin	70
Figure 4.15	NAD(P)H: DCPIP reductase activity as a function of DCPIP substrate	71
Figure 4.16	Mechanism of substrate-based inhibition of allosteric enzyme	72
Figure 4.17	NADH: DCPIP reductase activity as a function of electron donor concentration	73
Figure 4.18	Attempted inhibition of DCPIP reductase activity by dicoumarol	75

Figure 4.19	Schematic of dicoumarol binding with human NQO1 active site	76
Figure 4.20	Attempted inhibition of DCPIP reductase activity with different inhibitors	79
Figure 5.1	MRI image of MS brain.	83
Figure 5.2	Basic structure of neurons with myelin sheath in health and disease	85
Figure 5.3	Age-matched comparison of Cytochrome c reductase activity in health and diseased myelin	88
Figure 5.4	The pHMB-mediated inhibition as a function of cytochrome c reductase activity	91
Figure 5.5	Comparison of superoxide production rate in healthy and diseased myelin	92
Figure 5.6	Schematic of hypothesis of CB5R-induced BBB damage	93
Figure 5.7	Schematic of Calcium induced toxicity and axonal degeneration	94
Figure 5.8	Western blot of NQO1 in diseased and healthy myelin	95
Figure 5.9	Mechanism of activation of ARE pathway	97
Figure 5.10	Comparison of DCPIP reductase activity in healthy and diseased myelin.	98
Figure 6.1	Regulatory mechanism of sirt1 by CB5R and other oxidoreductases in plasma membrane	104
Figure 6.2	Architecture of ceramide signaling generated by NQO1/CoQ	106
Figure 6.3	CB5R and NQO1 in t-PMET	107
Figure 6.4	Role of NQO1 and CB5R in demyelination	108

List of Abbreviations

A	Absorbance
AFR	Ascorbate free radical
AGE	Advanced glycated product
ARE	Antioxidant response element
Asc	Ascorbate
ATP	Adenosine triphosphate
BCA	Bicinchoninic acid
BH	Brain homogenate
C	Concentration
Cb5	Cytochrome b5 (substrate)
DCPIP	2, 6-Dichlorophenol indophenol
CDKs	Cyclin-dependent kinases
CHAPS	3-[(3-Cholamidopropyl)dimethylammonio]-1-propanesulfonate
CNP	2, 3-cyclic nucleotide 3-phosphodiesterase
CoQ	Co-enzyme Q
CoH₂	CoQ reduced form
Cyto c	Cytochrome c
Cys	Cysteine residue
CB5R	Cytochrome b ₅ reductase
Dcyt b	Duodenal cytochrome b
DHA	Dehydroascorbate

Dicoumarol	3, 3-methylene bis-4- hydrocoumarin
DMSO	Dimethyl sulphoxide
DM-20	Deletion mutant of proteolipid protein
DP	Delipidated myelin
DRM	Detergent resistant membrane
DPI	Diphenyleneiodonium
E°	Electrode potential
ECL	Enhance chemiluminescence
EDTA	Ethylene diamine tetra-acetic acid
EGTA	Ethylene glycol tetra acetic acid
ENOX	External disulphide thiol exchanger
FAD	Flavin adenine dinucleotide
GAP	3- glyceraldehyde phosphate
GLUT 1	Glucose transporter 1
GSH	Glutathione reductase
H⁺	Hydrogen ion
HEPES	4-(2-hydroxyethyl)-1-piperazineethanesulfonic acid
H₂O₂	Hydrogen peroxide
HRP	Horseradish peroxidase
HSP70	Heat shock protein70
kb	Kilo base pair
KCl	Potassium chloride
KCN	Potassium cyanide

kDa	Kilo daltons
Keap 1	Kelch-like ECH-associated protein 1
L_d	Liquid-disordered phase
L_o	Liquid-ordered phase
MAG	Myelin-associated glycoprotein
MBP	Myelin basic protein
MCT 1	Monocarboxy transporter 1
MCT 2	Monocarboxy transporter 2
MD	Menadione
MDH₂	Menadiol
mNQO	Microsomal NAD(P)H: Quinone oxidoreductase
MOG	Myelin oligodendrocyte glycoprotein
MRI	Magnetic resonance imaging
MS	Multiple sclerosis
Na⁺	Sodium ion
NAA	N-acetyl aspartate
NaCl	Sodium chloride
NAD⁺	Oxidized form of Nicotinamide adenine dinucleotide (NADH)
NADH	Nicotinamide adenine dinucleotide
NF-κB	Nuclear factor kappa light-chain-enhancer of activated B cells
Na₃VO₄	Sodium vanadate
NO[•]	Nitric oxide
NOS	Nitric oxide synthase

NOA theory	Neurons-oligodendrocytes-astrocytes
NQO1	NAD(P)H: Quinone oxidoreductase 1
NQO2	NHR: Quinone oxidoreductase 2
Nrf2	Nuclear factor erythroid 2-related factor
NOX	NADH: Oxidases
O₂^{•-}	Superoxide radical
OLs	Oligodendrocytes cells
OONO⁻	Peroxynitrite ion
P53	Puma 53
PARP	Poly ADP-ribose polymerase
PBS	Phosphate buffer saline
Phos STOP	Phosphate inhibitor cocktail
PIC	Protease inhibitor cocktail
PLP	Proteolipid protein
PMSF	Phenylmethane sulfonylfluoride
PMRS	Plasma membrane redox system
PMS	Phenazinium methylsulphate
PNS	Peripheral nervous system
PPMS	Primary progressing MS
PRMS	Progressive relapsing MS
RRMS	Relapse-remitting MS
ROS	Reactive oxygen specie

SIRT 1	Sirtuin 1
SCs	Schwann cells
SE	Standard errors
SDS	Sodium dodecyl sulphate
SDS-PAGE	Sodium dodecyl sulphate polyacrylamide gel electrophoresis
SOD	Superoxide dismutase
SPMS	Secondary progressive MS
TBS	Tris buffer saline
TCA cycle	Tricarboxylic acid cycle
TEMED	Tetramethylethylenediamine
t-PMET	Trans plasma membrane electron transport
TTBS	Tris buffered saline with tween -20
TX-100	Triton-X-100
Vit C	Vitamin C
Vit E	Vitamin E
WST-1	Water soluble tetrazolium generation 1

Chapter 1

Introduction

The major focus of this thesis is the investigation of a trans-plasma membrane electron transport system (t-PMET) in the myelin membrane. An introduction to t-PMET alongside its vital components and their functions is described in this chapter. Different theories regarding myelin energetics are also presented. A hypothesis regarding myelin energetics is established which states that the t-PMET is assisting myelin membrane in maintaining the pyridine nucleotides pool. Lastly, the organization of this dissertation is given.

1.1 The Central Nervous System

Cells need energy to sustain life which they obtain from food. Mainly, the oxidation of food takes place in mitochondria, but starts in cytoplasm. Every cell type has different energy requirements according to its structure and function [1]. Cells, in particular skeletal muscles and neurons, need more energy than other cell types because of muscle movement and propagation of nerve impulses.

The nervous system is predisposed for all biological processes happening in the body and their communication with other body parts. The nervous system is divided into two distinct parts, the central nervous system (CNS) and the peripheral nervous system (PNS). The CNS, comprised of the brain and spinal cord, is believed to be the centre of

all biological processing. Alternatively, the PNS incorporates nerves in the body and plays a key role in reacting to stimulus transmitted by CNS [2].

Neurons are specialized cells in the nervous system that are capable of integrating thousands of inputs into a single output, known as the action potential [3]. The neuronal functional features such as the propagation of action potential and transportation of enzymes, make them energetically expensive. For instance, the mammalian brain is 2% of the total body weight but consumes 20% of the energy produced by the body [3]. To reduce this energy requirement, the brain is divided into two parts; grey matter which utilizes 1-1.6 $\mu\text{mol/g/min}$ glucose, and white matter which utilizes 0.3-0.4 $\mu\text{mol/g/min}$ glucose [4]. The difference in the energy requirements can be explained on two levels. Firstly, the neurons in grey matter have a high glucose requirement due to synapse formation. Secondly, neurons in the white matter are ensheathed with a specialized lipid-rich structure called "myelin" which encapsulates the neurons and conserves the energy [5, 6]. Zalc *et al.* defined the myelin and its function altogether in a very concise manner:

“Myelin is hypothesized to enable a large body size by maintaining timely communication between distant parts and to enhance precision in event timing by reducing the absolute temporal variability in communication between two points. These advantages are derived from the enhanced speed of nerve impulse conduction that myelinated fibre enjoys relative to unmyelinated ones of the same diameter” [7].

1.2 Myelin-Structure and Function:

Myelin is formed from the extended protrusions of the oligodendrocyte cells (OLs) in CNS, and the Schwann cells (SCs) in the PNS. OLs can myelinate multiple axons and form approximately 40 or more distinct layers of myelin membrane. OLs and SCs wrap their cytoplasmic extensions or processes around the axon to form concentric layers of wrapped plasma membrane (see Fig 1.1) [8].

Myelin can be different in composition and function, depending whether it originated from OLs and SCs. However, all myelin sheaths have a high lipid to protein ratio. Myelin is composed of 70-80% lipid and almost 15-30% protein by dry weight. The lipid content ratio is in the order of 2:2:1:1 of cholesterol, phospholipid, galactolipid, and plasmalogens [7].

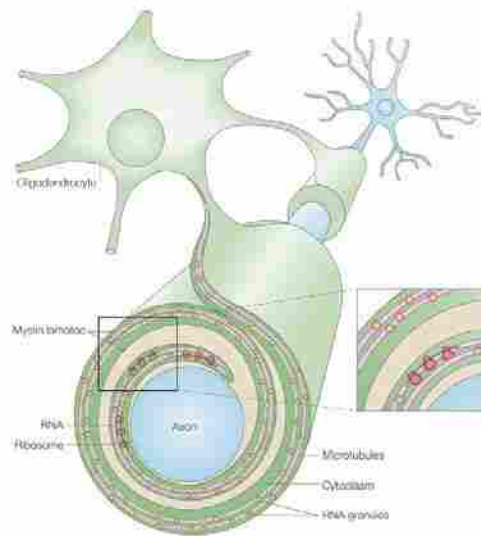


Fig1.1: The wrapping of the oligodendrocytes around axon. OLs cytoplasm is compacted to form a dense structure. In the CNS, one oligodendrocyte can myelinate more than one axon. Adapted from reference [7].

1.2.1: Major Proteins in the Myelin Membrane:

The major protein in myelin is proteolipid protein (PLP) which is approximately 30-45% of the total protein mass. The PLP is involved in septin and sirtuins shuttling as well as in transportation, strengthening and maintenance of myelin membrane [9]. It is believed that PLP mutation is responsible for several neurological disorders, as a result of the decreased axonal transportation [9]. The second most abundant protein is myelin basic protein (MBP) which comprises of almost 15-25% of the total protein content. The major role of MBP is to provide compaction to myelin sheath. The third most abundant protein is 2', 3'-cyclic nucleotide 3'-phosphodiesterase (CNP) that represents 5-15% of the total protein content present in the myelin. The CNP is involved in RNA binding to tubulin. The remaining 5-15% portion comprises of oligodendrocyte glycoprotein (MOG) and myelin associated glycoprotein (MAG), and more than 1200 different kinds of proteins [10, 11].

1.2.2: Advantages and Disadvantages of Myelin:

Communication is an issue due to large body size of gnathostomes where millisecond precision is required. The evolution of myelin membrane solved this problem. Some noticeable advantages of the myelin membrane are listed below:

- The evolution of myelin reduces the energy requirement for neuronal communication and boosts the speed of impulse propagation. Non-myelinated axons use considerably more energy per unit length of neuron than myelinated ones [12].

- Myelin gives the integrity to neurons and long term survival of neuron is made possible by myelin membrane [12].
- Myelin physically protects the CNS from autoimmune attack. It provides the protection against CD8⁺ and CD4⁺ activated T-cells [13].

However, a nearly completely insulated axon could be a double-edge-sword, as it restricts the access of extracellular metabolites to the axon [12]. Furthermore, the energy required in making myelin is greater than the energy conserved by myelin [12]. The following key questions are the most important aspects in myelinated neuron energetics and are the focus of research for last few decades:

- *Why and how OLs and SCs cells make myelin?*
- *How do neuronal cells meet their energy requirements in the presence of myelin?*

1.3: CNS Energetic Theories

Several theories are put forth to established the mechanism of interaction among neurons, OLs, astrocytes, and flow of metabolites into and out of the myelin sheath.

1.3.1: Neuron-Oligodendrocyte-Astrocyte (NOA) Interaction Theory

According to NOA theory, glucose from blood capillary is taken up by neurons, astrocytes, and oligodendrocytes (see Fig 1.2) [4]. This glucose is immediately metabolized into pyruvate through glycolysis. Pyruvate is converted into lactate, and this lactate can be absorbed by the cells with lower lactate concentration. Then the lactate is metabolized into alanine or acetyl CoA which can enter into the TCA cycle [14]. Aspartate is converted into N-acetyl aspartate (NAA) in the neurons. Acetyl CoA is

necessary for this conversion. This NAA is transported into the oligodendrocytes where it is converted back into aspartate and acetate. It is believed that acetate is extensively used in myelin lipid synthesis [4]. According to this theory, the shuttling of metabolites between the astrocytes, neurons, and oligodendrocytes is essential.

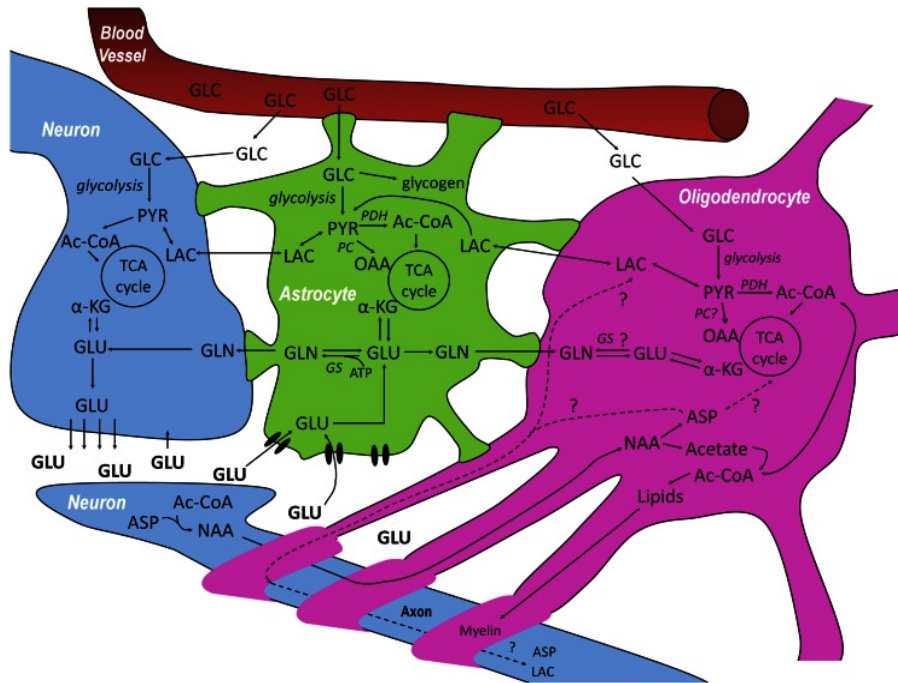


Fig 1.2: Schematic overview of NOA theory. The metabolic interaction between neuron-oligodendrocyte-astrocyte (NOA). Adapted from reference [4].

1.3.2: Nave Hypothetical Model

Klaus Nave and colleagues proposed a structural model to elaborate the transfer of glucose and its further processing in encapsulated neurons [15]. The hypothetical architecture is depicted in Fig 1.3.

It is believed that OLs and astrocytes are coupled together and assist neurons for energy production. Glucose is transported through glucose transporter protein 1 (GLUT 1) into the OLs and through connexin protein from astrocytes. Initially the glucose

undergoes oxidation in mature OLs, and the end glycolytic product, pyruvate, is converted into lactate.

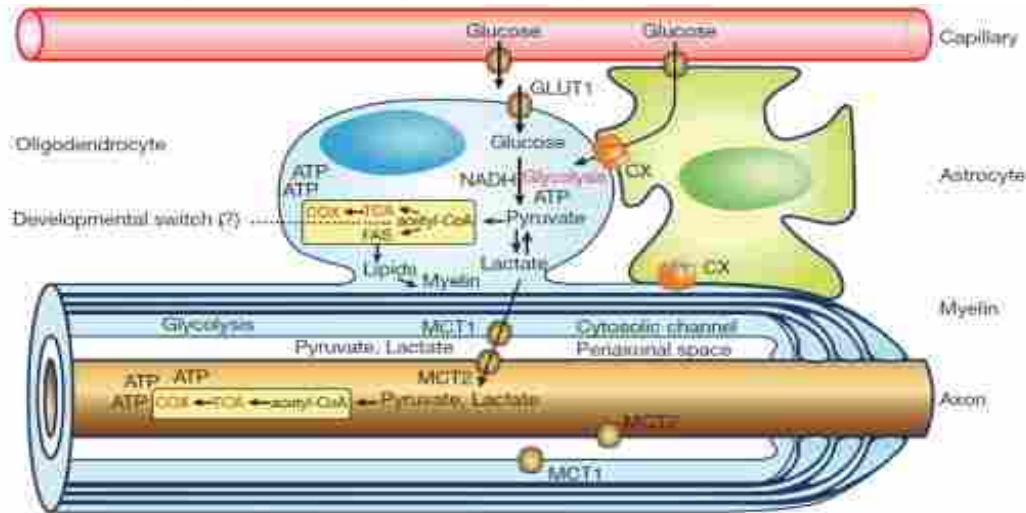


Fig 1.3: The hypothetical energy production model of myelinated axons by Nave. In this model, glucose is transported through glucose transporter protein (GLUT 1). From OLs, the end product of glycolysis, lactate, is transported to the underlying axon. Myelin sheath itself is also capable of maintaining glycolytic activity. Lactate produced from both the OLs and myelin membrane, enters into the axoplasm through MCT 2 where it enters into the TCA cycle for more ATP production. Adapted from reference [15].

The lactate is essentially shuttled across the myelin membrane by a transporter protein called monocarboxy transporter 1 (MCT-1). Through another transporter isoform MCT-2, it enters into the axoplasm. The lactate is used as an initial metabolite for TCA cycle. In axoplasm, the lactate is converted back to pyruvate which is utilized in the mitochondria for ATP production [15, 16]. According to this theory, glucose is utilized in the myelin sheath (OLs processes) where it undergoes the oxidation and the end product of glycolysis, pyruvate or lactate, is transported to the axon.

1.4: Proposed Alternative Model

For elucidation of myelinated-neurons energetics, an alternative model with a

myelin perspective is presented in the current research project. This model is not mutually exclusive to the Nave model, but hypothesizes another compensatory mechanism within myelin membrane.

It is hypothesized that to satisfy the energy requirement of myelin and to perform housekeeping functions, some compensatory mechanism such as trans-plasma membrane electron transport system (t-PMET) is assisting myelin membrane. Many components of mammalian t-PMET are now been identified. These are apparently ubiquitous and almost the same. The availability of a variety of substrates and inhibitors of t-PMET has made it possible to characterize and identify the structure of t-PMET in different cell types. Scientists have explored t-PMET in several cell types, but none have investigated its presence in myelin membrane.

Therefore, in this current research, it is hypothesised that

- The myelin membrane supports t-PMET through unidentified enzymes.
- The minimal structure of t-PMET consists of oxidoreductase enzymes, an internal electron donor and an external acceptor (see Fig 1.4).

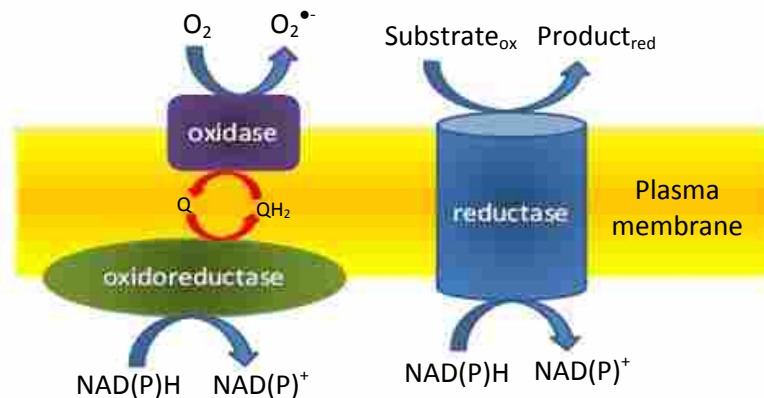


Fig 1.4: Possible redox activities in myelin t-PMET. The external acceptor (oxygen) is reduced by the t-PMET enzyme and reducing equivalents are derived from the $NAD(P)H$.

1.5: Trans-plasma Membrane Electron Transport System (t-PMET)

Trans-plasma membrane electron transport (t-PMET), also called as plasma membrane redox system (PMRS), was discovered in 1960, and emerged as an important system for cells [17]. The t-PMET utilizes almost 10% of the total oxygen consumption in the cells [10], and functions in almost every organism including yeast, plants, algae and animals [17]. In this system, the extracellular oxidants are reduced by t-PMET components at the expense of intracellular reducing agents. Some of the important functions associated with t-PMET are cell growth and death, proton pumping, ion channel activity, and antibody modification.

1.5.1 Types and Components of t-PMET:

The trans-plasma membrane electron transport system reduces the extracellular oxidants by two ways. One way is without enzymatic involvement and is referred to as shuttle based electron transfer. Second method is even more complex and is mediated through enzymes. The current focus of research is on the enzyme-dependent system. A proposed structure of various identified enzymes in a t-PMET system is shown in Fig 1.5.

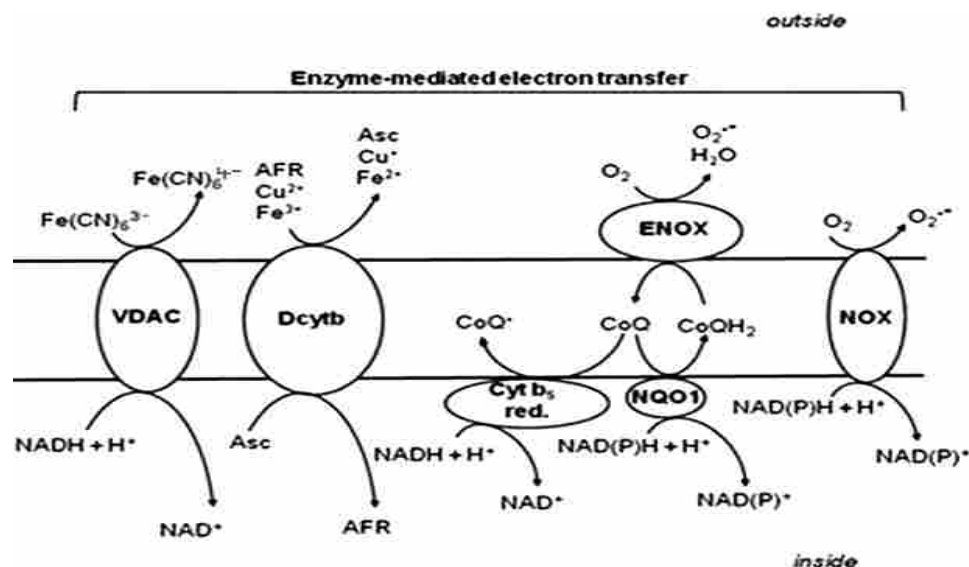


Fig1.5: Key components of t-PMET. Intracellular electrons provided by NADH or ascorbate, flow outward to reduce extracellular acceptors (oxygen, ascorbate free radical (AFR), ferric or cupric ions). Several enzymes contribute to t-PMET. Some of them are: voltage dependent anionic channel (VDAC), duodenal cytochrome b (Dcyt b), NAD(P)H oxidase (NOX) are trans-membrane proteins, while disulfide thiol exchanger (ENOX) are terminal donor of electron to oxygen and present at the outer surface of the membrane. Some important proteins such as cytochrome b5 reductase (CB5R), NAD(P)H quinone oxidoreductase 1 (NQO1) are important quinone reductases and present at the inner surface of plasma membrane. Co-enzyme Q (CoQ) is an important antioxidant and acts as an intermediate electron carrier. Adapted from reference [17].

1.5.1. A: Electron Donors

Intracellular reducing equivalents are derived either from NADH (reduced form of nicotinamide adenine dinucleotide) or NADPH (reduced form of nicotinamide dinucleotide phosphate). NADH is produced during catabolic processes such as glycolysis, whereas NADPH is produced as a by-product in the pentose phosphate pathway and is involved in the biosynthesis of fatty acids and cholesterol. The ratio of NADH/NAD⁺ or NADPH/NADP⁺ is very important for the cells to perform different biological functions as they directly affect the pH of the cell as well as redox state. In steady state conditions, proton influx and efflux is maintained and no significant change

in membrane potential is observed. But the accumulation of H^+ in cytosol results in hyperpolarization and membrane is depolarised when H^+ is pumped out into the extracellular space. This H^+ is derived from the pool of NADH or NADPH [13]. Ascorbate (Asc) and flavonoids (vitamin E, quercetin) are intracellular substrates other than NADH and NADPH. Their functions are also to protect the membrane from extracellular stressors. Ascorbate promotes the t-PMET by two ways: **A)** By acting as an electron donor in enzyme-mediated electron transport system, **B)** and acting as an electron donor in non-enzymatic shuttle based transfer, where Asc directly acts as a reducing agent and is oxidized to dehydroascorbate (DHA). This DHA is pumped across the membrane where it is again converted to reduced form [18].

1.5.1.B: Electron Acceptors

The most important extracellular electron acceptor is oxygen. When it is fully reduced, oxygen is converted to water, and when partially reduced, it can form reactive oxygen species (ROS), such as superoxide radical ($O_2^{\cdot-}$) or hydrogen peroxide (H_2O_2). Superoxide radicals play a dual function, it not only act as a signal transducer but also protects the cell. Other extracellular putative acceptors are ascorbate free radical (AFR), ferric and copper ions [17].

1.5.1 C: Intermediate Electron Carriers

The most important intermediate electron carrier is co-enzyme Q (CoQ), also known as ubiquinone. It is present between the lipid bilayer and links the inner surface of the cell to the outer environment. CoQ can be transformed to ubisemiquinone and ubiquinol (reduced quinone) by one and two electron reduction events, respectively. Some other intermediate electron carriers are flavins and vitamin E.

1.5.1.D: Oxidoreductases in t-PMET:

Enzymes are the important machinery in electron transfer. There are several different kinds of enzymes with different localization in the plasma membrane. Some of them are located at the outer surface like external NADH dependent oxidases (ENOX), some are trans-membrane proteins such as NADH dependent oxidase (NOX), duodenal cytochrome b (Dcytb), voltage dependent anionic channel (VDAC) and some are localized on the inner surface of the plasma membrane like cytochrome b5 reductase (CB5R) and NAD(P)H: quinone oxidoreductase 1 (NQO1).

The CB5R is present in plasma membrane, mitochondria and endoplasmic reticulum. It is a monomeric flavin protein and the prosthetic group, flavin adenine dinucleotide (FAD), is non-covalently bound. There are two known isoforms of this enzyme; a membrane-bound and soluble form, with molecular weights of 35 and 32 kDa, respectively. The major functions of CB5R involve fatty acid elongation, desaturation, cholesterol synthesis and it also reduces the AFR back to Asc [19]. NQO1 is another inner surface homodimeric flavo-protein with a molecular weight of ~30kDa for each subunit. The enzyme is involved in cellular defence, stabilization of p53 gene and chemo-protection [20].

External NADH dependent oxidase (ENOX) is cell surface protein considered to be the terminal electron donor to molecular oxygen. Three members of this family have been reported: ENOX 1, ENOX 2 and ENOX3. They control the cell growth by disulfide-thiol interchange activity [20].

Among trans-membrane proteins, NOX play a vital role in producing superoxide. On the basis of structure, NOX are classified into three groups: a) NOX 1-4 b) NOX 5

and c) DUOX 1-2. NOX 2 is well characterized in the t-PMET. NOX 1-4 are found in epithelial, muscle cells, kidney lungs and spleen cells. They perform various functions such as defence by invading the microbes through production of superoxide and they are considered to be the regulator of calcium in cells. DUOX 1-2 is mainly found in thyroid gland [21]. Duodenal cytochrome b (Dcytb) is novel protein that is induced in response to hypoxia and iron deficiency. Dcytb protein with a molecular weight of 33kDa plays a crucial role in iron metabolism [22].

Voltage dependent anion channel (VDAC) is another integral membrane protein with a molecular weight of ~30-35kDa. The channel's major function involves the trafficking of metabolites between extracellular space and cytoplasm. Another vital function of the channel is the release of apoptogenic proteins [23].

1.5.2: Functions of t-PMET:

Beside some general functions such as the trafficking of molecules, various physiological roles are also associated with t-PMET. The plasma membrane has a complex signalling system for regulating cellular metabolism and performing other vital functions for the cells such as maintaining homeostasis, pH control, proton pumping and antibody control.

Proton movement is one of the important functions of t-PMET. Proton movement is carried out by the Na^+/H^+ anti-porter, which facilitates the movement of the ions across the membrane. Due to ion exchange through plasma membrane, the internal and external pH gradient changes, which regulates cell volume sensing and apoptotic signaling [24].

Enzymes such as NOX2, NOX5 and DUOX are involved in sperm maturation and fertilization. Furthermore, since mitochondrial function is often defective in

spermatozoas, upregulation of t-PMET maintains the ratio of NAD^+/NADH [23]. The DUOX enzyme generates the hydrogen peroxide that not only helps the spermatozoa in defence against xenobiotics but also helps the cells in developing a cross-linking of envelope proteins, thus provides a physiological structure to avoid polyspermy [25] .

Another critical function of t-PMET is the maintenance of redox homeostasis. Alteration of membrane redox potential leads to dramatic change in platelets function in uremic patients. The deoxygenated erythrocytes, show decreased levels of NADPH and glutathione reductase (GSH), and therefore showing the depletion of membrane thiol pool and an increased oxidative stress. In this condition, t-PMET uses Asc as an electron donor. A single hemodialysis event in uremic patients triggers two responses: (1) removal of toxic compounds, and (2) regulates t-PMET efficiently [26].

Loss or overstimulation of t-PMET leads to different pathologies. Apoptosis is a process involved in cellular homeostasis and tissue development. The process must be tightly regulated, since defective apoptotic progression has been implicated in several diseases. For instance, excessive apoptosis causes hypotrophy, whereas an insufficient amount results in uncontrolled cell proliferation, such as cancer. Inhibition of t-PMET causes ROS generation, which in turn leads to a pro-oxidant environment at the plasma membrane and promotes apoptosis [24, 27] . The potential involvement of t-PMET in cell death is further suggested by the finding that NAD^+/NADH and CoQ/CoQH_2 ratios are important modulators of neutral sphingomyelinase, which catalyzes the generation of ceramide pathway from sphingomyelin, and allow the clustering of death receptors and transmission of an efficient death signal into the cells [28].

Normal tissues derive most of their energy by metabolizing glucose to carbon

dioxide and water through mitochondrial oxidative phosphorylation. Conversely, cancer cells convert glucose to lactate irrespective of oxygen presence or absence. This phenomenon, described by Warburg in the early 1900s (known as the “Warburg effect”), emphasizes that cancer cells rely less on mitochondrial activity than the normal cells. The role of t-PMET in cancer biology relies on the observation that the metabolic changes described above may perturb key redox couples, including the NAD(P)H/NAD(P)⁺ and CoQH₂/CoQ ratios, which play a crucial role in supporting cell survival, function, and growth of fast proliferating cells. Cancer cells usually exhibit elevated level of t-PMET [29]. It has been suggested that ENOX2 levels may be associated with the ability of tumour cells to acquire an aggressive phenotype [30]. Some NOX isoforms have been associated in early stages of carcinogenesis which implies the role of t-PMET in cancer cells. Most anti-cancerous drugs target the t-PMET inhibition.

The t-PMET system has a role in cardiovascular diseases, including hypertension, atherosclerosis, and vascular complications of diabetes. Hypertensive patients show increased NOX-dependent superoxide production in vascular smooth muscle cells [31]. When ubiquinone-dependent electron transport is disrupted, t-PMET becomes a source of ROS, triggering oxidative stress and apoptosis. This phenomenon has been proposed to be one of the factors responsible for the onset of age-related pathologies. Therefore, t-PMET system exerts a protective role by maintaining optimal levels of plasma antioxidants [28].

Experimental evidence suggests that some superoxide generating NOX isoforms may be involved in the clinical progression pathogenesis, as well as in several neurodegenerative disorders. For instance, in the brain of Alzheimer's patients, membrane

localization of p47phox (a NOX subunit) is increased, and at the same time, amyloid- β peptides can enhance NOX activity. Consistently, knockdown of p22phox inhibits amyloid- β peptide-induced neuronal apoptosis [32].

1.6 Thesis Organization

Due to complex anatomy of myelinated neurons, their energetics are difficult to explain. Several theories have been put forth hitherto. In this research, a theory of t-PMET association with myelin membrane is presented, and components of t-PMET were identified in myelin membrane. This thesis is divided into two parts. First part (chapter 1-4) explores putative components of t-PMET in myelin membrane. Second part (chapter 5) compares identified components between healthy and diseased myelin.

Chapter 2: Chapter 2 of this thesis deals with objectives and rationale. Methodology to achieve these objectives is also described in this chapter.

Chapter 3: CB5R is an enzyme present in plasma membrane electron transport system. In this chapter, CB5R existence in myelin membrane is investigated.

Chapter 4: NAD(P)H: Quinone oxidoreductase 1 (NQO1) is another t-PMET enzyme involved in defense against stress. This chapter deals with the investigation of NQO1 in myelin membrane.

Chapter 5: A neurodegenerative disorder, multiple sclerosis, is introduced. A comparison of previously identified enzymes activities is done with diseased myelin model.

Chapter 6: This chapter summarises the dissertation with conclusions and also reveals some future research directions.

Chapter 2

Objectives, Approaches and General Methodologies

This chapter describes the objectives and general methodologies of the current research work. Different approaches for studying t-PMET such as the measurement of reduction of artificial acceptors and superoxide production are described. The immunodetection of proteins and enzyme kinetics are other important aspects discussed in this chapter. Lastly, the impact and significance of current research work is elucidated.

2.1 Objectives

The t-PMET system allows the reduction of extracellular oxidants at the expense of intracellular reducing equivalents. In this way, cells not only respond to change in the redox microenvironment but also gain the ability to regulate their important house-keeping functions such as cell metabolism, proton pumping, ion channel activities, cell growth and death [33]. The purpose of this research is to characterize the proteins and enzymes that may be involved in t-PMET within the myelin membrane. A plethora of research has been done on t-PMET system of endothelial, phagocytotic and erythrocytic cells. However, researchers have not investigated the existence of t-PMET in myelin membrane. Detailed studies of t-PMET are important as its existence not only plays a key role in metabolism but it also has implication in various pathologies including neurodegenerative disorders [17].

The main objectives of this study are:

- i. To determine the enzyme redox activities in myelin membrane.
- ii. To establish the distribution and localization of each redox enzyme in different myelin membrane microdomains.
- iii. To compare healthy myelin with "diseased" myelin in terms of
 - a) oxidoreductase activities,
 - b) enzyme protein expression level, and
 - c) production of superoxide.

2.2 Methods of Studying t-PMET

The study of a complex biological system is divided frequently into three stages. First is the overall tissue structure determination (general structure of t-PMET is depicted in Fig 1.5). Second, the individual components must be identified, which is the paramount area of discussion in this research. The third stage is the determination of juxtaposition of these components, and elucidation of their structural and functional role with each other [34, 35]. Several methods are employed to study t-PMET [29, 34-36]. Some of these methods are listed below;

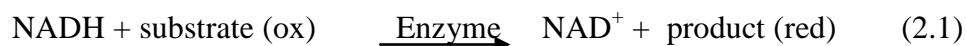
- i. Measurement of reduction of an artificial or exogenous electron acceptor
- ii. Measurement of disappearance of an electron donor
- iii. Measurement of oxygen consumption
- iv. Measurement of superoxide production

v. Measurement of ubiquinone reduction

In this research project, components of t-PMET were characterized or identified through measuring the reduction of the artificial acceptors, disappearance of an electron donor, and superoxide production. These approaches are described below.

2.3 General Approaches to Measure Redox Activities

The t-PMET system includes oxidoreductase enzymes. These oxidoreductase enzymes catalyze redox reactions; the transfer of electrons from one molecule to another molecule. An objective of this research was to determine the redox activities in myelin membrane which was accomplished through monitoring of electron transfer from electron donor to electron acceptor. The general activity can be measured with NADH or NADPH as an electron donor and an electron acceptor such as cytochrome c or tetrazolium salt.



The expression 2.1 illustrates the oxidoreductase reaction in which NADH in reduced form donates two electrons (as a hydride) and reduces the oxidized substrate (electron acceptor), produces the oxidized form of the electron donor, NAD^+ and the product. The electron transfer can be monitored spectrophotometrically at a specific wavelength following the oxidation of NADH or the reduction of the substrate. When NADH is monitored, a decrease in absorbance at 340nm is measured. As NADH donates electrons, the concentration of NAD^+ (oxidized form) increases, while

concentration of NADH (reduced form) decreases. The electron donor NADH has an characteristic absorption spectrum and a maximum absorption at 340nm.

Many oxidoreductase-catalyzed reactions are monitored with an artificial electron acceptor (substrate). The selection of artificial electron acceptor is crucial. There should be following characteristics in artificial acceptor [16]:

- Artificial acceptor must have strong chromophore in oxidized or reduced form, such as 2, 6-dichlorophenol indophenol (DCPIP).
- Artificial acceptor should carry large multiple negative charge; for example, ferricyanide.
- Artificial acceptor or endogeneous substrate must have high molecular weight, such as toluidine blue O or cytochrome c.

Due to high molecular weight and multiple negative charge, these substrate are impermeable to the membrane. To investigate the enzyme activities in myelin, a system was developed in which a sample of myelin membranes was reconstituted in a buffer (to maintain the pH of the system, usually Tris buffer), with a suitable substrate such as cytochrome c or dichlorophenolindophenol (DCPIP) (as final electron acceptor) and NAD(P)H (as the electron donor).

2.4 General Approach to Measure Superoxide Production

NAD(P)H oxidase or NOX, which is characterized as a superoxide generating enzyme, is another class of t-PMET enzymes. Superoxide plays a vital role in cellular defense, signal transduction, angiogenesis, blood pressure regulation, and biosynthesis

processes [37]. These enzymes use NAD(P)H as an internal electron donor and reduce the external oxygen by an one electron reduction into superoxide. The superoxide is spontaneously or enzymatically dismutated by superoxide dismutase (SOD) to hydrogen peroxide and oxygen. Hydrogen peroxide also acts as a messenger molecule [17]. Several methods are employed to detect superoxide production in cells. Some of them are:

- i. Detection of superoxide through lucigenin-derived chemiluminescence
- ii. Detection of superoxide through cytochrome c reduction
- iii. Detection of superoxide through WST-1 (water soluble tetrazolium generation 1) reduction

In this research, any measurable quantity of superoxide was detected by WST-1. Tetrazolium was reduced to formazan by superoxide which indicates the occurrence of a redox reaction and presence of superoxide radical. Expression 2.2 illustrates the non-enzymatic reaction. The formazan production can be detected at 438nm with an extinction co-efficient of $37\text{mM}^{-1}\text{ cm}^{-1}$.

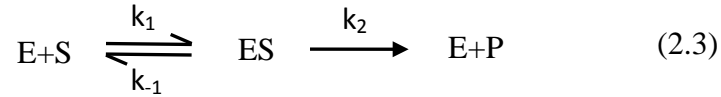


2.4.1 Enzyme Kinetics

There are several advantages of enzyme assays including their low cost, reliability and simple procedure. Besides these advantages, the most important advantage is the ability to investigate or study the kinetics and inhibition study of the enzyme.

Enzyme kinetic study is the branch of science that deals with reactions that are catalyzed by enzymes. This analysis provides useful parameters related to rate of reaction. When enzyme (E) binds to a substrate (S), it forms an enzyme-substrate

complex (ES). After sometime, this ES is regenerated to enzyme (E) and substrate is changed into product (P). This enzyme catalytic mechanism is described in equation below:



In kinetic analysis the enzyme rate is measured for a series of concentrations of the substrate, as shown in Fig 2.1

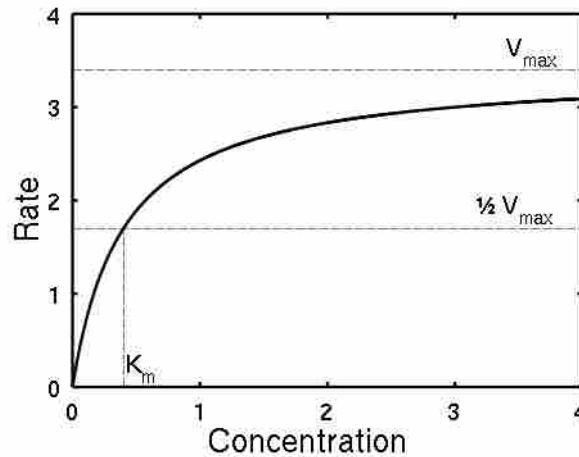


Fig 2.1: A typical Michaelis-Menten kinetics representation. V_{max} represents the enzyme maximum velocity while K_M represents the substrate concentration at which reaction attains its half maximum velocity. Taken from reference [38].

The mathematical modulation of Michaelis Menten model is described by the equation 2.4, and is used to study the asymptotic reaction. This equation graphically represents a hyperbola which is defined by two asymptotic parameters V_{max} and K_M .

$$V = \frac{V_{max}[S]}{K_M+[S]} \quad (2.4)$$

where

V_{max} = Maximum velocity of the reaction

$[S]$ = Substrate concentration

K_M = Michaelis constant or $1/2 V_{max}$

The V_{max} represents the maximal enzyme reaction velocity, when the enzyme is fully saturated with the substrate, and K_M reflects the affinity of enzyme-substrate interaction which is the substrate concentration to attain half maximum velocity.

The significance of Michaelis-Menten kinetics is that it provides the useful information about the rate of reaction, mechanism, and the enzyme nature. If the kinetic plot of an enzyme is similar to Fig 2.1, then the enzyme involves the single substrate. If plot is different from Fig 2.1, such as sigmoidal, then the enzyme may involve two substrates and may have ping-pong mechanism or could be allosteric in nature. Thus, Michaelis Menten equation describes chemical as well as some physical aspects of the enzyme.

The enzyme activity for oxidoreductases can be calculated following reduction of acceptor or oxidation of donor. According to Beer's law as concentration of substrate (chromophore in substrate) increases absorbance also increases. The general equation is

$$A = \epsilon lc \quad (2.5)$$

To monitor the enzyme activity, the change in absorbance of substrate over time is plotted. Enzyme activity can be calculated from the slope of the plot and the Beer's law relationship.

$$\text{Activity} = \text{Slope} \times 60\text{sec/min} \times 1/\epsilon \text{ (M}^{-1} \text{ cm}^{-1}\text{)} \times 1\text{(cm)} \times \text{volume (L)} \times 10^6 \mu\text{mol/mol}$$

where l = path length

ϵ = extinction coefficient

slope = $\Delta\text{Abs}/\text{min}$

2.5 General Methodologies

Some common methodologies and techniques that were utilized throughout the research project are discussed below.

2.5.1 Isolation of Myelin

Isolation of myelin from mouse brain was completed by the sucrose gradient method [39]. The brains tissues were homogenized with a Douncer homogenizer on ice in 10.5% (w/v) sucrose prepared in TNE (25mM Tris buffer, pH 7.4, 150mM sodium chloride and 5mM EDTA (ethylene diamine tetraacetic acid). The brain homogenate was layered on top of 2mL 30% (w/v) sucrose solution. The mixture was centrifuged using MLS-50 swinging bucket rotor at 35,000 rpm for one hour in the Optima Max ultracentrifuge (Beckman Coulter). The white myelin layer was carefully removed at the 30% (w/v) sucrose solution interface. After centrifugation myelin was diluted by ice-chilled milli Q water in a 1:1 ratio. To pellet the myelin membranes, an additional centrifugation at 35,000 rpm was performed for 30 minutes. The isolated myelin vesicles were osmotically shocked by addition of ice-chilled milli Q water and incubated on ice for 10 minutes, and followed by the subsequent centrifugation for 20 minutes at 22,300 rpm. The procedure of sucrose gradient separation and osmotic shock was repeated for better separation. Myelin pellets were resuspended in ~500 μ l of myelin storage buffer

[(500 μ l 2X TBS, 40 μ l PIC (protease inhibitor cocktail), 20 μ l 100mM Na₃VO₄, 20 μ l 100mM phenylmethane sulfonylfluoride (PMSF), 20 μ l Phos STOP (phosphatase inhibitor cocktail), 400 μ l water)]. After isolation, the concentration of myelin samples was determined using microplate procedure of bicinchoninic acid (BCA) protein assay (Pierce). All samples were read at 562 nm.

2.5.1(A) Myelin Detergent Fractionation

The myelin membrane consists of several microdomains but two microdomains, the radial component and lipid rafts, have been previously described [40]. Lipid rafts are region of plasma membrane rich in cholesterol and glycosphingolipids [40]. The membrane phase in which cholesterol and sphingolipids are rich and tightly packed is called the liquid ordered phase (L₀). This compactness creates thick, less fluid and a more ordered membrane structure. The proteins that are involved in signaling are mostly partitioned into lipid raft region [40]. The radial component is the structure within the compact myelin where closely associated cytoplasmic bilayer leaflets alternate with closely associated exofacial bilayer leaflets and radiates as a bicycle wheel spoke [41]. Radial component mostly consists of tight junctions between membrane layers, whereas the lipid rafts are a linear region within a membrane.

From most cells, lipid rafts can be isolated as detergent resistant membranes (DRMs). A detergent fractionation method can be used to separate the lipid raft microdomain from radial component in myelin. Hydrophobic proteins are difficult to separate and identify, as they are often present in cholesterol-rich microdomains (lipid rafts) of the membrane. Thus the procedure requires detergent for their purification. Detergents are chemical compounds that have both hydrophobic and hydrophilic

structure. The tails of detergent are essentially hydrophobic and the heads are hydrophilic. There are three types of such detergents: ionic, non-ionic, and zwitterionic.

Zwitterionic detergents such as CHAPS, (3-[(3-cholamidopropyl) dimethylammonio]- 2-hydroxy-1 propanesulfonate), which have head groups with both kind of charges can be used. The mechanism of action of these detergents is to disrupt the lipid-lipid and lipid-protein interactions. Due to disruptive ability of these detergents, they are considered even more efficient than non-ionic detergents. CHAPS, at 1.5% (w/v), has been used efficiently to isolate the lipid raft components from myelin membranes [42].

Being milder than ionic detergents, some non-ionic detergents are also utilized in protein extraction from myelin membranes [43]. Uncharged hydrophilic heads are the characteristic feature of non-ionic detergents such as triton X-100 (TX-100) and Tween-20. TX-100 has been used to separate the radial component of myelin sheath [44]. Sodium dodecyl sulfate (SDS), an anionic detergent, was not used in fractionation procedure due to its denaturing ability.

The overall procedure of detergent fractionation with myelin membrane is illustrated in Fig 2.2. Myelin (500 μ g) was added to 500 μ l of 2X Tris buffer saline (TBS; 50mM Tris/HCl pH 7.5, 280mM NaCl, 4mM EDTA) and 150 μ l of 1.5% (w/v) CHAPS detergent, with the final volume adjusted to 1000 μ l with water [40]. Sample mixtures were gently vortexed and subjected to 30 minute incubation on ice. Centrifugation at 5000xg for 10 minutes was done at 4°C. Supernatant was removed and called the **S1** fraction. Pellets were resuspended in 1mL of 3% (w/v) TX-100 solution and labeled as

P1. A gentle shaking was required to dissolve the pellet. Incubation of the pellet solution at room temperature was done for 30 minutes. The 2% (w/v) TX-100 was added and centrifugation was completed at 14000xg at room temperature for 15 minutes. This supernatant was labeled as **S2** and the pellet was dissolved in 1mL of 3% (w/v) TX-100 solution and labeled as **P2**. If a specific protein is present in **S1**, it may be localized in the lipid raft microdomain, whereas if it is present in **P1** and/or **P2** fraction, it may be localized in radial component of the myelin membrane.

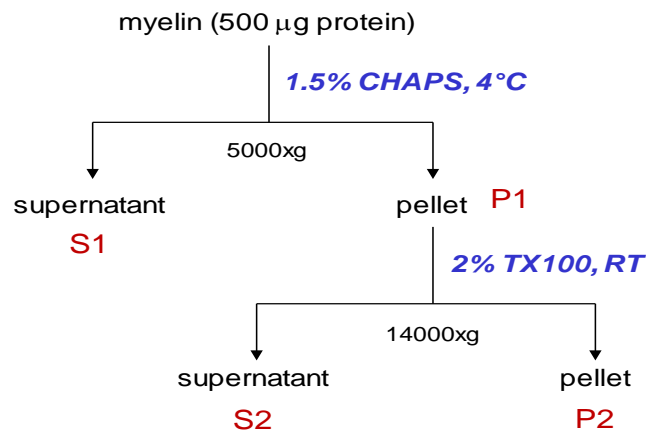


Fig 2.2: Schematic of the myelin detergent fractionation procedure. CHAPS is used to fractionate and isolate the lipid raft components from the myelin membrane, whereas TX-100 is utilized to fractionate the radial component.

2.5.1(B) Myelin Delipidation

To remove excessive lipid content for efficient electrophoresis of protein, myelin can be subjected to partial delipidation. Delipidation was achieved by treating the myelin with ether and ethanol in a 2:1 ratio. The myelin membranes (250-1000µg) were thawed on ice. The final volume was brought to 200µl by adding milli Q water. To the diluted myelin, 500µl of ether:ethanol (2:1 ratio) was added for lipid removal. Incubation of the

mixture was completed on ice for 10 minutes. Subsequently, centrifugation at 10,000xg for 10 minutes was completed at 4°C. The supernatant fraction containing the lipids was discarded. Pellets were partially air-dried, and then were dissolved in resuspension buffer (10mM Tris-HCl, pH 8.0 and 1% SDS).

2.5.1 (C) Sodium Dodecyl Sulfate-Polyacrylamide Gel Electrophoresis and Western Blotting

Once the myelin fractions were separated, 64µl of each fraction was added to 16µl of 5x sample loading buffer (0.5M Tris/HCl, pH 6.8, glycerol, 10% w/v SDS, 0.5% (w/v) bromophenol blue). Samples with loading buffer were boiled for 5 minutes which was used immediately or stored at -20°C after cooling for later usage.

The 12% and 14% resolving gels with 4% stacking gels (1mm, 8 x 7.3cm: Mini-Protean, BioRad) were used for Western blot analysis. The 10X running buffer or electrode buffer (25mM Tris/HCl, pH 8.3, 192mM glycine, 0.1% SDS) was diluted into 1:10 and ~500mL was utilized to run SDS-PAGE. Protein samples, either delipidated myelin or detergent fraction, in the loading buffer were loaded along with protein MW standards. Electric current was applied. For the first 20 minutes the applied voltage was 70V to facilitate the stacking of the proteins. After 20 minutes, the voltage was changed from 70V to 120V for an additional 80-90 minutes. After 90 minutes or when the dye front was out of the gel, the gel was disassembled and washed with transfer buffer (25mM Tris-HCl, 192mM glycine, pH 8.3, 20% methanol) for 5 minutes. Protein transfer onto the nitrocellulose membrane was accomplished by arranging the gel and membrane in the following order; fiber pad, 2 pieces of filter paper, gel, nitrocellulose membrane, 2 pieces of filter paper and at the very end fiber pad. Approximately 400-500

mL of ice-cold transfer buffer was required to fill the tank along with an ice pack. Current was set at 200mA for 2 hrs. After 2 hrs, the cassette was disassembled and nitrocellulose membrane was subjected to further western blot analysis after drying. The transfer of protein markers are indication of successful protein transfer.

For Western blot analysis, the membrane was blocked with 5% (w/v) milk solution (2.0g skim milk powder in 40 mL 1XTTBS) for 2.5-3 hrs. All antibodies and milk solutions were made in 1XTTBS solution by diluting 10XTTBS (247mM Tris, pH 7.6, 0.026M KCl, 0.137M NaCl, 0.5% (w/v) Tween-20) solution in 1:10. Two washings of one and five minutes with 1X TTBS were followed the blocking step. Subsequently, the membrane was incubated with primary antibody (concentration as provided by antibody supplier) for 1-4 hrs or more. After incubating with primary antibody, the membrane was washed once with 20mL 1XTTBS solution and for three more times each for 5 minutes. The membrane was incubated with a secondary antibody for 30-45 minutes (concentration as provided by antibody supplier). Secondary antibody incubation was followed by washing the membrane three times with 20mL 1XTTBS solution for 5 minutes. For imaging, the membrane was incubated with Super Signal West Femto reagent (Pierce) for 5 minutes as outlined by the manufacturer. Imaging was acquired immediately by a VersaDoc 4000 (Bio-Rad Ltd) system.

2.5.1 (D) Immunohistochemistry

Fluorescence microscopy images of myelin membrane proteins were acquired with a CCD camera (binning mode) attached to a 300 Nikon epifluorescent microscope. The oil immersion 100X objective was used in this study. Myelin samples were diluted

into 1:1000 by volume and applied to the glass slide. The 10 μ l of diluted sample was incubated with 40 μ l primary antibody at room temperature for 1hr. The dilution of primary antibody was provided by the supplier and was prepared in PBS buffer (5mM sodium phosphate, 137mM NaCl and 27mM KCl, pH 7.0). After incubation with the primary antibody, samples were washed three times with PBS buffer and subsequently, incubated with fluorescently tag secondary antibody for 30 minutes at room temperature. The secondary antibodies were also prepared in PBS (secondary antibody dilution as provided by the supplier). After washing with PBS, image was taken by 300 Nikon epifluorescent microscope.

2.6 Research Significance

Myelin, a multilayered sheath, not only provides integrity and insulation to the neurons but it is also metabolically active. It is still controversial that to meet its energy requirements, myelin must either be self-sufficient (utilizing the t-PMET system) or dependent on distal mitochondria. Over recent years, the theories of oligodendrocyte, astrocyte, neuron and myelin interaction for myelin energetics have emerged [4, 12, 15]. In the current research, the theory of t-PMET association with myelin membrane for its energy requirement is presented for the first time. This research project investigated the association of t-PMET with myelin membrane. The identified component's activity and expression level were measured in the demyelinated system. The role of t-PMET in health and disease will further assist in deciphering the functions of these identified enzymes and their role in demyelination.

Chapter 3

Investigation of Cytochrome b5 Reductase in the Myelin Membrane

The central theme of this chapter is to investigate the presence of cytochrome b5 reductase (CB5R) in myelin membrane through its associated activity of NADH: cytochrome c reductase. The kinetic parameters V_{\max} and K_M were determined to describe the reductase activity. Furthermore, para-hydroxymercuribenzoic acid (pHMB), a potent inhibitor of CB5R was used. Western blot analysis and immunohistochemistry were performed to confirm the presence of CB5R in myelin membrane. Lastly, detergent fractions of myelin were assayed for comparing the enzyme activity and localization in the membrane microdomains.

3.1 Introduction

Cytochrome b5 reductase (CB5R), is an NADH-dependent, FAD-containing integral membrane protein [45]. The CB5R catalyzes two coupled, single electron reductions of substrates such as Cb5 or CoQ. A pair of electrons, as hydride ion, from NADH are transferred to the flavin ring of FAD, and then from the reduced form of FAD these electrons are transferred one at a time to two molecules of Cb5. Overall, the electrons are transferred from the two electron carrier (NADH) to the one electron carrier (Cb5). The FAD can cycle from the fully reduced form of FADH⁻ to the semiquinone and then back to the fully oxidized form FAD. The catalytic mechanism is shown in Fig 3.1.

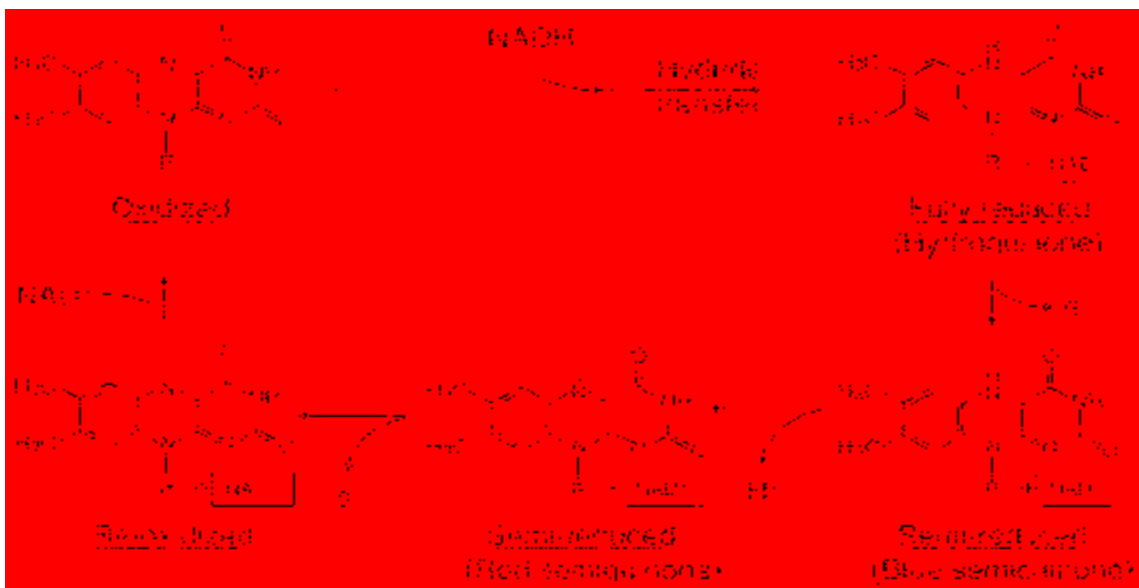


Fig 3.1: Catalytic cycle of FAD in CB5R. The two electrons are transferred via hydride transfer from NADH to the fully oxidized form of FAD to give the reduced form. One electron from FADH is transferred to the substrate (Cb5) or single electron acceptor to yield the neutral blue semiquinone which is deprotonated to the anionic red semiquinone. A second electron is transferred to another single electron acceptor. Figure taken from reference [46].

In humans, CB5R is encoded by four genes CB5R1, CB5R2, CB5R3 and CB5R4. The isoform, CB5R3 has ubiquitous expression and is present in mitochondria, nucleus, endoplasmic reticulum and plasma membrane. The CB5R3 is encoded by the gene present on chromosome number 22 and this gene is 32 kb in length (with 9 exons and 8 introns) [47]. Two isoforms of CB5R are known. One isoform is membrane-bound with a molecular weight of ~35kDa, while second isoform is soluble with a molecular weight of ~33kDa. The soluble form is mostly found in the erythrocytes [48]. The difference in two forms lies in their N-termini. In membrane-bound form, the N-terminus is myristoylated and hydrophobic. This hydrophobicity of the chain facilitates the enzyme insertion into the membranes. The soluble form is produced by the alternate splicing of membrane-bound form [48, 49].

The X-ray crystallographic studies have resolved the enzyme fold and structure. Overall, the enzyme consists of two functional lobes (Fig 3.2A). The prosthetic group, FAD, binding site is present on N-terminus lobe. This FAD binding domain (Lys33-His144, in the human sequence) consists of six antiparallel β -strands [36]. The NADH binding site lies in the C-terminus lobe (Gly171- Phe300) and has an $\alpha\beta$ motif. The N-terminus and C-terminus lobes of enzyme is linked by a small peptide, which is a short random coil of 25 amino acids [36]. This short random coil acts as a hinge and is thought to facilitate the efficient transfer of electron from NADH to FAD by holding their binding sites in close proximity to one another (Fig 3.2B) [50].

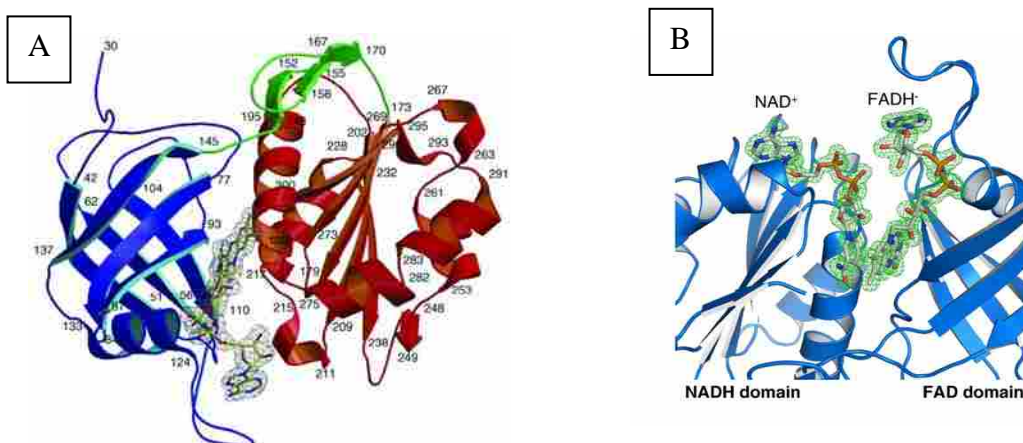


Fig 3.2: Overall structure of human CB5R. Panel (A): FAD binding domain is in blue, while NADH binding domain is in red. The linker domain is in green. Adopted from reference [46]. **Panel (B):** Interface of NADH and FAD domains. Adopted from reference [53].

The distance between the FAD binding domain and NADH binding domain is $\sim 11\text{\AA}$ [36]. How is efficient electron transfer facilitated? A highly conserved flavin-binding sequence is present in FAD domain. This region contains the residues Arg63, Tyr65 and Thr66 in porcine liver. The amino acid residue Thr66 is thought to be responsible for electron transfer from FAD ring and destabilizes the FAD molecule. The NAD^+ molecule is confined in the cavity between NADH- and FAD-domains and

interacts with the surrounding atoms in the enzyme. The NAD^+ is distorted and acquires an "L-shaped" conformation [46]. The adenine ring stacks itself parallel to the aromatic ring of Phe223 in the groove. This groove is created by Phe223, Pro247, Pro249 and Met250. To superimpose the NADH binding domain over FAD domain, almost a $30\text{-}40^\circ$ twist is required for proper orientation of two binding domains. This orientation is usually acquired by the water-mediated lateral movement of FAD binding domain.

One of the most important functions of CB5R in plasma membrane is to reduce the CoQ. This reduced pool of CoQ prevents lipid peroxidation and protects the cell from oxidative stress [51, 52]. CB5R is also involved in fatty acid chain elongation and desaturation. Cholesterol synthesis is another well described function of CB5R [53]. CB5R can regenerate some antioxidant molecules such as ascorbate (Asc) and α -tocopherol [54]. The major function of the soluble form of enzyme in erythrocytes is to reduce methemoglobin back to hemoglobin as shown in the Fig 3.3 [55].

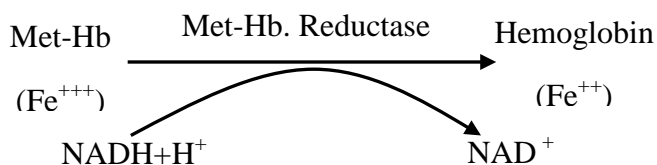


Fig 3.3: Reduction of hemoglobin by non-myristolated CB5R form. Methemoglobin is reduced to hemoglobin by soluble form of CB5R while the NADH is utilized as an electron donor source. CB5R is also known as methemoglobin reductase.

The metabolic disease associated with the deficiency of CB5R is called methemoglobinemia. There are two types of this deficiency. Type I involves the deficiency of soluble form of CB5R in red blood cells. In this type of disease, a well-

tolerated cyanosis with mild symptoms of headache, fatigue and shortness of breath is observed [56]. Type II is even more severe than type I, and in type II, deficiency of both forms is observed in red blood cells as well as in leukocytes. The patients with type II deficiency have severe neurological disorders due to inefficient desaturation of fatty acids [56].

3.2 Materials and Methods

The methods and materials used for the experimentation with their manufacturer are listed below:

Myelin (see section 2.5.1), cytochrome c (Sigma 7752), para-hydroxymercuribenzoic acid (pHMB) (Sigma 55540), TX-100 (Sigma t-9284), Tris (Bio-basic 77-86-1), β -NADH (Sigma N6005), KCN (Sigma 60178), CHAPS (Sigma C-5070), SDS (Sigma L-4390), ethanol (BDH B10324-78), ether (EMD Ex-194-6), potassium chloride (KCl; Sigma 4504), sodium chloride (NaCl; Sigma C-3014), Tween-20 (Bio-Rad 161-0781), Dual Colour Precision Plus protein standards (Bio-Rad 161-0374), goat anti-CB5R antibody (Pierce PA5-19196), rabbit anti-goat IgG-HRP secondary antibody (Sigma A-5420), Super Signal West Femto reagents (Thermo scientific 34094), ammonium persulphate (MP biomedical 802829), tetramethylethylenediamine (TEMED) (Bio-Rad 161-0800).

3.2.1 Western Blot Analysis and Immunohistochemistry

For the SDS-PAGE separation, a 14% resolving gel with 4% stacking gel was prepared for the investigation of CB5R in brain homogenate, S1 fraction and delipidated

myelin sample. Myelin fractionation and delipidation was achieved by following the protocol described in section 2.5.1(A & B) in detail. Gels were loaded with final volume of 16 μ l of delipidated myelin, 20 μ l of S1 detergent fraction, along with the 5X sample loading buffer and 10 μ l of 1:10 dilution brain homogenate, 20 μ l of 1:50 dilution brain homogenate. Gel was loaded with 5 μ l of 1:10 dilution of Dual Colour Precision Plus protein standard. The complete conditions of SDS-PAGE and Western blotting are outlined in section 2.5.1 (B). For Western blots, membranes were blocked with 5% (w/v) milk solution for 3 hrs. Subsequently, the membrane was incubated with 3mL of primary antibody (goat anti-CB5R at a 1:500 dilution) in 1XTTBS solution for 5hrs. After washing, membrane was incubated with secondary antibody (anti-goat IgG-HRP) for 30 minutes at a 1:80,000 dilution.

Immunofluorescence was done according to the procedure described in section 2.5.1(D). Myelin was diluted in a 1:1000 applied to the slide. The 10 μ l of diluted myelin sample was incubated with primary (goat-anti-CB5R) antibody for 1 hrs at room temperature. The primary antibody was prepared in the dilution of 1:200. After washing 3 times with PBS solution membrane was incubated with secondary fluorescent antibody Dylight 549 in 1:500 dilution for 30 minutes at room temperature. After washing, images were taken from Nikon epifluorescence microscope.

3.2.2 NADH Dependent Cytochrome c Reductase Assay

The rate of change of cytochrome c reduction by CB5R was monitored spectrophotometrically by using 96-well microplate format [57]. A total volume of 200 μ l was used for each well and reaction is initiated by the addition of electron donor NADH. Sample blanks, containing no enzyme, were run in the same manner.

The activity was determined essentially as described by Navas and co-workers [57]. The reaction mixture contained 50mM Tris/HCl buffer pH 7.6 with 0.5% (w/v) TX-100, 10-30µg protein (myelin), substrate cytochrome c from 50-600µM and 250µM NADH. Enzyme activity was determined by monitoring the enzyme-dependent increase in absorbance at 550nm for 5 minutes at the intervals of 20-40 seconds at 37°C. For inhibition studies, different concentrations up to 10µM of pHMB were used. The 20mM stock solution of pHMB was prepared by dissolving 0.036g pHMB into 5mL milliQ. The activity was expressed as $\Delta\text{Abs}/\text{min}$ or micromoles of cytochrome c reduced per minute using an extinction coefficient of $29.5\text{mM}^{-1}\text{cm}^{-1}$.

3.2.3 Methodology of Detergent Fraction Assay

For detergent fractionation, the myelin was treated as the procedure described in section 2.5(A). The overall procedure of the detergent fraction assay was similar as described in section 3.2.2 with only exception that 1.5% (w/v) CHAPS supernatant and pellet (S1, P1) were assayed with supernatant and pellet of 2% (w/v) TX-100 (S2, P2). The assay mixture contained 50mM Tris/HCl buffer pH 7.6 with 0.5% (w/v) TX-100, 50µl of each detergent fraction, 100µM of cytochrome c and 250µM NADH. For controls, 20µg of myelin was used instead of detergent fractions. Total volume in well was made up to 200µl by addition of water. The activity was measured as described above. The enzyme activity in myelin was compared with the activities in different detergent fractions (S1, S2, P1 and P2).

3.2.4 Kinetic and Statistical Analysis

For kinetic analysis, online curve and surface fitting resources from zunzun.com (least square fit model) were used to estimate the V_{\max} and K_M parameters of CB5R with cytochrome c substrate. Statistical analysis was performed using Microsoft Excel 2010. T-tests were used for all analysis including the myelin dose response, substrate dose response and on inhibition test. Statistical significance was established at $p \leq 0.05$ at 95% confidence level.

3.3 Results and Discussion

Borgese *et al.* determined the sub-cellular localization of CB5R using radioimmunoblotting analysis in rat liver, and found that CB5R is present in smooth microsomes, Golgi bodies, lysosomes, the plasma membrane and the outer membrane of mitochondria [58]. In this current study, Western blot analysis and immunohistochemistry identified the CB5R in the myelin membrane (see Fig 3.4). In Fig 3.4A, immunohistology of CB5R confirmed the enzyme localization in myelin membrane. To further investigate the distribution within the membrane, Western blot analysis was performed on the detergent fractions (Fig 3.4B). CB5R was present in the S1 fraction, whole myelin, and in brain homogenates (see Fig 3.4B). The blot also showed that CB5R is expressed in two isoforms; one with a molecular weight of ~35kDa which may represent the form bound to membrane while the other isoform with molecular weight of ~33kDa which may represent the form lacking myristoylated region.

The myristoylation confers hydrophobicity to the protein and facilitates the insertion of the protein into the membrane. The form lacking the myristoylated moiety

still may be associated with the myelin membrane, and thus be a tightly bound peripheral membrane protein either through various protein-protein or lipid-protein interactions. Another possibility is that the non-myristoylated form was produced as a degraded product of CB5R membrane bound form. The non-myristoylated form as a peripheral membrane protein might be an additional system for reduction of CoQ pool to avoid lipid peroxidation and ascorbate regeneration. Previous studies demonstrated that both the non-myristoylated (soluble) and myristoylated form (membrane-bound), were detected in cultured neurons, whereas the membrane-bound form was only detected in synaptic plasma membrane vesicles [59].

The detection of CB5R in the S1 fraction indicates that the enzyme may be localized in the lipid raft microdomain. Further separation of this fraction on a sucrose buoyant density gradient would confirm this [41]. Samhan *et al.* found evidence that CB5R is present in lipid rafts and is associated with caveolin-rich regions of plasma membrane of neuronal cells [60]. Caveolin is the most abundant protein in the caveolae microdomain and controls the cholesterol trafficking.

A



B

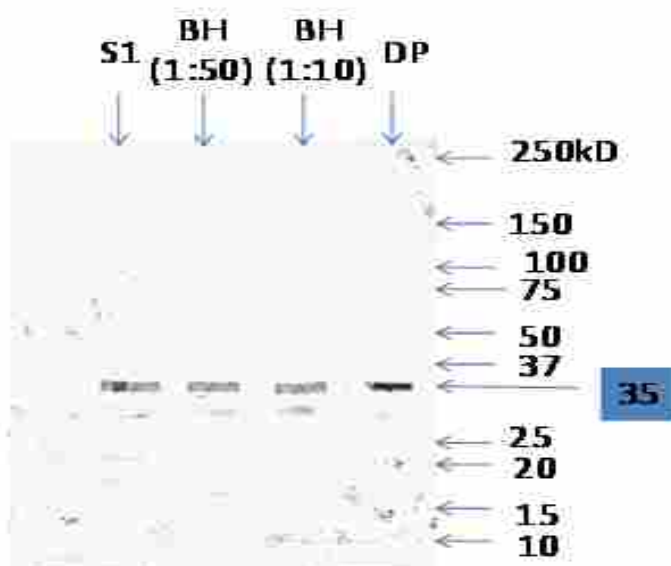
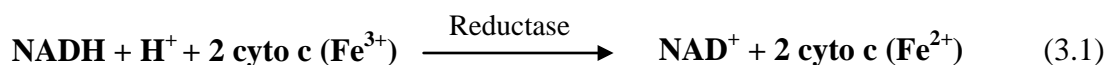


Fig 3.4: Immunodetection of CB5R in the myelin membrane. Panel (A): Immunofluorescent image of CB5R in myelin membrane. Diluted myelin (1:1000) was incubated with cytochrome b5 primary antibody in 1:200 dilution for one hour and after washing subsequently incubated with secondary antibody anti-goat DyLight 549 in a 1:500 dilution for 30 minutes. Image was taken with 100X oil immersion lens and with Nikon 300 epifluorescent microscope. **Panel (B): Western blot for cytochrome b5 reductase.** A 14% resolving gel with 4% stacking gel was prepared for the examination of CB5R in brain homogenate (BH), S1 fraction and delipidated myelin sample (DP). Proteins were transferred to nitrocellulose membrane at 200mA for 2 hrs. Membrane was blocked with milk solution and then subsequently incubated with primary and secondary antibodies. For enhanced chemiluminescence, ECL substrate was used and immediately after that image was taken with the 4000 VersaDoc imaging system.

3.2 Measurement of Cytochrome b₅ Reductase Activity in Myelin Membrane

The endogenous substrates of CB5R enzyme are cytochrome b₅ (Cb5) and CoQ. Recombinant Cb5 is available commercially but it is cost prohibited. High levels of Cb5 are found in liver cells but its extraction from liver is difficult [57]. In cells, the reduction of Cb5 is essential, as it is a key player in cholesterol synthesis [61]. For experimental purposes, an analog of Cb5, cytochrome c, is extensively used. The CB5R activity is determined spectrophotometrically as the NADH-dependent reduction of cytochrome c and also quantified with the inhibitor pHMB [62]. The measurement of cytochrome c reduction was taken at 550nm as it is the wavelength at which cytochrome c (reduced form) shows maximum absorption. The enzyme activity was determined by following the reduction of cytochrome c with the electron donor, NADH. Hence, by measuring the rate of reduction of cytochrome c, the CB5R activity can be estimated. Following reaction is catalyzed by CB5R. Moreover, the standard electrode potential E° (235mV) of cytochrome c ($\text{Fe}^{3+}/\text{Fe}^{2+}$) oxidized form is fairly large (positive value) and thus the ferrous form readily to accepts an electron [63].



The enzymatic activity of CB5R in myelin membrane was measured by the associated activity of cytochrome c reductase. A typical rate of reaction of cytochrome c reduction with the myelin membrane is illustrated in Fig 3.5. The slope (change in absorbance/min) and enzyme activity were calculated as described in section 2.4.1. All slopes were corrected for the background (negative control without enzyme).

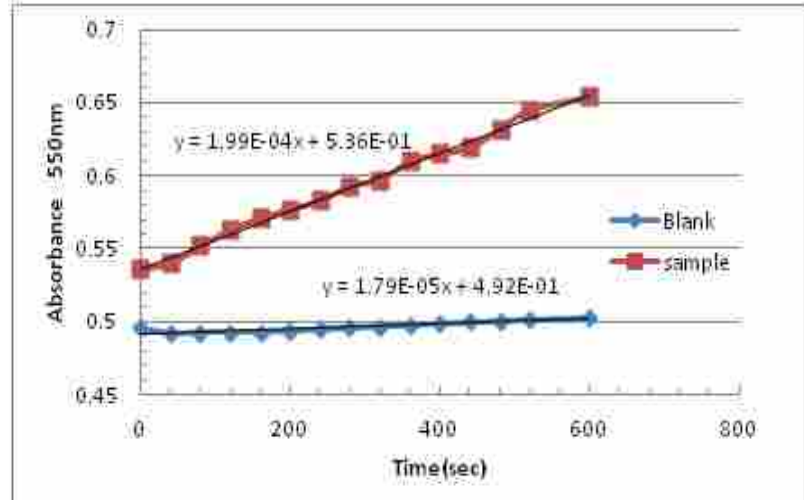


Fig 3.5: A typical graph depicting cytochrome c reductase activity. Rate of change of cytochrome c reduction was determined by plotting the absorbance versus time. Same procedure was used for blanks as well. Sample contains myelin, water, buffer, cytochrome c and NADH. The blank (negative control) contains no myelin.

3.5.1 Enzyme Assay with Myelin Detergent Fractions

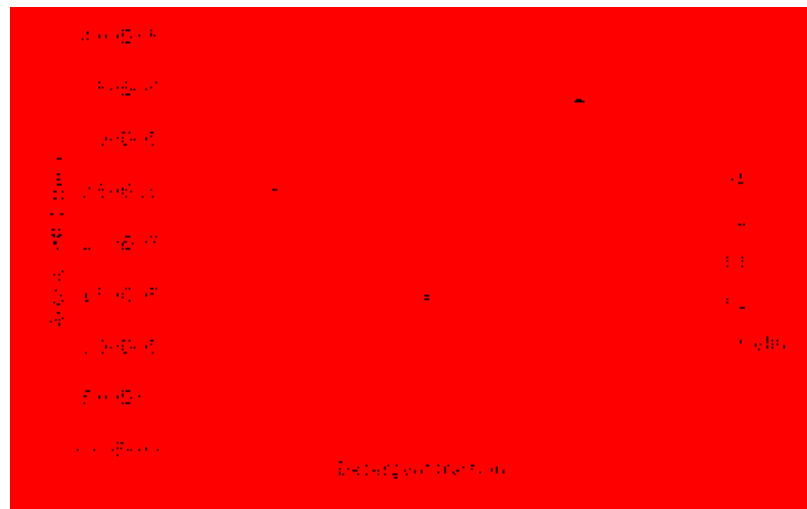


Fig 3.6: Comparison of myelin detergent fractions for NADH:cytochrome c reductase activity. The activity of enzyme in non-treated myelin is taken as the control. The rate of each fraction (50 μ l) and myelin (20 μ g) was assayed in the presence of 100 μ M of cyto c and 250 μ M NADH at 37 $^{\circ}$ C over 5 minutes (see methods for complete details). All error bars are \pm SE.

The enzyme activity in whole myelin sample was compared to the different myelin detergent fractions (see Fig 3.6). On an equi-volume basis, the highest activity was observed in the S1 fraction ($2.44 \times 10^{-4} \mu\text{M}/\text{min}$) and the lowest activity was in the P2 fraction ($1.37 \times 10^{-7} \mu\text{M}/\text{min}$) and thus, most of the CB5R associated activity is distributed into the CHAPS supernatant fraction. This also supports the findings of Western blot. The enzyme activities in detergent fractions, other than S1, can be seen. These activities might be due to the presence of other reductases, oxidases or dehydrogenases.

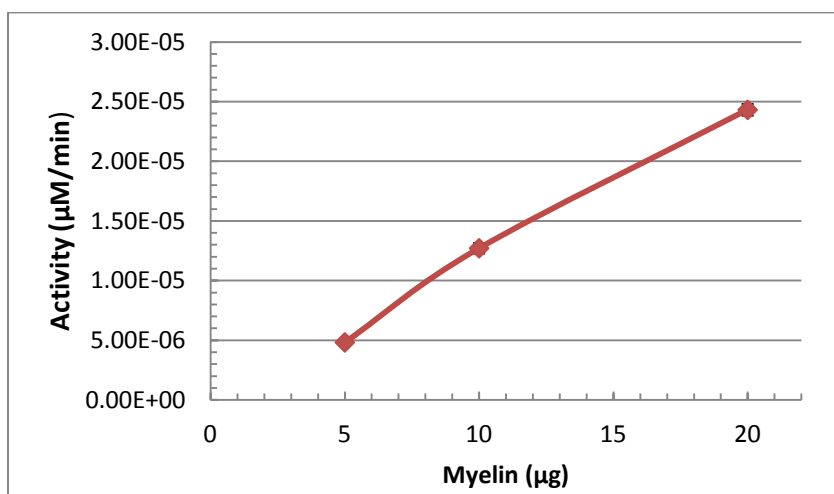
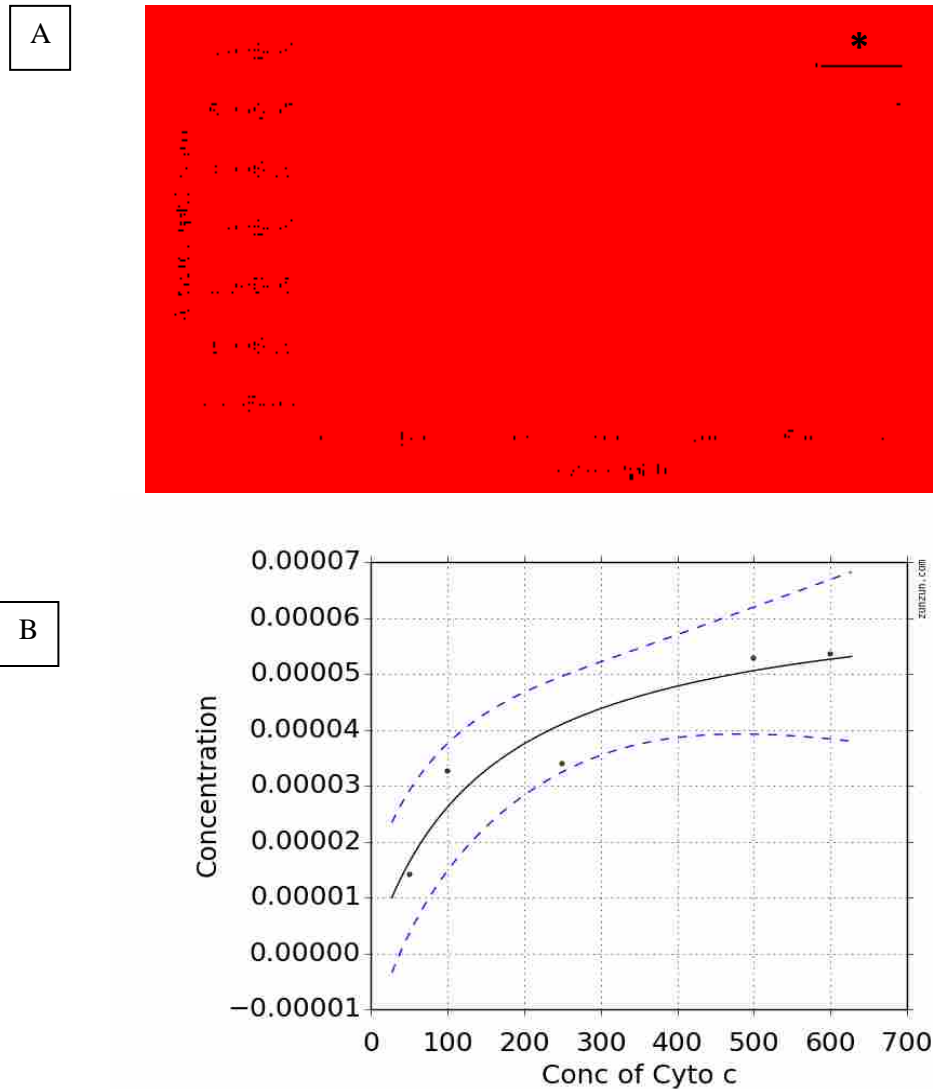


Fig 3.7: NADH: cytochrome c reductase activity as a function of amount of myelin. 50mM Tris-HCl buffer pH 7.6 with 0.5% (w/v) TX-100, was assayed with 5, 10, 20 μg myelin, 100 μM cytochrome c and 250 μM NADH. Measurement was taken spectrophotometrically at 550nm at 37°C. Results are produced in duplicate and corrected for background. The error bars are \pm SE (standard error).

Further characterization of NADH: cytochrome c reductase activity was completed with whole myelin. Fig 3.7 illustrates that the enzyme activity is directly proportional to the amount of protein added. Thus the NADH: cytochrome c reductase activity is a function of myelin concentration. Dose response of myelin also shows that enzyme(s) is in active form.

Enzyme activity at various substrate concentrations is very important in determining enzyme steady-state kinetics model. An evaluation of the dose response of the substrate, cytochrome c, was done to generate the kinetic curve (see Fig 3.8).



3.8: NADH: cytochrome c reductase activity as a function of amount of substrate. Panel (A) Enzyme activity in myelin. 50mM Tris/HCl buffer pH 7.6 with 0.5% (w/v) TX-100, was assayed with 20 μg myelin, 50, 100, 250, 500 and 600 μM cytochrome c and 250 μM NADH. Measurements were taken spectrophotometrically at 550nm at 37 $^{\circ}\text{C}$. Results are produced in duplicate and corrected for background. The error bars are \pm SE (standard error). The t-test results indicate no statistical significance (*p=0.35) of more than 95% confidence interval in increase in enzyme activity between 500 and 600 μM of cytochrome c concentration. **Panel (B)** Data fitted with kinetic software (zunzun.com) to determine apparent K_M and V_{max} . The solid line shows the data, whereas dashed line depicts the 95% CI.

Substrate dose response curve showed that enzyme follows a hyperbolic curve representing the typical Michaelis Menten model. At 600 μ M, the enzyme is saturated with substrate and reaches at its maximum rate V_{\max} and reaction follows the zero order kinetics and becomes independent of amount of substrate added. The kinetic parameters, V_{\max} and K_M were estimated as 6.59×10^{-5} μ M/min and 151 μ M, respectively.

Enzyme inhibitors are important in studying metabolic reactions and pharmacological modeling. Some physiological inhibitors as well as artificial inhibitors are well known and are used in drugs. Typically in kinetic studies of an enzyme, the assays are validated when a potent inhibitor reduces the specific enzymatic activity. The myelin samples were exposed to progressive increasing concentration of pHMB (see Fig 3.9), which is a well-known competitive reversible inhibitor of CB5R enzyme [57].

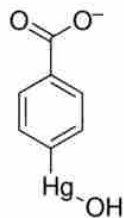


Fig 3. 9: Structure of pHMB. Para-(hydroxymercuribenzoate (pHMB) also known as 4-(hydroxymercurio)benzoate forms mercury-sulfur covalent bond with thiol group of cysteine residues.

Organic mercurial compounds such as pHMB and para-chloromercuribenzene sulfonate (pCMBS) reacts with cysteine sulfhydryl groups. The pHMB is relatively hydrophobic in nature and can partition into the membrane, reacting with more "buried" sulfhydryl groups. In contrast, pCMBS can react only with "exposed" sulfhydryl groups.

A myelin sample without inhibitor was used as the control and considered as having 100% oxidoreductase activity (see Fig 3.10). The cytochrome c reductase activity was significantly decreased by increasing concentration of the inhibitor, pHMB. At 10 μ M of pHMB the enzyme activity was over 90% inhibited. In addition, 50% inhibition (IC_{50}) of enzyme activity was achieved by 1 μ M pHMB. Enzyme activity assay of cytochrome c reductase and pHMB-mediated inhibition is another confirmation of presence of CB5R enzyme in myelin membrane. In human CB5R, four cysteine residues (Cys203, Cys273, Cys283 and Cys297) are present. Among four residues, two residues, Cys273 and Cys283 are located near the NADH binding domain. The Cys273 plays a vital role in the electron transfer and also aids in maintaining the native conformation of the protein [64].

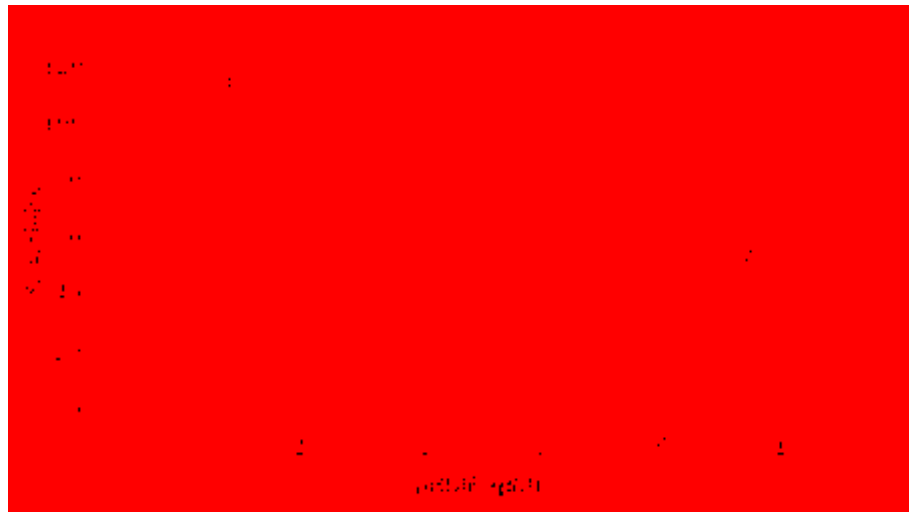


Fig 3.10: Inhibition of cytochrome c reductase activity by pHMB. Measurements were taken at 550nm at 37°C. Results are produced in triplicates and corrected for background. The 20 μ g myelin was assayed with 100 μ M cytochrome c and 250 μ M NADH. The error bars are \pm SE. The t-test results indicate a statistical significance of more than 95% between 0 and 0.1 μ M (* $p=0.01$) and between 5 and 10 μ M pHMB (** $p= 0.04$).

Since it was established that CB5R is present in myelin membrane, it is now necessary to differentiate the detected activity from mitochondria to ensure that activity is at the level of plasma membrane. To achieve this purpose, potassium cyanide (KCN) was used. Cyanide is a potent inhibitor of cellular respiration, acting on mitochondrial cytochrome c oxidase (complex IV), by blocking the electron transfer, inhibits the oxidative phosphorylation. A previous study showed that 1.0mM of KCN inhibits 70% activity of cytochrome c oxidase in mitochondria [65]. Effect of KCN inhibition on CB5R is depicted in Fig 3.11. The cytochrome c reductase activity in the myelin membrane is insensitive to the inhibitor KCN. In addition, the insensitivity to KCN shows that cytochrome c reductase activity is at the level of plasma membrane and there is no mitochondrial contribution or contamination.

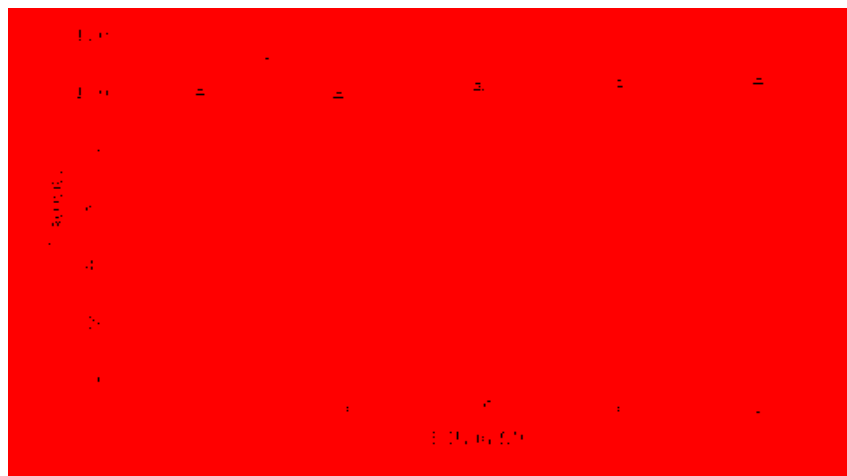


Fig 3.11: Attempted inhibition of cytochrome c reductase activity by KCN. The activity of 10 μ g myelin was assayed with 50mM Tris buffer, 100 μ M cytochrome c and various concentrations (0, 0.1, 0.5, 2.0 mM) of KCN. Reduction of activity is monitored for 5 minutes at the interval of 20 second at 550nm. Reactants were allowed to react at 37 °C. Results were produced in triplicate and corrected for non-enzymatic activity. The error bars are \pm SE. The t-test results indicate a statistical significance of more than 95% confidence. The value of t-test is *p = 0.438.

3.6 Conclusions

In this study, for the first time, the presence of t-PMET enzyme, CB5R, was detected in myelin membrane. CB5R is present in functional enzymatic form and may be localized to the lipid raft domain. The CB5R activity was measured with an assay utilizing the NADH-dependent cytochrome c reduction. The substrate dose-response curve revealed that enzyme follows the Michaelis Menten model and their kinetic parameters V_{\max} and K_M were estimated as $6.59 \times 10^{-5} \mu\text{M}/\text{min}$ and $151\mu\text{M}$, respectively. The enzyme activity was 90% inhibited with $10\mu\text{M}$ pHMB. Furthermore, both the myristoylated and non-myristoylated enzyme are associated with the myelin membrane. The function(s) of the isoforms of CB5R in myelin remains to be elucidated. The confirmed presence of CB5R in myelin membrane supports the hypothesis that t-PMET is assisting myelin membrane.

CHAPTER 4

Investigation of NAD(P)H: Quinone Oxidoreductase 1 (NQO1) in the Myelin Membrane

In the following chapter, a study was conducted to investigate the presence of NQO1 enzyme and its associated activities in the myelin membrane using various substrates such as menadione, dichlorophenol indophenol (DCPIP) and phenazinium methyl sulfate (PMS). To examine enzyme specificity, various inhibitors such as DPI, pHMB and the potent inhibitor of NQO1, dicoumarol, were used. The NQO1 presence was also verified with immunohistochemistry and Western blotting.

4.1 Introduction

NAD(P)H: quinone oxidoreductase 1 or NQO1, previously known as DT-diaphorase and quinone reductase, is a flavo-homodimeric protein and it catalyzes the two electron reduction of various quinones and quinone imines. Each subunit has a predicted molecular weight of 30kDa. In humans, the NQO1 gene is located on the 16th chromosome and is ~20 kb in length [66, 67]. NQO1 can utilize, NADH or NADPH, both as an electron donor. In erythrocytes, NQO1 has electron donor preference for NADPH [68, 69]. The localization of NQO1 within the cell is dependent on the cell type and the function of this enzyme in this particular cell [70]. Ross *et al.* described the enzyme's presence in the nucleus; however, under oxidative stress, through an unknown

mechanism, the enzyme can be translocated to the plasma membrane [70]. Other researchers described the NQO1 as a cytosolic protein but the presence in the nucleus, mitochondria and plasma membrane has been confirmed [17].

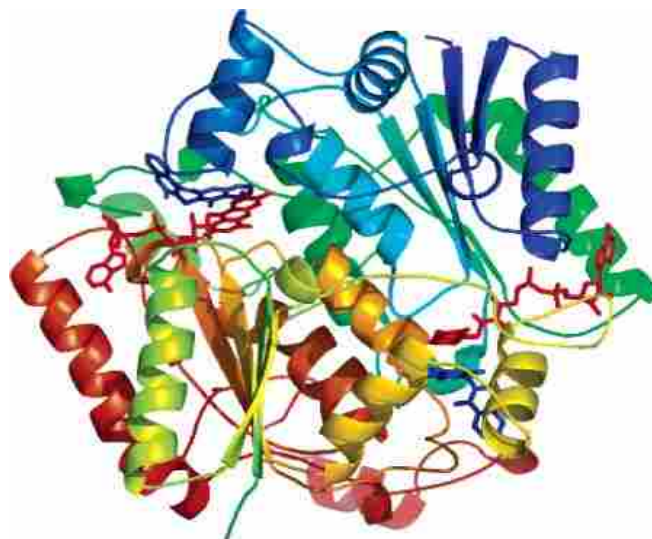


Fig 4.1: Structure of the human NQO1 enzyme. The two different lobes are represented by the two different colours. The FAD binding domain is at the interface of the dimers. Figure taken from reference [71].

This homo-dimeric flavoprotein has its catalytic site at the dimer interface. Each monomer subunit consists of 273 amino acid residues and its own prosthetic group, FAD [72]. Each monomer contains two domains; a catalytic N-terminus domain which is larger and comprised of 1-220 amino acid residues, and the small C-terminus domain from residues 221-273 (Fig 4.1) [72]. The one side of the catalytic pocket is formed by FAD-binding domain while other side of the wall is formed by the residues of the larger domain [68, 73]. The amino acid residues Tyr155 and His161, (in the human sequence) are present in the active site (Fig 4.2). The NQO1 enzyme is capable of metabolizing a wide range of substrates. Due to this ability of the enzyme, the binding site of substrate can accommodate a large variety of ring containing compounds and the enzyme shows an induced-fit model [72].

NQO1 catalyzes the two-electron transfer from NAD(P)H to FAD and then from FADH₂ to a quinone (for example, CoQ) by a ping-pong mechanism [72]. The nicotinamide ring of NAD(P)H stacks parallel to the FAD isoalloxazine ring and facilitates the efficient transfer of electrons. The donor, NADH, in the form of NAD⁺ is released after transferring electrons. Then the quinone binds to the enzyme, and it becomes reduced and released. Dicoumarol is a potent competitive inhibitor of NQO1 enzyme. Dicoumarol interacts with FAD, and prevents NAD(P)H binding [71]. The schematic of the catalytic mechanism is shown in Fig 4.2. In the enzyme, the NADPH binding site and quinone binding site are overlapping.



Fig 4.2: A proposed catalytic mechanism of human NQO1. NADH donates its electron to the FAD prosthetic group. The electrons from FADH₂ are transferred to the substrate CoQ. In the active site, Tyr and His acts as a proton/acceptor. Figure from reference [17].

One of the major functions of NQO1 in the plasma membrane is cellular defence, by reducing the pool of CoQ. CoQ is also an endogenous physiological substrate of NQO1 and the other endogenous substrates are unknown [74]. NQO1 reduces the CoQ by a two electron reduction, thus avoiding the formation of the semiquinone and subsequently, O_2^- and H_2O_2 formation [75]. In addition, NQO1 also demonstrates superoxide scavenging activity [76]. Another important function of the enzyme in the plasma membrane as well as in other localizations is the detoxification of xenobiotics [68, 77]. Moreover, enzyme is involved in stabilizing the p53 gene product [78]. The functions of NQO1 are summarized in Fig 4.3.

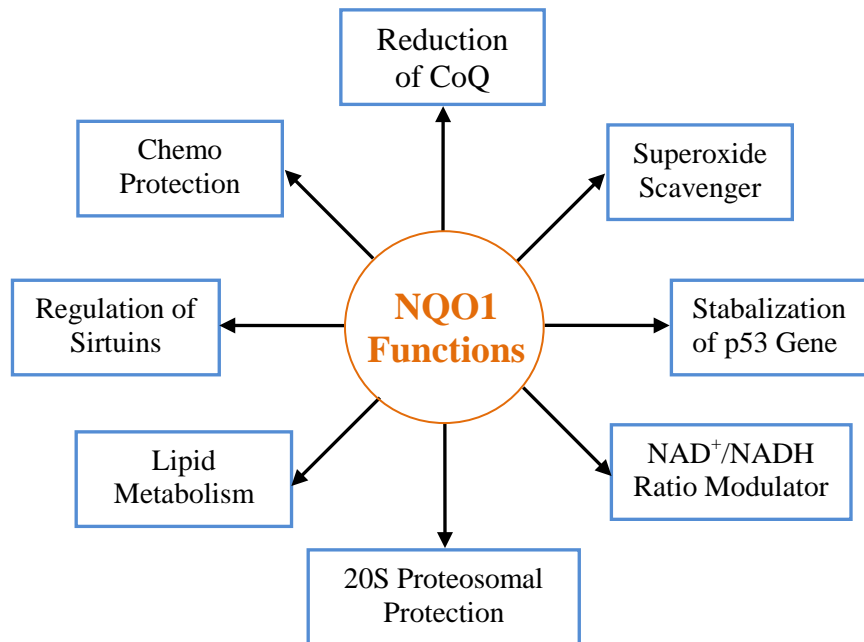


Fig 4.3: Schematic of functions of NQO 1 enzyme. Important functions of NQO1 enzymes are modulation of electron donor ratios, protection from proteasomal attack and reduction of CoQ. Some functions are tissue specific.

4.2 Materials and Methods

The reagents and materials used for the experimentation with their supplier and product number are listed below:

Myelin from mouse brains (see section 2.5.1), Tris (Bio-Basic 77-86-1), menadione (2-methyl-1,4-naphthoquinone; Sigma M5625), DCPIP (2,4-dichlorophenol indophenol; Sigma 33125), dicoumarol (3,3'-methylene-bis(4-hydroxycoumarin); Sigma M-1390), DPI (diphenyliodonium chloride; Santa Cruz sc-202584), pHMB (Sigma 55540), dimethyl sulphoxide (DMSO) (Fisher Scientific Co. BPB231), cytochrome c (Sigma 7752), rotenone (Sigma R8875), KCN (Sigma 60178), chloramphenicol (Sigma C0378), rabbit anti-NQO1 antibody; Pierce), mouse anti-rabbit IgG-HRP secondary antibody (Sigma A0545), super-signal West Femto reagent (Thermo Scientific).

4.2.1 Enzyme Activity Assays

The NQO1 activity was measured by three related activities; menadione-mediated cytochrome c reductase activity, PMS-mediated WST-1 reductase and DCPIP reductase activity. In all of these activities, NADH or NADPH is utilized as an electron donor. The general procedure of enzyme assay was the same as described in section 2.3. All three procedures for measuring enzyme activities are described below:

(A) Menadione-Mediated Cytochrome c Reductase Activity

Myelin protein (20-40 μ g) was assayed with 10 μ M menadione, 70 μ M cytochrome c and 250 μ M NADH, in final concentration. The buffer was 50mM Tris/HCl, pH 7.6 with 0.1% TX-100. Total volume in the well was 200 μ l and adjusted with the milli Q

water. The various concentrations of inhibitors dicoumarol (0, 50, 100, 500 μ M) and DPI (0, 10, 50, 100 μ M) were used. Measurements were taken at 550nm, at 37°C and monitored for 5 minutes at the kinetic interval of 20 seconds. The extinction coefficient of reduced cytochrome c at 550nm was taken as 29.5mM⁻¹cm⁻¹ [79].

(B) PMS-Mediated WST-1 Reductase Activity

Water soluble tetrazolium generation 1 (WST-1) is another diagnostic tool used to measure the NQO1 activity [80]. An intermediate electron carrier, PMS, is also used in conjunction with WST-1. The activity was measured as reduction of WST-1 increase in absorbance at 37°C for 15 minutes at an interval of 30 seconds. The extinction coefficient of the reduced formazan at 438nm was taken as 37 mM⁻¹cm⁻¹ [80].

The assay mixture consists of 100mM potassium phosphate, 2mM EGTA buffer (pH 7.0), 200 μ M of NADH, 20 μ M PMS and 10 μ g myelin. To initiate the reaction 300 μ M of WST-1 was added to the mixture. To determine the specificity of the activity, various concentrations of dicoumarol (0, 10, 20, 50 and 100 μ M) were used.

(C) DCPIP Reductase Activity

The same method as described previously was used to measure the DCPIP reductase activity [81]. The myelin (20-40 μ g) was assayed with increasing concentrations (0-600 μ M) of DCPIP. NQO1 activity was measured with or without the addition of FAD. To measure the activity with FAD, 5 μ M of FAD was used. The following inhibitors were tested: dicoumarol (0, 10, 25, 50, 75, 100, 250, 500 μ M) prepared in DMSO or in 0.1N NaOH, DPI (0, 10, 100, 500 μ M) 30mM stock solution in DMSO, pHMB (0, 1, 5, 10, 50, 100 μ M) 20mM stock solution in water, KCN (0, 3, 5, 10, 50 μ M) 10mM solution in

water, chloramphenicol (0, 50, 100, 200, 400, 500 μ M) 10mM in DMSO, rotenone (0, 20, 50, 100, 500 μ M) 10mM solution in DMSO and DMSO (w/v) (0, 2.5, 5, 7.5, 10, 17.5%) were used. The structures of these inhibitors are drawn in Table 4.1. The buffer contained 25mM Tris/HCl, pH 7.4, 0.01% (w/v) Tween-20 and 0.07% (w/v) BSA in final concentration. To initiate the reaction, 200 μ M of NADH was added. Activity was measured as a decrease in absorbance at 600nm, at 37°C and monitored for 5 minutes at 20-40 seconds interval. The extinction coefficient of oxidized form of DCPIP at 600nm was taken as 21.0 mM⁻¹ cm⁻¹ [81].

4.2.2 Measurement of Reductase Activity in Detergent Fractions

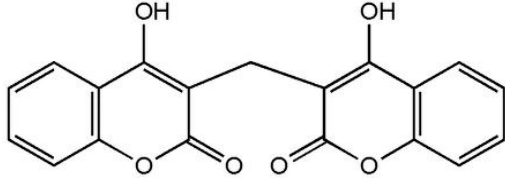
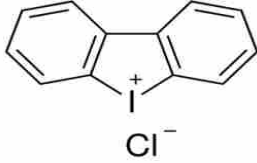
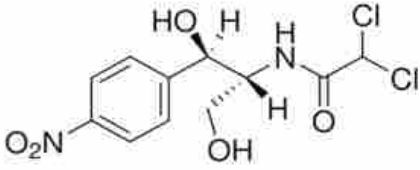
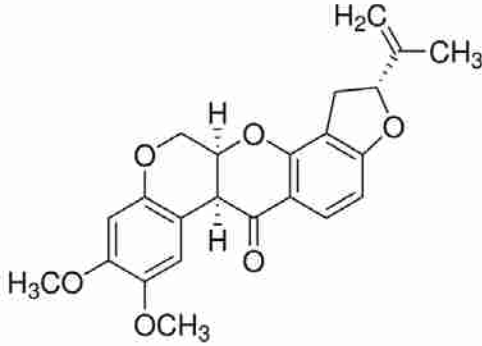
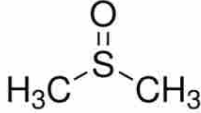
For detergent fractionation, myelin was treated as the procedure described in section 2.5.1(A). The menadione-mediated cytochrome c reductase assay was conducted with the 1.5% (w/v) CHAPS supernatant (S1) and pellet (P1) and the 2% (w/v) TX-100 supernatant (S2) and pellet (P2). The assay mixture contained 50mM Tris/HCl buffer (pH 7.6 with 0.5% TX-100), 50 μ l of each detergent fraction, 100 μ M of cytochrome c and 250 μ M of NADH. For the positive control, 20 μ g of myelin was used instead of detergent fractions. The total volume in the well was made up to 200 μ l by addition of water. The enzyme activity in myelin was compared with the activities in different detergent fractions (S1, S2, P1 and P2).

4.2.3 Western Blot Analysis and Immunohistology

For the SDS-PAGE separation, a 14% resolving gel with 4% stacking gel was prepared for the investigation of NQO1 in the brain homogenate and detergent fraction

samples (S1, S2, P1 and P2). The procedure of SDS-PAGE and Western blotting was followed as outlined in section 2.5.1(C). Gels were loaded with final volume of 20 μ l of

TABLE 4.1: Chemical structures of used inhibitors. Inhibitors analogue to NAD(P)H are shown with their chemical structure.

INHIBITOR	CHEMICAL STRUCTURE
Dicoumarol	
Diphenyleneiodonium	
Chloramphenicol	
Rotenone	
Dimethyl sulphoxide	

each detergent fraction, along with the 5X sample loading buffer and 10 μ l of 1:10 dilution brain homogenate, 20 μ l of 1:50 dilution brain homogenate. Gels were loaded

with 5µl of 1:10 dilution of Dual Colour Precision Plus protein standard (Bio-Rad). For the Western blot, the membrane was incubated with 3mL of primary rabbit anti-NQO1 antibody for 5hrs. The dilution of antibody was 1:1000. After washing, the membrane was incubated with a secondary antibody, anti-rabbit IgG-HRP, for 30 minutes at a 1:80,000 dilution. After washing three times with 1XTTBS, the membrane was incubated with 3mL of super signal west femto solution for 5 minutes and image was taken immediately.

To confirm the NQO1 presence in the myelin membrane, immunohistochemistry was also performed. To achieve this, myelin was diluted to a 1:1000 ratio. The diluted of myelin (10µl) is incubated with 40µl of NQO1 primary antibody (Pierce PA5-19624) in a 1:200 dilution and 40µl of primary antibody of myelin basic protein (MBP) (Millipore LV 1583525) in a 1:200 dilution for 1 hour at room temperature [19]. Subsequently, myelin is incubated with secondary anti-rabbit IgG antibody Dylight 549 (Thermo Scientific 35557) and anti-rat IgG Dylight 488 (Millipore MAB386). The dilution of each secondary antibody was 1:500. The image was taken with the Nikon fluorescent microscope with 100x oil immersion lens.

4.2.4 Kinetic and Statistical Analysis

For kinetic analysis, online curve and surface fitting resources from zunzun.com (least-square model) were used to estimate the V_{max} and K_M parameters of NQO1. Statistical analysis was performed using Microsoft Excel 2010. The t-test was used for all analysis including myelin dose response, substrate dose response and on inhibition test. Statistical significance was established at $p \leq 0.05$ for a 95% confidence level.

4.3 Results and Discussion

NQO1 is present in a variety of cells and tissues and its localization in the cell depends on the cell's function. Jaiswal *et al.* described the NQO1 activity in almost all cell types [82]. Although NQO1 is mainly a cytosolic protein, but it is also present in other cell fractions. In humans, NQO1 is present abundantly in epithelial and endothelial cells but overexpressed in lung, colon and breast cancer [83]. Hyun *et al.* found the NQO1 in plasma membrane of neuroblastoma cells [84]. NQO1 has been detected in astrocytes and myelin-laden macrophages within MS lesions. In addition, NQO1 was found in a subset of OLs at the borders of active plaques [85]. The NQO2 and mNQO are the two major isoforms of NQO. NQO2 is 43 amino acids shorter than NQO1. The nucleotide sequence from exon 3-6 is highly conserved between NQO1 and NQO2 [87]. Contrary to NQO1, which is expressed in almost all cell types, NQO2 is expressed in heart, lungs, brain, liver and skeletal muscles. NQO2 can use DCPIP as a substrate but uses NADH as an electron donor poorly [87]. The preferential electron donor of NQO2 is dihydronicotinamide riboside (NRH) and the enzyme functions mainly as a nitroreductase [87]. Microsomal NQO (mNQO), another isoform of NQO, which is highly insensitive to dicoumarol is identified in liver microsomes and its molecular weight found to be ~18kDa [88].

4.3.1 Immuno Detection of NQO1 in the Myelin Membrane

To confirm the presence of NQO1 in the myelin membrane Western blot and immunohistochemistry were performed. Fig 4.4 A & B represents the results of Western blot and immunofluorescent image, respectively. The Western blot and

immunohistochemistry confirmed that the enzyme is present in the myelin membrane. Furthermore, Western blot revealed the truncated form of the NQO1 in the myelin membrane as demonstrated by the band at ~13kDa (see Fig 4.4A).

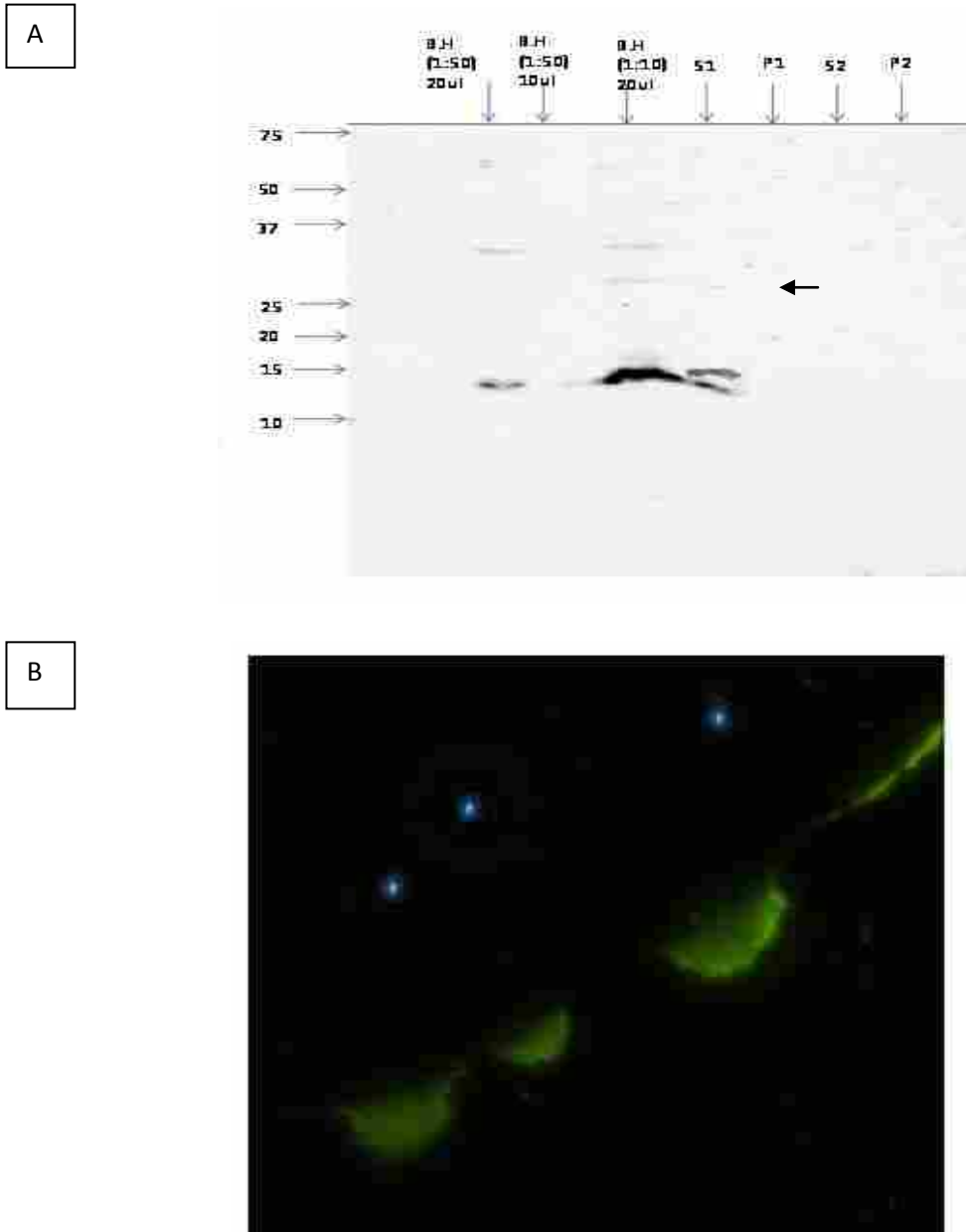


Fig 4.4: Immuno detection of NQO1. Panel (A): NQO 1 Western blot: Blot was made with 14 % resolving and 4 % stacking gel. Blot shows brain homogenate and detergent fractions (S1, S2, P1, P2) samples. Image was taken with 4000 VersaDoc. **Panel (B): Immunoflourescent image of NQO1:** Nikon Fluorescent microscope (100X oil immersion lens) is used to detect NQO1. Green colour shows the NQO1 while the blue colour shows the myelin basic protein (MBP).

In addition, the Western blot confirmed that the enzyme is present in the S1 detergent fraction at ~13kDa as well as at ~27kDa (a very faint band can be seen). In the brain homogenate, a very prominent band at ~13kDa can be seen along with two other, relatively light, bands at 27 and 30kDa, respectively. The NQO1 full length is represented by the band at 30kDa. Immunofluorescent image also confirmed the presence of NQO1 in the myelin membrane. Moreover, the image reveals that NQO1 and MBP are not co-localized (Fig 4.4 B).

Gasdaska *et al.* discovered a novel alternatively splice form of NQO1 mRNA (Fig 4.5) in normal and tumour colon cells [89]. The new isoform lacks the exon 4 (corresponding to mRNA residues 102-139), which corresponds to the quinone binding domain. This non-functional form is 114 base pairs smaller than NQO1 full length (20 kb) form, and is subjected to the further degradation. In rat NQO1, different residues regulate different functions. Likewise, Tyr128 is significant for dicoumarol binding and Lys76, Phe116, Glu117 and Asp163 for NADPH binding [89]. The reason for the non-functional form could be the absence of these above mentioned amino acid residues.

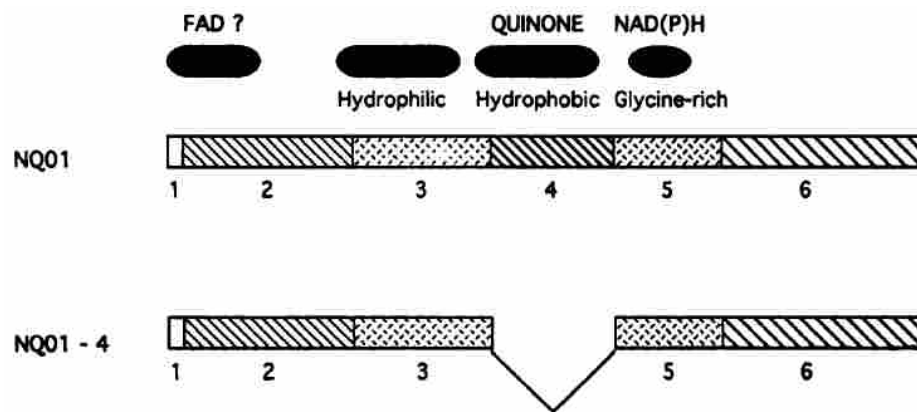


Fig 4.5: Structure of NQO1 mRNA and position of spliced exon 4. Fig taken from reference [89].

Jaiswal *et al.* discovered the two isoforms of NQO, NQO1 and NQO2, in rat liver cells in addition to microsomal NQO (mNQO). Moreover, they found that rat mNQO has a molecular weight of ~18kDa. In addition, mNQO was found along with the full length, ~29kDa, cytosolic rat NQO1. Interestingly, mNQO showed the approximately three to four times more affinity for electron donor NADH over NADPH. The estimated molecular weight of the truncated form that we found in mouse myelin membranes was ~13kDa, whereas the molecular weight of rat mNQO is ~18kDa.

In Fig 4.4A, the brain homogenate (1:10 dilution) and S1 fraction have a band at ~27-28kDa which may represents NQO1, or NQO2. Mouse NQO1 and NQO2 have a 49% sequence homology and the antibody used in the experiment was polyclonal [90]. Thus, there is a possibility that NQO1 antibody binds to the NQO2 which has a molecular weight of ~26kDa. As mentioned earlier, NQO1 has two domains, one is the compact N-terminus (1-220 amino acid residues), and the other C-terminus (221-273) is less compact. Previous studies showed that the NQO1 carboxy-terminus is cleaved off due to the proteolytic attack in the absence of NAD(P)H or FAD [90]. Another possibility is that ~ 27kDa band is generated due to the degradation of NQO1 in absence of electron donor or prosthetic group.

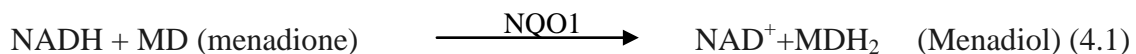
4.3.2 NQO1 Associated Activities in the Myelin Membrane

In this research study, NQO1 activity was measured through three associated activities; menadione-mediated cytochrome c reductase activity, PMS-mediated WST-1 reductase activity and lastly, DCPIP reductase activity. The potent inhibitor, dicoumarol, should affect all three activities.

4.3.2 (A): Menadione -Mediated Cytochrome c Reductase Activity

Quinones belong to the Vitamin k3 class, and are used as intermediate electron carriers for various reactions. Menadione-mediated cytochrome c reduction by NQO1 is monitored as increase in absorbance at 550nm [79].

The NQO1 cannot reduce the cytochrome c directly, thus a mediator, menadione, is required. The electron flow from NADH via menadione will reduce the cytochrome c (oxidized form). As a consequence, the concentration of cytochrome c (reduced form) will gradually increase with correspondence to its absorbance. Thus, NQO1 will catalyze the two electron reduction of menadione to menadiol with NADH as the electron donor (expression 4.1). Then non-enzymatically, menadiol will reduce cytochrome c (expression 4.2).



A typical rate of menadione-mediated cytochrome c reduction with myelin is illustrated in Fig 4.6. The initial reaction rate was determined by plotting the absorbance against time for sample and negative control (blanks). All reaction rates were corrected for the non-enzymatic reduction of cytochrome c and menadione.

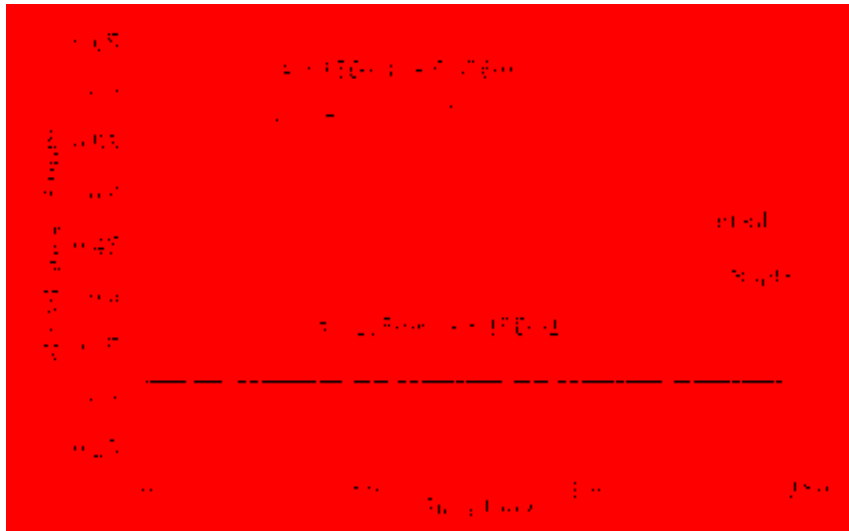


Fig 4.6: Typical reaction rate of menadione-mediated cytochrome c reduction by myelin. The sample contains myelin whereas, the negative control contains no myelin and represents the non-enzymatic reduction.

Enzyme Assay with Myelin Detergent Fractions

To determine the enzyme localization in the myelin membrane and its microdomain, a strategy was developed to compare the menadione-mediated cytochrome c reductase activity of enzyme in different myelin detergent fractions. To obtain myelin fractions, 500 μ g of myelin was treated as described in section 2.5.1(A). An enzyme activity assay as described above was performed with detergent fractions of CHAPS extract S1 and P1 (the supernatant and pellet, respectively) and TX-100 extract S2 and P2, (supernatant and pellet).

By comparing the activities of myelin detergent fractions (S1, S2, P1 and P2) on equi-volume basis with the activity of whole myelin, it can be concluded that most of the reductase activity is distributed into the S1 fraction (Fig 4.7). The activity in S1 fraction

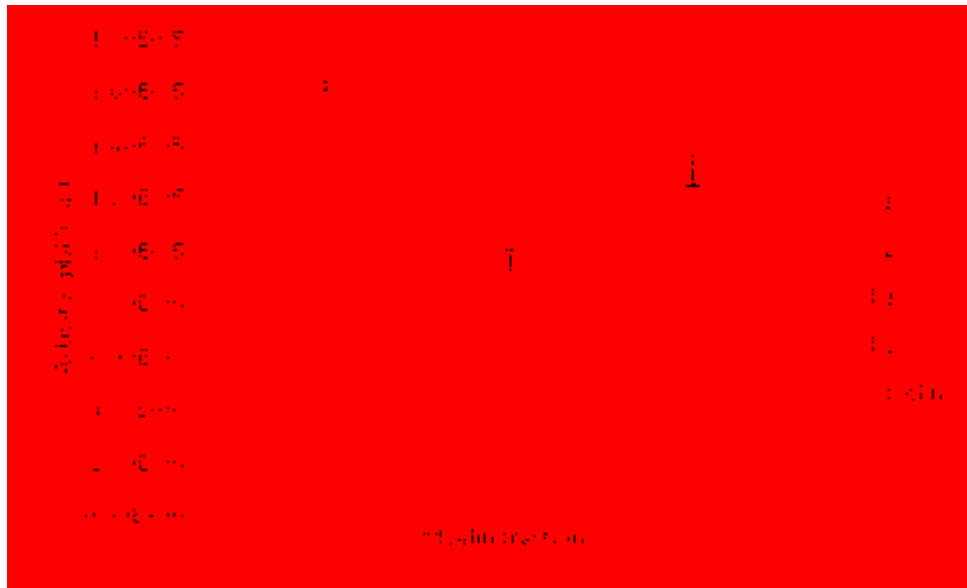


Fig 4.7: Comparison of myelin detergent fractions for menadione-mediated cytochrome c reductase activity. The reaction rate of each fraction (50 μ l) and myelin (20 μ g) was assayed in the presence of 70 μ M cytochrome c, 10 μ M menadione and 250 μ M of NADH at 37°C over 5 minutes. All results were produced in triplicate and corrected for non-enzymatic activity. The error bars are \pm SE.

is higher than control myelin sample may be due to the enzyme semi-purification. Furthermore, Western blot analysis result (Fig 4.4A) also confirmed the enzyme presence in S1 fraction. NQO1 and the reductase activity are either in the membrane region, completely solubilized by CHAPS, or in detergent resistant membranes representing lipid rafts. The activities in other fractions (S2, P1, and P2) might be due to the presence of other oxidoreductases.

Further characterization of the menadione-mediated cytochrome c reductase activity was completed with whole myelin. Fig 4.8 illustrates the result of enzyme dose-response analysis. Fig 4.8 depicts that rate of absorbance per unit time is proportional to the amount of protein added. In short, there is a direct relationship in reduced cyto c



Fig. 4.8: Cytochrome c reduction via menadione activity as a function of amount of myelin. Assay contained 50mM buffer with 20, 30, or 40µg of myelin protein and 70µM cyto c, 10µM menadione and 200µM NADH. Measurement was taken spectrophotometrically at 550nm at 37°C. Results are produced in duplicate and corrected for background. The error bars are ±SE (standard error).

concentration and enzyme activity. Furthermore, it can be assumed that cytochrome c reduced form is produced by the activity of menadione-mediated cytochrome c reductase activity, which may be due NQO1 presence in myelin membrane.

Several inhibitors, such as rotenone, DPI and capasicin, are typically used to inhibit the activities of oxidoreductases and flavoproteins. Dicoumarol, a competitive inhibitor, is widely used to inhibit the activity of NQO1 [90]. Dicoumarol inhibits the activity of Vitamin K dependent reductases and has an anti-coagulant property by decreasing the prothrombin level in Vitamin-K dependent proteins [91]. NQO1 is very sensitive to dicoumarol and typically, 10nM to 10µM is required to inhibit the activity in different species including humans [91].

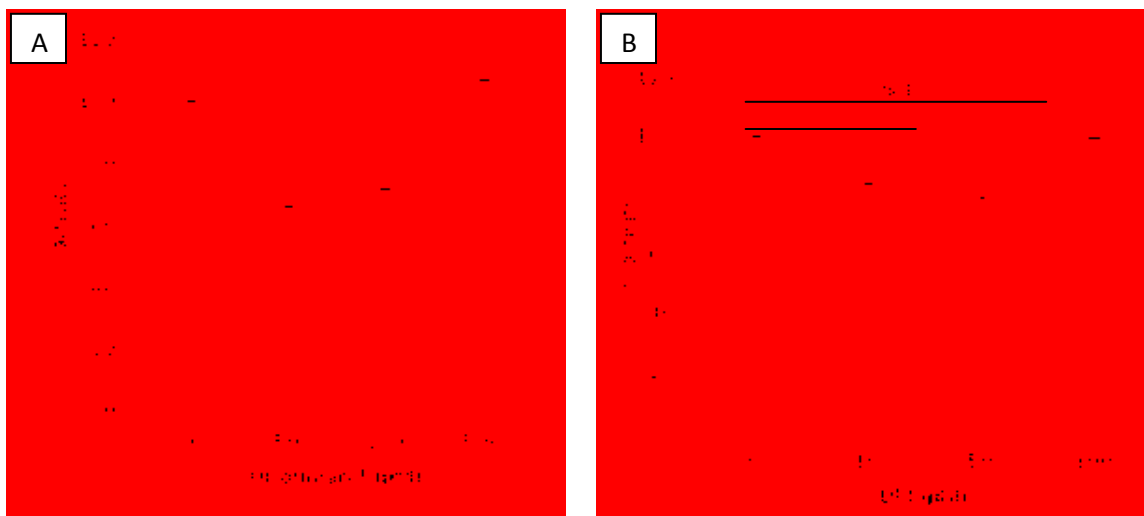


Fig 4.9: Attempted inhibition of menadione-mediated cytochrome c reductase activity by inhibitors: (A): Dose response of dicoumarol: Assay mixture consists of 50mM Tris buffer, 20μg myelin in (1:3) dilution, 10μM menadione, 70μM cytochrome c, 0, 50, 100, 500μM dicoumarol and finally 200μM NADH. **Panel (B): Dose response of DPI:** 50mM Tris buffer, 20μg myelin, 10μM menadione and 70μM cytochrome c, 200μM of NADH and 0, 10, 50, 100μM DPI. The statistical analysis showed the p values as *p= 0.028 and **p= 0.051. For both panels, (A) & (B), Measurement was taken spectrophotometrically at 550nm at 37°C. Electron transfer was monitored for 5 minutes at the interval of 20 sec. Results were produced in triplicate and corrected for non- enzymatic activity. The error bars are ± SE (standard error).

Result of dicoumarol-dependent inhibition is shown in the Fig 4. 9 (A). It is evident from the results that 35% activity of cytochrome c reductase was inhibited with 50μM dicoumarol but the cytochrome c reductase activity was increased at higher concentration (500μM) of dicoumarol (Fig 4.9A). The increase in activity might be due to dicoumarol in the buffer. Only a modest degree of inhibition (35%) was observed at 50μM dicoumarol. Typically, NQO1 is fully inhibited with nanomolar concentrations of dicoumarol. It may be concluded that oxidoreductase activity is not only due to the NQO1 but other enzymatic activities are also contributing.

DPI is another inhibitor of flavoproteins such as NADPH oxidases. It is also a potent inhibitor of nitric oxide synthase (NOS) in macrophages and endothelial cells. Typically, 20-25μM of DPI is required to inhibit 80% of NOS activity in endothelial

cells. The results of DPI-dependent inhibition of menadione-mediated cytochrome c reductase in myelin is shown in Fig 4.9(B). The activity is partially inhibited (~20%), by 50 μ M DPI. Besides NQO1, there are several other flavoproteins that are present in the myelin membrane such as CB5R. As mentioned earlier, a recent study shows that CB5R and neuronal NOS (nNOS) are associated with the caveolin protein in microdomains [92, 93]. If various flavoproteins are closely associated the inhibition of one may affect the activity of another.

4.3.2 (B): PMS-Mediated WST-1 Reductase Activity

As menadione reductase activity is not inhibited by dicoumarol, another substrate, water soluble tetrazolium generation 1 (WST-1) was used along with the electron carrier 1-methoxy-5-methyl phenazinium methyl sulfate (PMS). Water soluble tetrazolium generation 1 (WST-1) reduction is another tool that was used to investigate and measure the NQO1 activity in myelin membrane [80]. The WST-1 carries multiple sulfonate groups that confer the overall negative charge to WST-1 and prevent its transport across the membrane [80, 94]. The reduced WST-1 (formazan) shows maximum absorption at 438nm. The NADH-dependent reduction of PMS is catalyzed by NQO1 then the reduced PMS is recycled with the tetrazolium to the formazan (see Fig 4.10).

The effect of dicoumarol on PMS-mediated WST-1 reduction was determined in the myelin (see Fig 4.11). No inhibition was observed for dicoumarol concentrations up to the 100 μ M, thus again indicating NQO1 may not be the enzyme responsible for this catalysis.

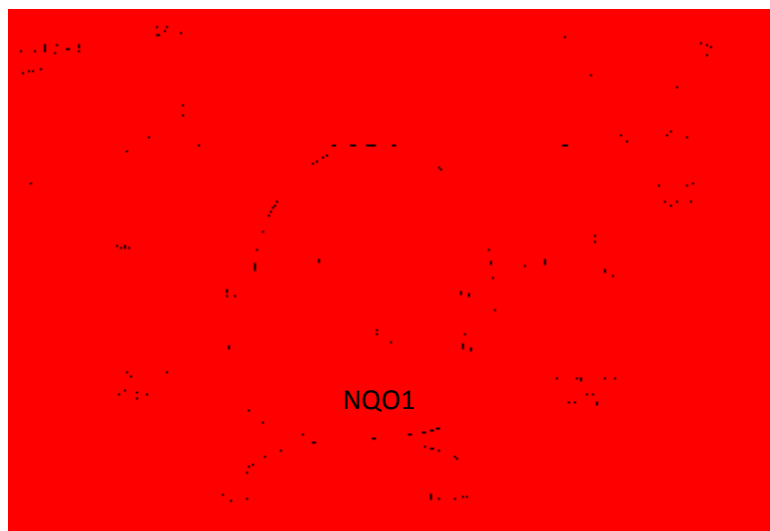


Fig 4.10: Modified mechanism of reduction of WST-1 by intermediate electron carrier PMS. The intermediate electron carrier itself oxidises. Modified from reference [94].



Fig 4.11: Attempted inhibition of WST-1 reductase activity by dicoumarol. Myelin (10µg) was assayed with 300µM WST and various concentrations (0, 10, 20, 50, 100µM) of dicoumarol. NADH (250µM) was used as an electron donor. Results were produced in triplicate and corrected for non-enzymatic activity. The temperature was kept at 37°C and measurements were taken at 438nm.

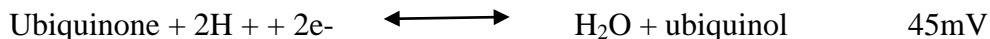
4.3.2 (C): DCPIP Reductase Activity

The activities of cytochrome c reduction via menadione and WST-1 reductase were not inhibited by dicoumarol. To further investigate the putative NQO1 activity, the substrate was changed to DCPIP. Although, DCPIP is a substrate for various enzymes, it

is an excellent substrate with NAD(P)H for measuring NQO1 activity [95]. The standard reduction potential is as follows:



and



Due to the greater standard potential, E° , DCPIP is a better electron acceptor than ubiquinone or menadione [63].

Lee *et al.* determined the NQO1 activity as the NADH-dependent reduction of DCPIP [81]. As DCPIP is reduced by enzyme, the concentration of oxidized form increased at 600nm [81]. The enzyme catalyzed reaction is shown for DCPIP reduction with NADH as the hydride donor.

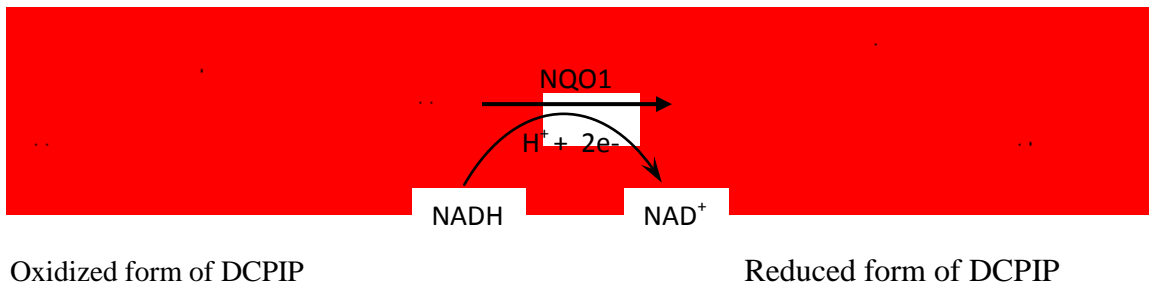


Fig 4.12: Reduction of DCPIP by NQO1. The DCPIP oxidized form is reduced by NQO1 via hydride transfer.

The transfer of electrons or reduction of substrate from electron donor (NADH) to terminal acceptor (DCPIP or CoQ) is catalyzed by two electron transfers in a two step reaction; first from NAD(P)H to FAD and then to the substrate (DCPIP or COQ). A typical rate of reaction of DCPIP reductase is illustrated in Fig 4.13. The decrease in absorbance over time in the sample can be seen due to the reduction of DCPIP.

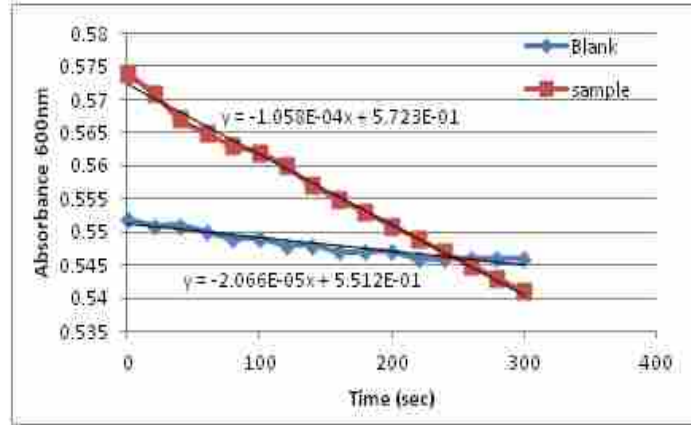


Fig 4.13: Typical reaction rate of NADH-dependent reduction of DCPIP in the myelin. The sample contains myelin, whereas, the negative control contains no myelin and represents the non-enzymatic reduction.

Further characterization of the DCPIP reductase activity was completed with the whole myelin. The activity of enzyme was measured in three regimes; dose response of enzyme, substrate dose response, and inhibitor(s) dose response. For the steady-state kinetics, the activity was determined with various concentrations of substrate and enzyme (see Fig 4.14 and 4.15). The result of myelin-dose response showed that there is a direct relation between absorbance and amount of protein, thus protein is present in active state.

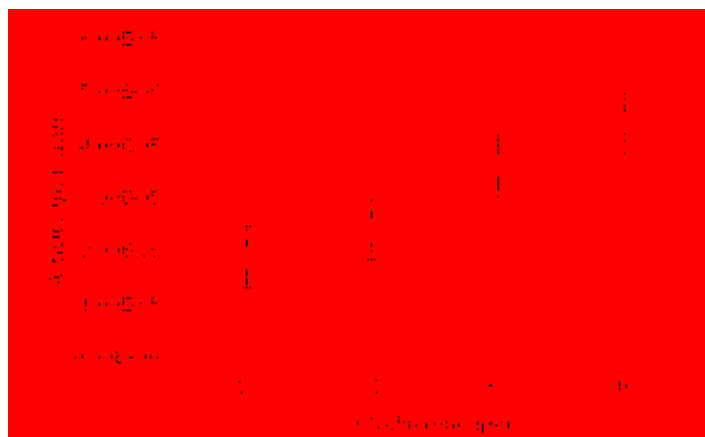


Fig. 4.14: DCPIP reductase activity as a function of amount of myelin. DCPIP (50µM) was assayed with various amounts of myelin (10, 20, 30, 40µg). To initiate the reaction, 250µM NADH was added. Measurement was taken spectrophotometrically at 600nm at 37°C. Results are produced in duplicate and corrected for background. The error bars are ±SE (standard error).

A



B

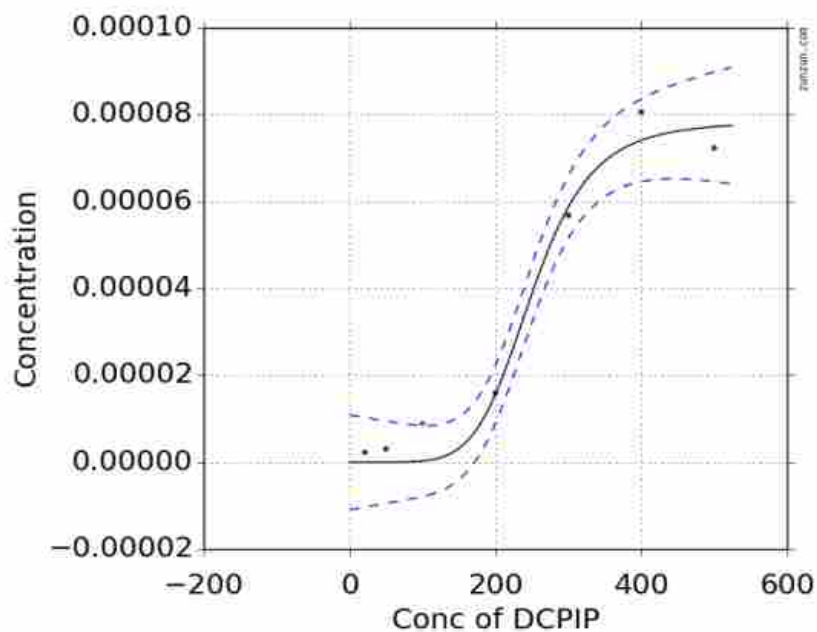


Fig 4.15: NAD(P)H: DCPIP reductase activity as a function of DCPIP substrate: Panel (A): Substrate dependent dose response curve generated on the basis of various substrate concentrations 20, 50, 100, 200, 300, 400 and 500 μ M with 10 μ g protein, 25mM Tris buffer and 2.5mM NADH. Electron transfer was monitored at 37°C at 600nm for 5 minutes at the interval of 20 seconds. All results are produced in duplicate and corrected for background. The error bars are \pm SE. t-test results indicate an statistical significance of more than 95% (**p=0.039) confidence in decrease in enzyme activity between 400 μ M and 500 μ M substrate concentration. **Panel B):** Data fitted with kinetic software (zunuz.com) to determine apparent K_M and V_{max} . The curve was generated by fitting the 2D Hills equation. Solid line represents the data while dashed line represents the 95% confidence of interval.

The curve of the DCPIP substrate dependent enzyme activity is sigmoidal. A sigmoidal curve suggests that the enzyme is allosteric in nature. The substrate inhibition can be seen at the highest concentration of DCPIP. This finding is in strong agreement with a study by Gustafson *et al.* which showed the inhibition of purified NQO1 activity with DCPIP substrate at 300 μ M [96]. The substrate-based inhibition is considered as physiological phenomenon not a pathological phenomenon. This phenomenon is demonstrated by almost 20% of the enzymes, out of which, 90% were allosteric enzymes [97]. Allosteric enzymes have two binding sites, one catalytic binding site, and another non-catalytic or allosteric binding site. In the non-catalytic site the second substrate binds and acts as an allosteric inhibitor by changing the conformation of the enzyme. As a consequence of this conformational change the enzyme can no longer bind to the substrate [97]. The mechanism is shown in Fig 4.16.

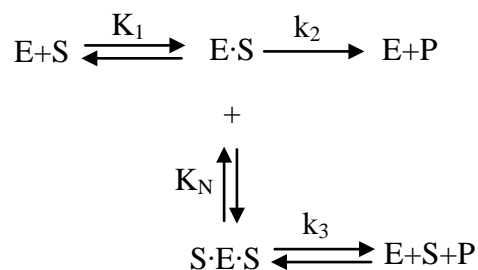


Fig 4.16 Mechanism of substrate-based inhibition of allosteric enzyme. Two molecules of substrate bind to the enzyme at a time at high concentration and inhibits enzyme activity. K_1 , k_2 , K_N and k_3 are the dissociation constants.

Furthermore, the DCPIP reductase activity is due to the enzyme that can use more than one substrate and have ping-pong mechanism. The enzyme that is using the DCPIP substrate does not follow the Michaelis Menten model. Using kinetic software, the kinetic parameters, V_{max} and $K_{0.5}$ were determined as $7.83 \times 10^{-5} \mu\text{M}/\text{min}$ and $251 \mu\text{M}$, respectively. Cytosolic NQO1 is NADPH dependent protein but it can use both the

electron donors; NADH and NADPH, with same V_{max} value, but the K_M for NADH is twice as that of NADPH [69, 77]. The dose response of electron donor NADH/ NADPH was determined in Fig 4.17. The estimated values of V_{max} and K_M for NADPH were determined as $6.86 \times 10^{-5} \mu\text{M}/\text{min}$ and $210 \mu\text{M}$, respectively. In addition, the V_{max} and K_M values for NADH were estimated $6.54 \times 10^{-5} \mu\text{M}/\text{min}$ and $54.7 \mu\text{M}$, respectively. The K_M value of NADPH is almost more than thrice as that of NADH, which shows that enzyme that is using DCPIP has NADH preference, contrary to NQO1, which has NADPH preference in several cells types.

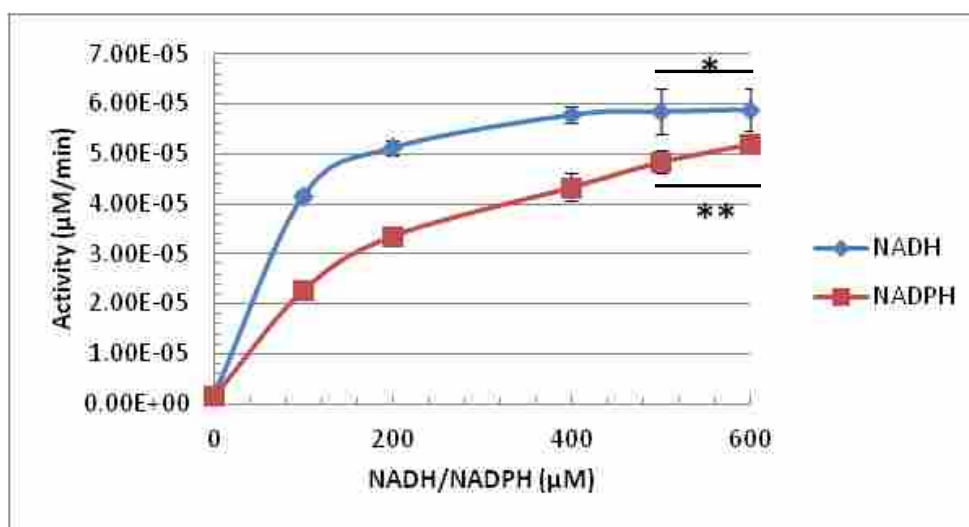


Fig 4.17: NADH: DCPIP reductase activity as a function of electron donor concentration. Both assays used the 25mM Tris buffer, 10µg myelin, 100µM DCPIP, various concentrations of NADH (0, 100, 200, 400, 500 and 600µM) and various concentrations of NADPH (0, 100, 200, 400, 500 and 600 µM). Measurement was taken at 600nm at 37°C. Results were produced in triplicate and corrected for non-enzymatic activity. The error bars are \pm SE. t-test results indicate a statistical significance of more than 95%, with * $p = 0.172$ for NADH and ** $p = 0.312$ for NADPH, respectively, between 500µM and 600µM electron donor concentration.

Jaiswal *et al.* illustrated that mNQO utilizes NADH as an electron donor with three times greater affinity than NADPH [88]. In our findings, K_M value of NADPH is

more than three times greater than the NADH (Fig 4.17) and thus, the enzyme shows the same greater affinity for NADH as with the mNQO. On the basis of K_M value, insensitivity to dicoumarol and molecular size, it can be speculated that DCPIP reductase activity might be due to mNQO but not due to NQO1.

Specifically, the enzyme assays are validated when a potent inhibitor abolishes the activity. The myelin samples were exposed to progressive increasing concentration of dicoumarol. To determine the inhibitory effect of dicoumarol, enzymes in the myelin were subjected to increasing concentration of dicoumarol (dissolved in DMSO or in 0.1N NaOH). Results are shown in Fig 4.18 (A & B), respectively. As FAD is an important component of electron transfer system in NQO1. To inhibit the activity of DCPIP, enzyme assay was supplemented with FAD and dicoumarol (Fig 4.18C). Although the FAD group is tightly associated with flavoenzymes, the supplementation was completed in case some loss occurred with the isolation or treatment of the myelin.

A myelin sample without inhibitor was used as a control and considered as having 100% oxidoreductase activity (in this case, NADH: DCPIP reductase). Dicoumarol in both solvents, DMSO and NaOH, did not show inhibitory effect on DCPIP reductase activity (Fig 4.18 A & B). Moreover, addition of FAD with dicoumarol showed that DCPIP reductase activity is also insensitive to its addition.

All NQO1 enzymes catalyze the two electron reduction reactions. Dicoumarol binds to the each catalytic site and the interaction is facilitated by FAD. Like the NADH, the plane of dicoumarol stacks parallel to the isoalloxazine ring of FAD at a distance of 4Å [71]. The coumarin ring of dicoumarol makes a hydrogen bond with His161. The schematic of NQO1 interaction is shown in Fig 4.19 [71].

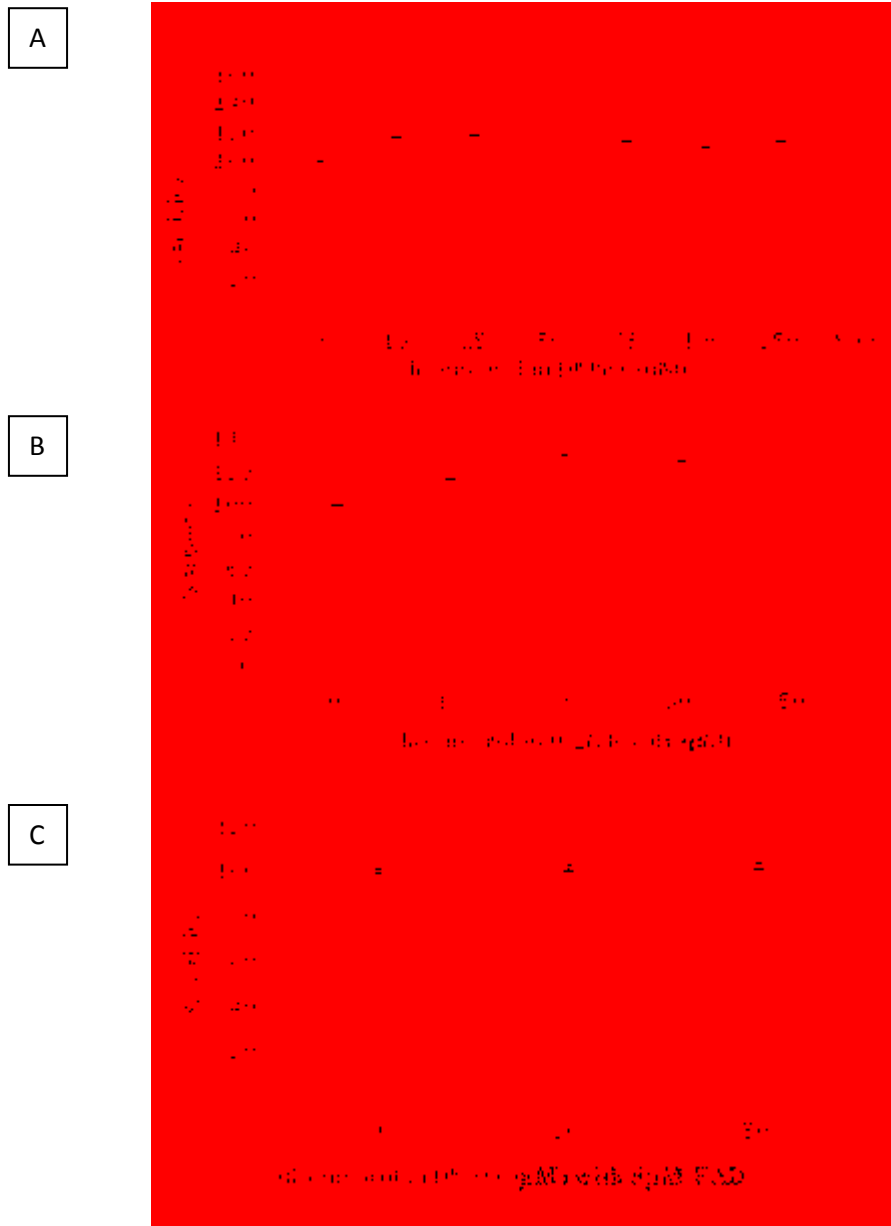


Fig 4.18: Attempted inhibition of DCPIP reductase activity by dicoumarol. The reaction rate of 10µg myelin was assayed with 50mM Tris/HCl buffer, in the presence of 50µM DCPIP substrate, 200µM NADH and various concentrations of inhibitors. Activity was measured at 600nm and at 37°C. Results were corrected for non-enzymatic activity and produced in duplicate **Panel (A)** Reductase activity with dicoumarol in DMSO with 0, 10, 25, 50, 75, 100, 250, 500µM. **Panel (B)** dicoumarol in 0.1N NaOH with 0, 10, 20, 30, 50µM. **Panel (C)** 5µM FAD with 0, 20, 50µM dicoumarol. The error bars are ±SE.

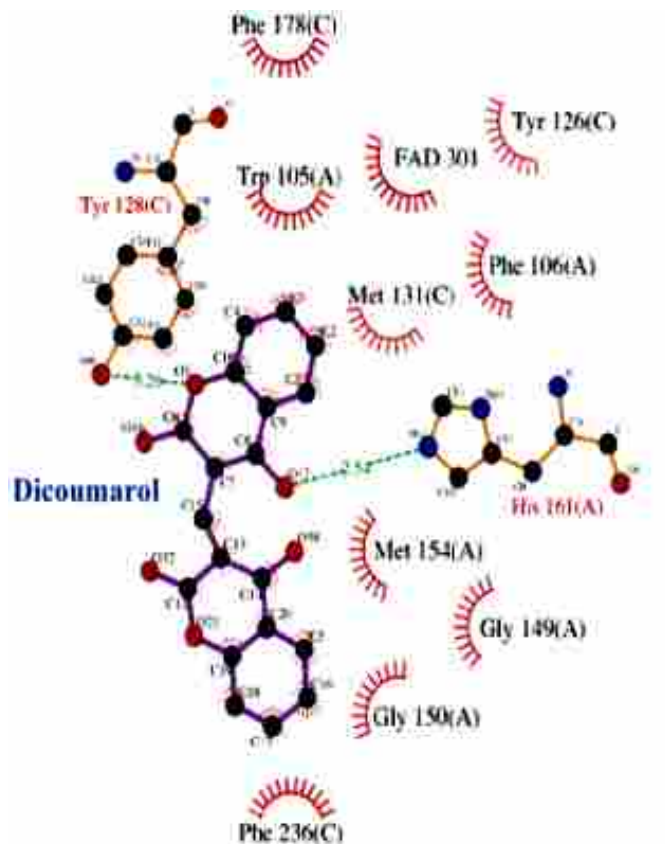


Fig 4.19: Schematic of dicoumarol binding with human NQO1 active site. Figure taken from reference [71].

Using dicoumarol as an inhibitor has two disadvantages: first is the lack of specificity and second is its competitive mechanism of inhibition [98]. The concentration of dicoumarol required to inhibit the DT-diaphorase activity varies with quinone acceptor, which may lead to false conclusions of either involvement or estimation of NQO1 [99]. The mechanism-based inhibitor, ES936, is a better inhibitor of NQO1 rather than dicoumarol. It is non-competitive inhibitor and only 100nM can inhibit more than 95% NQO1 activity in 30 minutes [98].

As DCPIP reductase activity is not inhibited by dicoumarol, it can be concluded that it is not the NQO1 that is catalyzing the reaction. Then what enzyme(s) are responsible for the DCPIP reductase activity? The DCPIP reductase activity was examined through various oxidoreductase inhibitors due to utilization of DCPIP substrate by several other enzymes. The inhibitory effects of DPI, pHMB, chloramphenicol, rotenone, KCN and DMSO were determined (Fig 4.20 A-F).

High concentrations of DPI (500 μ M) did not inhibit the activity of DCPIP reductase in myelin (Fig 4.20 A). Studies have shown that DPI does not inhibit the activities of various quinone reductases, including NQO1 and some other flavoproteins [100]. Thus, it is not surprising if DPI does not inhibit the DCPIP reductase activity. Another explanation could be that the enzyme that is using the DCPIP is not a flavoenzyme. DCPIP reductase activity was 50% inhibited by pHMB at 50 μ M (see Fig 4.20 B). Since pHMB is not a known inhibitor of NQO1-associated DCPIP reductase activity it can be concluded that activity is associated with an enzymes, carrying a cysteine residues or sulfhydryl group.

In order to preclude any associated mitochondrial activity, an inhibitor KCN, was used. Potassium cyanide is a potent inhibitor of cellular respiration, and ultimately blocks the oxidative phosphorylation. The DCPIP reductase activity showed the 50% inhibition with 10 μ M KCN (Fig 4.20 C). Although is an potent inhibitor of cytochrome c oxidase (complex IV of the mitochondrial electron transport chain), KCN is also a general inhibitor of several heme proteins, metallo enzymes, malic enzyme, creatine phosphokinase and Cu, Zn superoxide dismutase [101, 102]. There is a possibility that

activity of one of those enzymes is inhibited by KCN and can utilize DCPIP as a substrate.

Chloramphenicol did not inhibit the DCPIP reductase activity (Fig 4.20D). Chloramphenicol prevents protein chain elongation by inhibiting the peptidyl transferase activity [103]. It specifically binds to the 50S ribosomal subunit, preventing peptide bond formation. Usually it is used as an antibiotic and 10-20 μ M of chloramphenicol inhibits 85% activity of the peptidyl transferase [103]. The result confirmed that DCPIP is not utilized by an enzyme involved in protein synthesis.

As well, DCPIP reductase activity was not inhibited by rotenone (Fig 4.20 E). Rotenone is a specific inhibitor of mitochondrial complex I. It inhibits the electron transfer from iron-sulfur center to ubiquinone and eventually inhibits the ATP synthesis. Almost 10pM of rotenone inhibits 50% of the complex I activity [104], unlike our finding, where 500 μ M of rotenone did not inhibit the activity. It can be concluded that the activity what we find is distinct from mitochondrial complex I activity.

Lastly, about 80% of the DCPIP reductase activity is inhibited by 17.5% (v/v) DMSO (Fig 4.20 F). DMSO is a polar organic solvent and widely used in biology as a differentiation inducer, and it also apprehends the growth of cells at G1 and M phase [105]. DMSO enhances the permeability of the membranes by forming a pore, loosening the structure or by collapsing the lipid bilayer in cholesterol-rich domain [106]. Moreover, in DMSO-dependent assays, its volume is typically kept as low as 0.1-5 % (v/v) [106] and in our experiment, we use 2.5-17% DMSO. Most likely the inhibition by DMSO is due to protein denaturation.

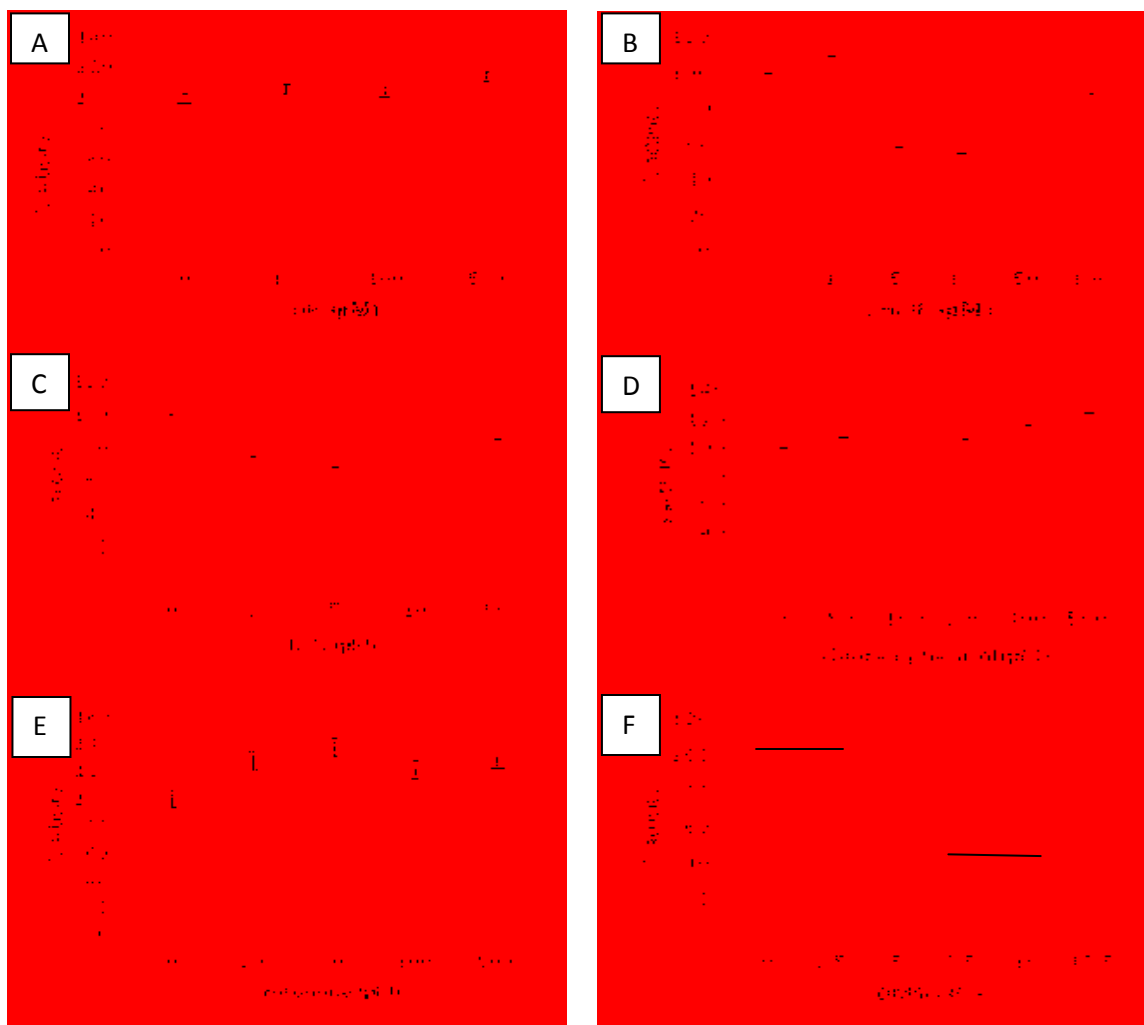


Fig 4.20: Attempted inhibition of DCPIP reductase activity with different inhibitors: The reaction rate of 10 μ g myelin was assayed with 50mM Tris/HCl buffer, in the presence of 50 μ M DCPIP substrate, 200 μ M NADH and various concentrations of inhibitors. **Panel (A):** With DPI at 0, 10, 100, 500 μ M. **Panel (B):** with 0, 1, 5, 10, 50, 100 μ M of pHMB. **Panel (C):** With KCN at 0, 3, 5, 10, 50 μ M. **Panel (D):** With chloramphenicol at 0, 50, 100, 200, 400, 500 μ M. **Panel (E):** With rotenone at 0, 20, 50, 100, 500 μ M. **Panel (F):** With DMSO at 2.5, 5.0, 7.5, 10.0, 17.5% (v/v). Activity was measured at 600nm and at 37 °C. Results were corrected for non-enzymatic activity and produced in duplicate. The error bars are \pm SE and 95% CI was established. The p values in Panel (F) are as follows: *p= 0.088, **p = 0.0806.

Fiore *et al.* described this denaturation activity as NADH-dependent DCPIP reductase activity [105]. In addition, DMSO was considered as a potent inhibitor of cyclin-dependent kinases (CDKs). The CDKs are a family of protein kinases that play

a role in cell cycle regulation. The CDKs are also involved in regulating and transcription of mRNA and are also involved in neuronal cells differentiation [105].

Zurbriggen *et al.* discovered DCPIP reductase activity in the plasma membrane of mouse neuroblastoma cell line NB41A3 [107]. The activity was not inhibited by dicoumarol, antimycin or rotenone, but the activity was inhibited by treating the cells with DMSO [107]. Furthermore, the same group concluded that DCPIP reductase activity is due to the unnamed enzyme which is similar to glyceraldehyde 3-phosphate dehydrogenase (GAP). There might be a possibility that activity is solely due to isozyme of GAP or could be a combination of two or more enzymes.

Several inhibitors were used to inhibit the NQO1 associated DCPIP reductase activity, some of them (KCN, pHMB and DMSO) partially inhibited the activity and some of them did not inhibit the activity (dicoumarol, rotenone, chloramphenicol). But our major focus was the dicoumarol-dependent inhibition of DCPIP reductase activity, which was not achieved due to the non-functionality of the enzyme. There could be a possibility that a novel isoform of NQO1, which is resistant to dicoumarol, is present.

4.4 Conclusions

In this study, the putative NQO1 presence in myelin membrane was investigated. Western blotting and immunohistochemistry of NQO1 detected the enzyme in myelin membrane. Furthermore, current study showed that NQO1 is present in a truncated form which may not be responsible for the observed dicoumarol-insensitive DCPIP reductase activity. Studies showed that NQO1 expression is tissue specific, ubiquitous, tightly controlled by a gene and highly inducible. Previous studies showed that if NQO1

is overexpressed, the cell becomes death resistant; this occurs in cancer cells. Several xenobiotics, aging and oxidative stress can modulate its expression. Furthermore, if enzyme is not required, it undergoes the posttranslational modification and degraded by proteosomal attack.

The equivalence of the three possible methods for measuring NQO1 activity; NADH-dependent cytochrome c reduction via menadione, DCPIP reduction and WST-1 reduction into formazan was assessed in myelin samples. The activity of NQO1 was quantified by the use of the potent inhibitor dicoumarol. Several other inhibitors including DPI, pHMB, and rotonone were used in an attempt to inhibit the activity. DPI reduced the 20% activity of menadione-mediated cytochrome c reductase [93, 108]. With the DCPIP reductase assay, DPI did not inhibit any of the activity. Menadione-mediated cytochrome c reductase activity was almost 35% inhibited by 50 μ M dicoumarol; however, the DCPIP reductase activity was insensitive to dicoumarol. Overall, the level of dicoumarol inhibition is far away from literature values for NQO1, where picomoles of dicoumarol completely inhibit the activity. It can be concluded that DCPIP reductase activity may be due to the other oxidoreductases and dehydrogenases which are residing in the myelin membrane. These enzymes can use the substrate DCPIP but they were partially or fully insensitive to dicoumarol. Secondly, there is a possibility that any other novel isoform of NQO1, resistant to dicoumarol is present in myelin such as mNQO. The electron donor of NQO2 is NRH (dihydronicotinamide riboside) but it can utilize NADH and NADPH, very poorly. Wu *et al.* estimated the $K_{0.5}$ value of NQO2 in liver cell culture as 252 μ M when it was using DCPIP as a substrate [109]. This value is very close to our estimated value of $K_{0.5}$ which is 251 μ M, whereas with NRH electron donor and DCPIP

substrate the K_M value of NQO2 is $30\mu\text{M}$ [109]. Furthermore, NQO2 is almost insensitive to dicoumarol [109]. It can be speculated that DCPIP reductase activity may be due to NQO2.

Purification and protein sequencing can give the insight into the truncated isoform present in the myelin membrane. For future NQO1 investigations ES936 inhibitor should be used instead of dicoumarol.

Chapter 5

Comparison of Oxidoreductases in Healthy and Diseased Myelin

In this chapter, the previously investigated enzymes, CB5R and NQO1 are examined in a demyelinating mouse model. The demyelination process is associated with a pathology called multiple sclerosis (MS), and most commonly diagnosed in young adults. The ND4 spontaneously demyelinating mouse model with age-matched controls was used in this study. Furthermore, the level of superoxide production was also investigated in healthy and diseased mouse myelin.

5.1 Introduction

Multiple sclerosis (MS), also known as disseminated sclerosis or encephalomyelitis disseminata, is considered to be an inflammatory disease in which the insulating sheath, the myelin membrane, in the brain and/or the spinal cord is damaged. This process is called demyelination [110]. Due to the damage of the myelin sheath and the disruption of macromolecules, plaques in white matter can be seen (see Fig 5.1)

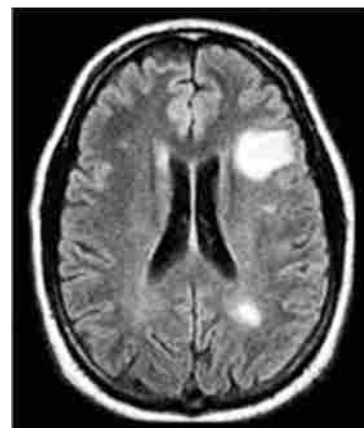


Fig 5.1: MRI image of MS brain. The white areas are lesions or plaques. Fig adapted from reference [111].

The symptoms of MS correlate with the affected region. Contrary to the PNS,

in the CNS the repair mechanism of myelin is complex and limited since one oligodendrocyte cell is myelinating more than one axons.

The actual cause of MS is unknown but it is believed that MS is a combination of several genetic, infectious and environmental factors [111]. Some common signs and symptoms among MS patients include a loss of sensitivity or changes in sensation such as tingling, pins and needles or numbness, muscle weakness, very weak reflexes, muscle spasms, or difficulty in moving; difficulties with coordination and balance (ataxia); problems with speech or swallowing, visual problems such as; blurry vision or peripheral vision loss, (nyctagmus, optic neuritis or double vision), and fatigue [111].

On the basis of symptoms, MS can be categorized into four classes [112]. The first class is the relapse-remitting MS (RRMS) in which the signs and symptoms are characterized by random appearance of symptoms that can last from hours to months but patient recovers over a period of time. This is the most common type of MS and almost 80% patients show these signs and symptoms in the beginning. RRMS is further divided into two subtypes: 1- Benign MS: In this subclass the recovery is almost complete and only limited progression in disability even after 20 years is observed. 2- Clinically isolated syndrome: In this subclass, the patients have an attack which is suggestive of promising demyelination, but the symptoms are insufficient [110]. The second class is the primary progressive MS (PPMS) in which the improvement in disability is very minor. This class is more equally distributed in men and women. Otherwise, in all other classes women are more prone to disease. The third class is the secondary progressive MS (SPMS). In this type there is no defined time between the periods of symptoms. The disability worsens with each episode

of attack. Lastly, progressive relapsing MS (PRMS) is the class of MS in which patients have progressive neurological decline from the onset of the disease. This class may result in complete disability [110].

Although, the mechanism of action of MS is unknown it is believed that body's own immune system, T-cells, attacks the myelin membrane and destroys it. In normal circumstances, the blood brain barrier (BBB) is impermeable to these cells, but in diseased condition, the BBB becomes permeable and T-cells destroy the myelin sheath (see Fig 5.2 A & B). Recently, Wu, *et al.* discovered that kallikrein (KLKB), a serine protease and modulator of the T-cell antigenic determinant, is robustly upregulated in the demyelinating brain [113].

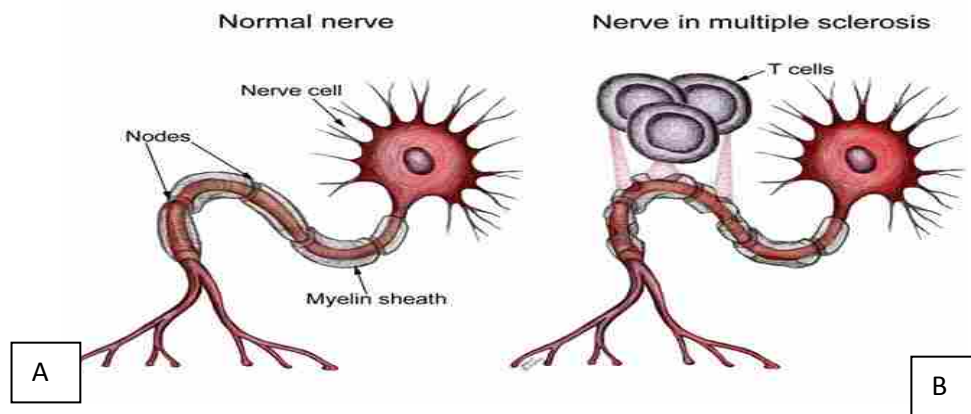


Fig 5.2: Basic structure of neurons with myelin sheath in health and disease. (A) Healthy myelinated neuron. (B) Demyelination due to the attack of T-cells. Fig taken from reference [110].

5.1.1 Model of Demyelination

As the MS disease is considered multifactorial, comprehensive animal model or models are required for its study. The available demyelinating models include viral-induced demyelinating models, immune-mediated demyelinated models, and

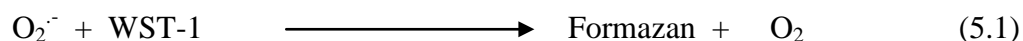
genetically-induced demyelinated models. Artificial chemical-induced demyelination can be induced by the exposure to cuprizone, a copper chelator. In this research project, a transgenic mouse model, ND4 mice, was used. In ND4 mouse model, PLP is down regulated due to an over-expression of a deletion mutant of PLP (DM-20) [114]. There are almost 70 copies of the transgene encoding for the DM-20 protein in ND4 mouse [114]. The ND4 mouse is clinically healthy at 3 months of age and has minimal inflammatory signs. Around 3 months of age, without the injection of a myelin-specific antigen such as myelin basic protein, ND4 mice spontaneously undergo demyelination [114]. It is therefore, one of the genetically modified animal models for the study of demyelinating disease and offers intrinsic manifestations of MS symptoms without any external injections. In the ND4 model, demyelination is asymptomatic at 3 months of age. Typically, by 8-10 months mice showed tremors and unsteady gait and have 17% myelin as compared to a normal mouse [114]. Moreover, the disrupted myelin can be seen at 8 months of age and myelin debris can be seen in astrocytes [114].

5.2 Material and Methods

For CB5R and NQO1 investigations, the materials and methodology is the same as described in section 3.2 and 4.2, respectively.

5.2.1 Measurement of Superoxide Detection

Increased superoxide production is the hallmark of increased oxidative stress. Superoxide detection was carried out using a WST-1 reduction assay, in diseased and healthy myelin of the same age. The superoxide reduces WST-1 into formazan (equation 5.1).



The assay mixture contained 100mM potassium phosphate, 2mM EGTA buffer (pH 7.0), various concentrations (20, 30, 40 μ g) of healthy and diseased myelin, 50 μ M NADH, and to initiate the electron flow, 300 μ M WST-1 was added. The total volume per sample was brought up to 200 μ l with the addition of phosphate buffer. The reduction of WST-1 into formazan was monitored at 37°C for 15 minutes at kinetic interval of 30 seconds. The increase in absorbance at 438nm was monitored with an extinction coefficient of 37.0 mM⁻¹cm⁻¹ for formazan.

5.3 Results and Discussion

5.3.1 Investigation of Cytochrome b5 Reductase Activities in Diseased and Healthy Myelin

CB5R is an enzyme that has been found in myelin membrane (see chapter 3). To investigate the CB5R activities in diseased myelin, two age groups of ND4 mouse model were used. The 7.7 month old mice represent the age group before physical symptoms of demyelination are apparent, whereas the 11.3 month ND4 mice have significant symptoms of demyelination. The cytochrome c reductase activity was measured in both age groups of diseased and healthy mouse myelin (see Fig 5.3). The kinetic parameters, K_M and V_{max} , were not determined as the enzyme activities did not reach saturation (plateau curve). Fig 5.3 A & B represent dose response of myelin in both age groups, which illustrates that the reduction reaction is directly proportional to the amount of protein added. Overall, healthy myelin showed a greater activity as compared to diseased myelin on an the basis of equal amount of protein.

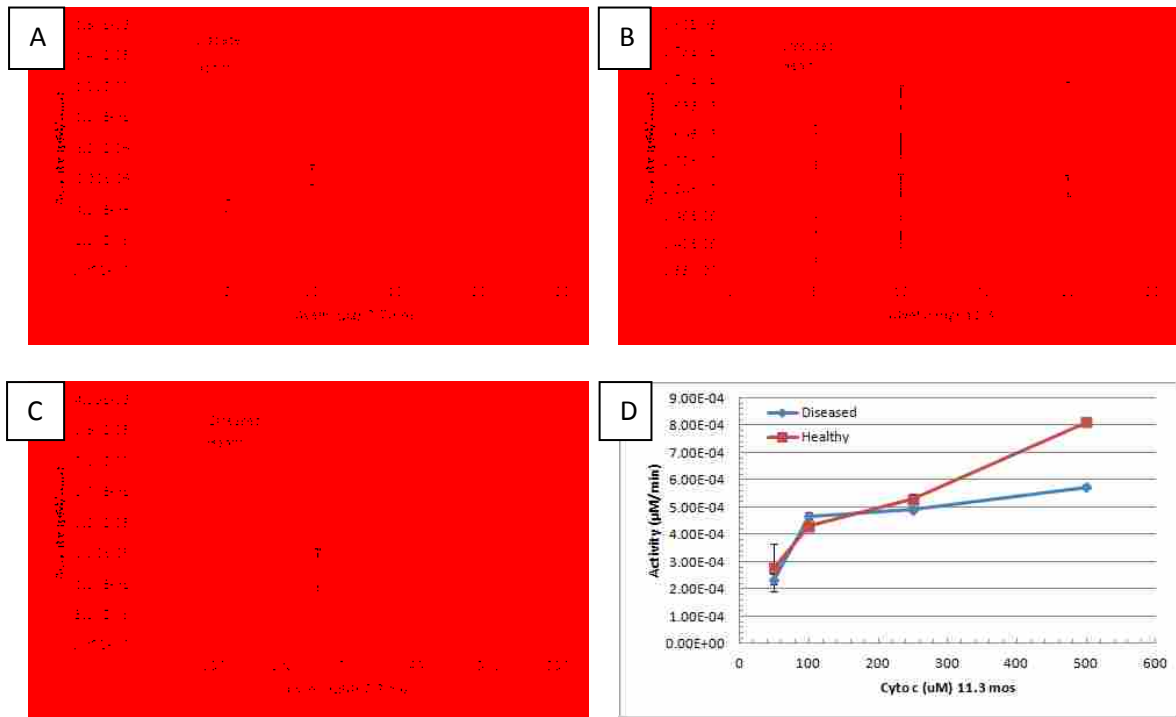


Fig 5.3: Age-matched comparison of cytochrome c reductase activity in healthy and diseased myelin. Panel A and B represents activity as function of myelin protein with 100 μ M cytochrome c for the two age groups. Panel C and D represents the activity as a function of cytochrome c with 10 μ g for both ages. The reaction was initiated with 250 μ M NADH. All assays were performed at 37 $^{\circ}$ C in a total volume of 200 μ l per well. Measurement was taken at 550nm. All error bars represent \pm SE.

Interestingly, all of these activities are lower when were compared with the activity of CB5R found in chapter 3, where the age of the mice were approximately 2 month and the enzyme activity of 20 μ g of myelin with 100 μ M of cytochrome c was 0.28 μ mol/min. When examining reductase activity in healthy mouse myelin, at 2, 7.7, and 11.3 months of age, the findings suggests that CB5R activity fluctuates over the lifespan. However, in healthy myelin from 7.7 to 11.3 months, the activity greatly increases (p= 0.001). This same statistically significant trend is seen in the diseased myelin, from 7.7 to 11.3 months (p= 0.032).

Table 5.1: Comparison of cytochrome c reductase activity with 20 μ g myelin and 100 μ M cytochrome c in healthy and diseased samples. Enzyme activity from healthy and diseased myelin were calculated from the reaction rates in figure 5.3 A and B using the extinction coefficient of 29.5mM⁻¹cm⁻¹ for the reduced cytochrome c at 550nm.

Mice Age (Months)	Diseased myelin activity (μ mol/min)	Healthy myelin activity (μ mol/min)	P values
7.7	0.132 \pm (3.252E-06)	0.165 \pm SD (2.333E-05)	p=0.324
11.3	0.180 \pm SD (9.899E-06)	0.205 \pm SD (9.192E-06)	p=0.016
P values	p = 0.032	p= 0.001	

Another comparison was made between healthy and diseased myelin, this time with 10 μ g myelin and 500 μ M cytochrome c is utilized (see table 5.2). In comparing the

Table 5.2: Comparison of cytochrome c reductase activity with 10 μ g myelin and 500 μ M cytochrome c in healthy and diseased samples. Enzyme activity from healthy and diseased myelin were calculated from the reaction rates in figure 5.3 C and D using the extinction co-efficient of 29.5mM⁻¹cm⁻¹ for the reduced cytochrome c at 550nm.

Mice Age (Months)	Diseased myelin activity (μ mol/min)	Healthy myelin activity (μ mol/min)	p- values (D vs H)
7.7	0.425 \pm SD (7.990E-06)	0.232 \pm SD (7.778E-05)	p=0.010
11.3	0.456 \pm SD (5.656E-06)	0.687 \pm SD (3.535E-06)	p=0.008
p-value (age comparison)	p = 0.024	p = 0.001	

enzyme activities with 500 μ M cytochrome c between the 7.7 and 11.3 months old healthy mice, the activities were statistically greater in the myelin of the older mice (p=0.001). When comparing activities between diseased and healthy myelin at the same age, the younger mouse diseased myelin showed the greatest activity (p=0.01 and p=0.008, respectively). However, the older mice, healthy mouse showed the greatest activity. Interestingly, when these activities were compared with the activity of CB5R found in chapter 3, where the age of the mice were approximately 2 months, the enzyme activity of 10 μ g of myelin with 500 μ M of cytochrome c was 0.673 μ mol/min. However,

again in the healthy myelin from 7.7 to 11.3 months there is greater activity ($p= 0.001$). In diseased myelin there is increase in activity in older mice ($p= 0.024$).

Lastly, the pHMB-dependent inhibition of the enzyme activity demonstrated that at 7.7 months of age the disease myelin cytochrome c reductase activity is more susceptible to pHMB inhibition (see Fig 5.4). However, in the 11.3 months age group, the pHMB inhibitory effect is almost the same in diseased and healthy myelin, as shown statistically. In chapter 3, the $1\mu\text{M}$ of pHMB inhibited the 50% enzyme activity in myelin from ~2 months old mice. This decreased effect of pHMB inhibition with age may be related to an increased level of protein expression.

Several reactive oxygen species (ROS), such as superoxide radical (O_2^-) and hydrogen peroxide (H_2O_2), play a crucial role in cell signaling [115, 116]. These species performed very vital functions for cells as phagocytosis, hormone synthesis and apoptosis [117]. Various pathological conditions are associated with the increased oxidative stress [115]. Oxidative stress is a condition in which level of ROS such as superoxide radical, hydrogen peroxide and peroxynitrite are elevated. These elevated ROS can damage the protein and lipids. Oxidative stress increases over a significant time period, and thus it is an age-related phenomenon. In the aging process, ROS damage the mitochondrial DNA (mDNA) and results in impaired mitochondrial function energy production and the subsequent reliance on glycolysis. This results in the hyper-reactivity of t-PMET [118].



Fig 5.4: The pHMB-mediated inhibition as a function of cytochrome c reductase activity. The reaction was initiated with 250µM NADH, 10µg myelin, and 100µM of cytochrome c in the presence or absence of 1µM pHMB. Measurement was taken at 550nm at 37°C. All error bars are ±SE. The t-test values, *p=0.083 and **p=0.294 are established at 95% CI.

In various cells NOX is responsible for producing superoxide [17]. In this study the superoxide production was carried out in healthy and diseased myelin of the same age to investigate the levels with the disease progression. To detect any measureable quantity of superoxide, oxidation of WST-1 into formazan was followed at 438nm. This reaction was NADH-dependent (see equation below).



Fig 5.5 shows that superoxide production has a direct relation with the amount of protein. The diseased myelin, as we hypothesized, showed the greater superoxide production as compared to healthy myelin. Furthermore, both groups of protein showed a plateau curve which may be due to the insufficient substrate. In all cells, generally, superoxide dismutase (SOD) enzyme is responsible for dismutating the superoxide ($\text{O}_2^{\cdot-}$) into H_2O_2 and O_2 . But, at a threshold level of ROS, the SOD activity decreases and as a consequence superoxide damages the macromolecules.

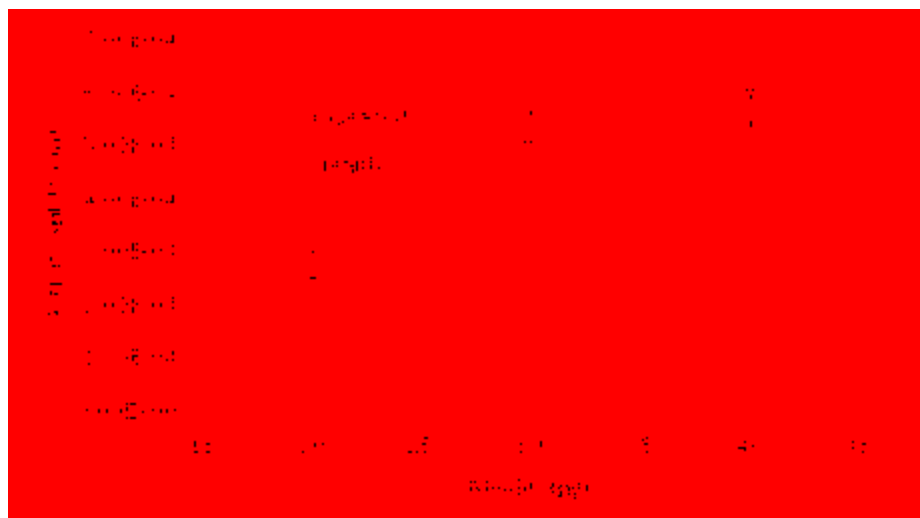


Fig 5.5: Comparison of superoxide production rates in healthy and diseased myelin: Various concentrations of 5.34 months old mouse myelin (20, 30, 40μg) were assayed with 300μM of WST-1. To initiate the reaction 250μM of NADH was added. In each well, volume of reaction mixture was made up to 200μl by adding 100mM potassium phosphate buffer with 2mM EGTA buffer, pH 7.0. Measurements were taken at 438nm at 37°C. Results were produced in duplicates and corrected for non-enzymatic activity. The error bars are ±SE.

Due to limited availability of related published literature it was not possible to compare the activities of CB5R with different model systems. As mentioned earlier recent research published in March 2014 showed that CB5R and NOS are associated through the caveolin protein in lipid cholesterol-raft region [92]. Furthermore, CB5R itself is involved in superoxide production and superoxide production increases with age [115].

Previous studies discovered that CB5R also regulates the release of nitric oxide [108, 119, 120]. In light of previous and current study scenarios it can be postulated that modulation in CB5R activity may trigger the uncontrolled NO[•] production and release. The NO[•] is the first known endogenous inhibitor of superoxide dismutase (SOD) and competes for the availability of superoxide radical (O₂^{•-}) to form peroxynitrite (OONO⁻)

[121]. The OONO^- is a very toxic species, and has the ability to damage the BBB [122]. The schematic of the CB5R-dependent BBB dysfunction is illustrated in Fig 5.6.

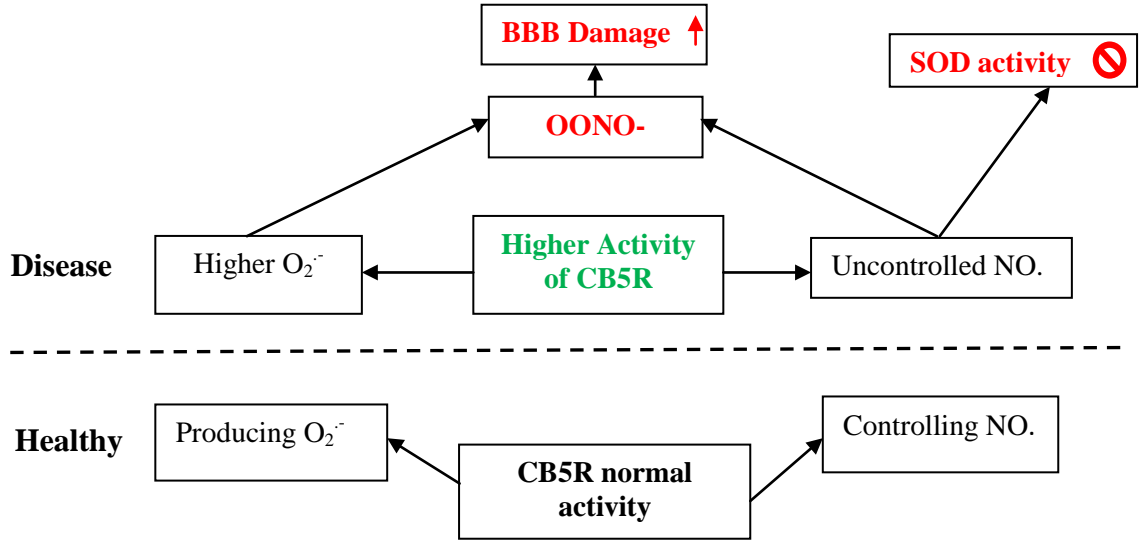


Fig 5.6: Schematic of hypothesis of CB5R-induced BBB damage. In healthy cells CB5R controls the release of nitric oxide and also a producer of superoxide radical. In diseased state with the disruption of CB5R function, nitric oxide release is uncontrolled and superoxide production may increase. It is hypothesized that the uncontrolled nitric oxide and superoxide forms the peroxynitrite specie which is very harmful to the cells. Studies shows that peroxynitrite can damage the blood brain barrier.

In neuronal cells the "L-shaped" calcium channels are present in close proximity to CB5R within the lipid raft region [19]. These calcium channels are also found in oligodendrocytes [123]. The calcium channels are also called sodium-calcium exchanger. This exchanger is an antiporter membrane protein that removes calcium from the cells. It removes a single calcium ion in exchange for the three sodium ions [124]. It can be proposed that both of the isoforms of CB5R may regulate calcium homeostasis and influx of Ca^{2+} into the cells by their association with Ca^{2+} channels. Previous studies also show that calcium toxicity as one of the major cause of axonal degeneration [125]. In axonal inflammation Na^+ channels redistribution affects the $\text{Na}^+/\text{Ca}^{++}$ exchange and increases the

calcium influx into the cells [125]. The high calcium level initiates the calcium-dependent proteolytic degradation. Furthermore, excessive Ca^{++} entry releases the glutamate and this glutamate and Ca^{++} harm the axon and cause degeneration. The schematic of the procedure is shown in Fig 5.7.

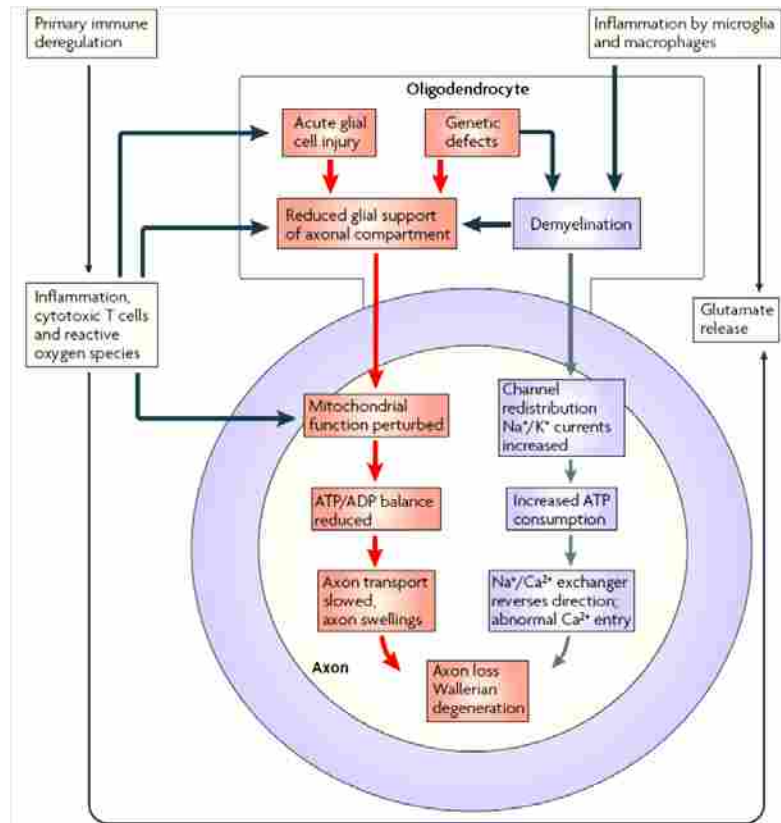


Fig 5.7: Schematic of calcium induced toxicity and axonal degeneration. Two pathways for axonal injury are shown. First pathway shown in red color, deals with the mitochondrial dysfunction. Second pathway shown in blue, deals with the consequence of demyelination and calcium toxicity. Oxidative stress redistributes the channel organization in the myelin membrane and as a consequence energy depletes and excessive calcium enters the cells. This increase in calcium triggers the glutamate release which is harmful to the cells. Fig adapted from reference [12].

5.3.2 Investigation of NQO1 in Healthy and Diseased Myelin

5.3.2.1 Immuno-Detection of NQO1 in Diseased and Healthy Myelin

NQO1 has been previously identified in the myelin membrane (see chapter 4), but mainly in a truncated, non-functional form. Although various associated reductase

activities were present, none were inhibited by dicoumarol, a NQO1 specific inhibitor.

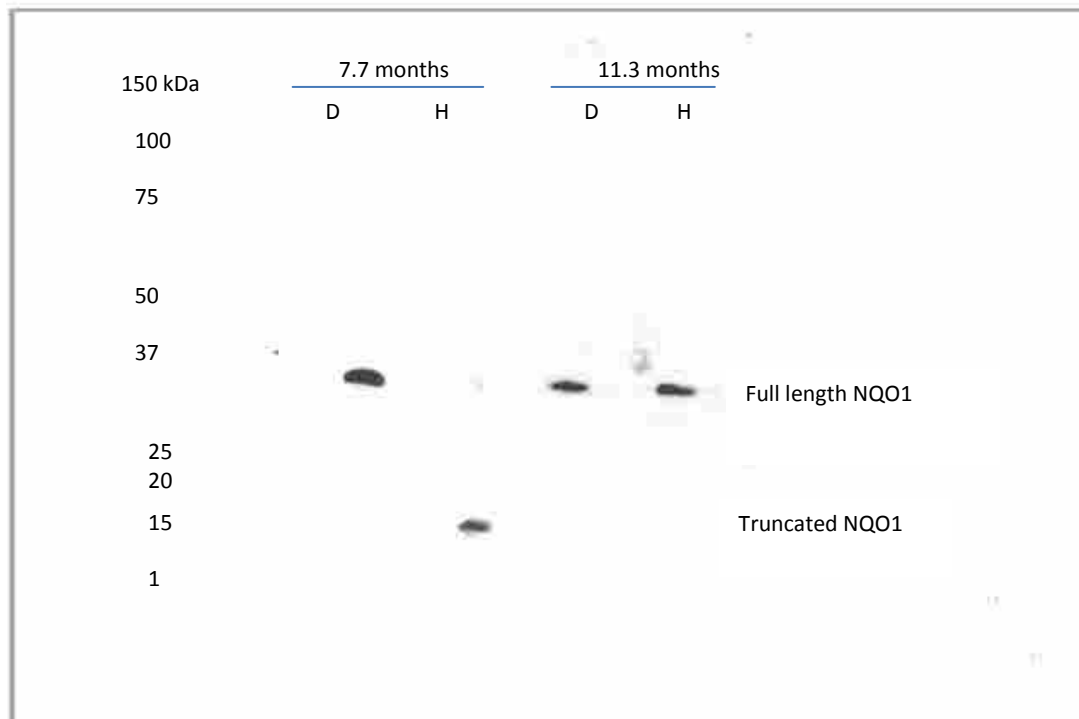


Fig 5.8: Western blot of NQO1 in diseased and healthy myelin. A 14% resolving gel along with 4% stacking gel was prepared to examine the NQO1 expression level in diseased and healthy myelin of different ages. A volume of 16 μ l of delipidated myelin (disease and healthy of both age groups) (in final volume) with 5x sample loading buffer was loaded. Dual Colour Precision Plus protein standard (5 μ l) in 1:10 dilution was also loaded with sample. The protein on the gel were electrotransferred to a nitrocellulose membrane, which was incubated with primary NQO1 antibody in a 1:1000 dilution for 4 hrs. Subsequently after washing, membrane was incubated with secondary antibody anti-rabbit IgG in a 1:80,000 dilution for 30 minutes. Image was taken with 4000 VersaDoc. Letter "D" represents diseased myelin, whereas "H" represents healthy myelin.

Western blot analysis of NQO1 in diseased and healthy myelin was performed between two age groups. In diseased myelin of both ages, NQO1 was detected at ~30kDa, whereas in the middle-aged healthy myelin (7.7 months) a truncated form was detected, as previously observed in the young mice (~2 months) (see Fig 4.4 A). Contrary to 7.7 months old healthy myelin, in 11.3 months old healthy mouse myelin, only the full-length NQO1 was detectable. This might be due to the age of the mouse.

The healthy mouse of 11.3 months has completed almost 65% of its life span and the presence of full length NQO1 in myelin membrane may be related to the higher oxidative stress levels found with aging. Aging is a biological process in which the free radicals produced by metabolic processes damage the macromolecules of the cells. They also damage the mitochondria and as a consequence the ratio of pyridine nucleotides, NADH/NAD⁺ is disrupted [126]. To maintain the ratio of NADH/NAD⁺, t-PMET is activated in an aged brain [118] (see further discussion in chapter 6).

Previous studies are in agreement with current results. They show that NQO1 accumulates in the aged brain, and in addition the age-related elevated level of NQO1 might be cellular protection mechanism [127]. Another theory postulates that as NQO1 is involved in lipid metabolism [128] there is a possibility that it is involved in myelinogenesis, and after birth its level gradually falls and it became inactive [86].

The NQO1 is highly inducible enzyme [82]. Generally, it is believed that the expression of NQO1 is under the control of a promoter, called antioxidant response element (ARE) [129, 130]. This factor is the adaptive mechanism of cell against oxidative stress [131]. The ARE-related genes are involved in several functions of the cell as a response to external stimulus such as glutathione regulation, catalase expression, proteosomal degradation and redox status [132]. The Nrf2 is the key signaling protein, that post-translationally regulates the ARE pathway. Under normal circumstances in cytosol the Nrf2 is conjugated with kelch-like ECH-associated protein 1 (Keap1). Keap 1 protein initiates the ubiquitinal degradation of Nrf2. Nrf2 dissociates from Keap1 by two ways: 1- directly by phosphorylation, 2- indirectly by signal induction due to endogenous or exogenous factors. After dissociation, Nrf2 binds to the promotor ARE

sequence in the nucleus and activates the transcription of antioxidant elements such as NQO1 and glutathione reductase (see Fig 5.9) [84]. In addition, Hyun *et al.* describes that two transcriptional factors, Nrf2, NF- κ B and HSP70 have elevated levels in a system with high oxidative stress [84].

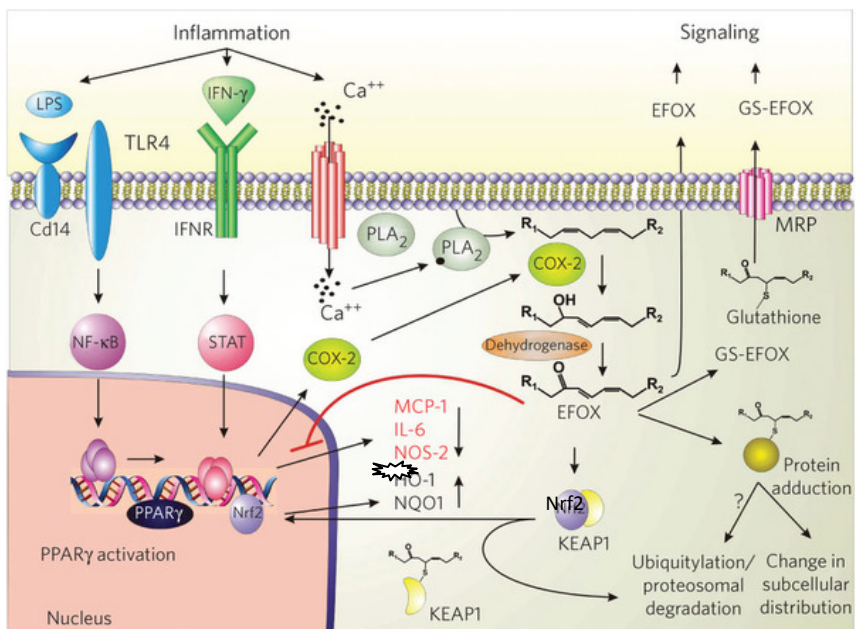


Fig 5.9: Mechanism of activation of ARE pathway. The antioxidant responsive element (ARE) is a regulatory element of genes encoding phase II detoxification enzymes and antioxidant proteins, such as NQO1 and glutathione S-transferases. Interestingly, it has been reported that Nrf2 regulates a wide array of ARE-driven genes in various cell types. The DNA binding sequence of Nrf2 and ARE sequence are very similar, and many studies demonstrated that Nrf2 binds to the ARE sites leading to up-regulation of downstream genes. The function of Nrf2 and its downstream target genes suggests that the Nrf2-ARE pathway is important in the cellular antioxidant defense system. Fig adapted from reference [84].

The Ross group identified the NQO1 localization in the nucleus of several colon and lung cancer cells using 3D-confocal microscopy [70]. The translocation of NQO1 proteins into the nucleus occurred through a nuclear pore complex [133]. The function of the nuclear NQO1 is to protect the DNA from damage and its repair through activation of Sirtuins 1 (SIRT1) and poly ADP-ribose polymerase (PARP) enzymes [61]. Further,

David *et al.* describes the NQO1 presence in mitotic spindle as well as in centrosomes in human pancreatic cancer cell [133]. Using the double-labeling immunostaining and specific antibodies against NQO1 they discovered that NQO1 is attached to alpha-tubulin in the mitotic spindle fiber [133].

5.3.2.2 Measurement of DCPIP Reductase Activity in Healthy and Diseased Myelin

To further characterize the NQO1, the DCPIP reductase activity was compared in diseased and healthy myelin in 7.7 months old mice (see Fig 5. 10). In both diseased and healthy myelin the activity increased with the concentration of DCPIP substrate. The DCPIP reductase activity was partially inhibited by dicoumarol in both groups. However, the statistical analysis indicated that there is almost the same level of inhibition in both groups. This partial inhibition (~40-45%) in older and diseased myelin is in contrast to the lack of inhibition of the DCPIP reductase activity in myelin from young mice (see chapter 4).

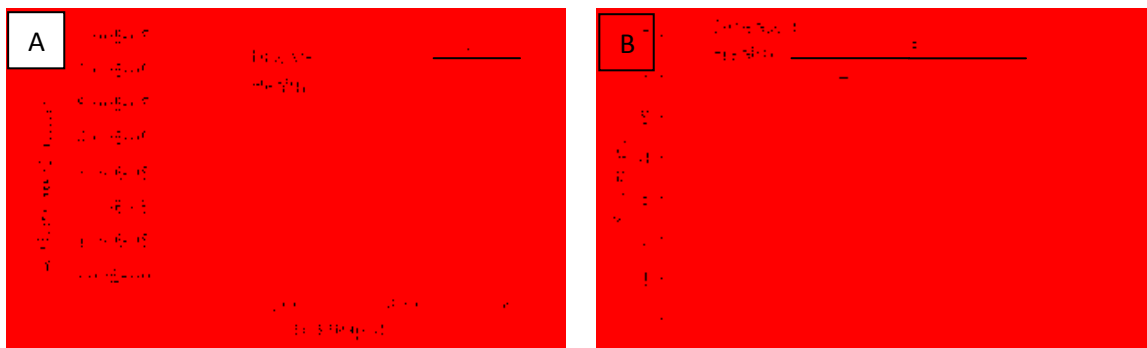


Fig 5.10: Comparison of DCPIP reductase activity in healthy and diseased myelin. Panel (A): Reductase activity as a function of DCPIP substrate concentration. Myelin (20μg) was assayed with various concentrations (10, 25, 100, 500μM) of DCPIP. The value of *p= 0.356. **Panel (B):** Inhibition of reductase activity with dicoumarol. The activity was measured with 20μg of protein and 50μM DCPIP in the presence of 50μM dicoumarol. The age of the mouse was 7.7 months. The t-test value of *p=0.255 established at 95% CI. To initiate the reaction 200μM of NADH was added and the final volume per well was 200μl. The measurement was taken at 600nm at 37°C for 5 minutes. All error bars are ±SE.

5.5 Conclusions

A preliminary study that compared the redox activities in age-matched healthy and diseased myelin was conducted. On the basis of current research findings it can be concluded that CB5R activity increases overall with age. As well, in healthy myelin the activity of CB5R was enhanced relative to age-matched diseased myelin. CB5R may be responsible for superoxide production, and high levels of oxidative stress occur in aging and in disease processes. It is hypothesized that superoxide spontaneously reacts with nitric oxide to form the reactive peroxynitrite ion that confers the permeability to BBB. Moreover, it could be one of the factors in etiology of MS.

The NQO1 was detected in the full length form at 30kDa by Western blot analysis in the diseased myelin from 7.7 and 11.3 months old mice. Only in the older healthy myelin (11.3 months) the full length form was detected; in the middle-aged myelin (7.7 months) a truncated form (~13 kDa) of the enzyme was found. Diseased state and age, correlate with the presence of full length NQO1. Moreover, the expression of NQO1 is under the control of the ARE factor, and can be induced by pathology and aging.

Chapter 6

Summary, Conclusions and Future Directions

This dissertation has utilized various kinetic assays and immunodetection techniques to identify the oxidoreductases in the CNS myelin. The conclusions based on the research work performed are drawn in this chapter. The identified proteins are compared on the basis of activities, structure and function. Moreover, a number of future avenues that can be explored to enhance present research are highlighted.

6.1 Summary and Conclusions

A study on the characterization of t-PMET in the myelin membrane was conducted. On the basis of current research, specific activities of all oxidoreductase are calculated in Table 6.1

Table 6.1: Specific activities of oxidoreductases with various substrates.

Oxidoreductase activity	Specific activity (nmol/min/mg)
NADH: cytochrome c reductase activity	3.401
NADH: DCPIP reductase activity	0.891
NADPH: DCPIP reductase activity	0.208
NADH: menadione reductase activity (with cytochrome c)	0.871
NADH: PMS reductase activity (with WST-1)	0.633
NADH-dependent WST-1 reduction	0.499

The specific activity of NADH: cytochrome c reductase (3.401nmol/min/mg) is greater in all above calculated oxidoreductase activities. The enzymes activities of NADH: DCPIP reductase and NADH: menadione reductase, 0.891 and 0.871 nm/min/mg respectively, are almost the same. In addition, NADH is the preferred electron donor for the enzyme which uses DCPIP as a substrate. Furthermore, NADPH: DCPIP reductase activity is lowest (0.208nm/min/mg) of all measured oxidoreductase activities.

Current study discovered that CB5R, a member of t-PMET system, is expressed in the mouse myelin membrane. The activity of CB5R was measured through cytochrome c reductase and was inhibited by pHMB, a specific inhibitor of CB5R. Furthermore, the CB5R has estimated V_{max} and K_M values as $6.58 \times 10^{-5} \mu\text{M}/\text{min}$ and $151\mu\text{M}$, respectively. The sulfhydryl agent pHMB, inhibited almost ~90% activity at a concentration of $10\mu\text{M}$. Differential detergent fractionation of myelin suggests that the CB5R may be localized in the lipid raft microdomains of myelin membrane. Furthermore, two bands detected by Western blotting may indicate the myristoylated and non-myristoylated forms of the protein.

The CB5R activity was also investigated in a diseased myelin model and compared to control healthy mouse myelin. The results illustrate the variation in activity over the normal growth period. In the healthy control, the 2 months old mouse myelin showed greater activity than the 7.7 months old mouse myelin; however, the greatest activity was in the 11.3 month old. Overall, the activity of CB5R increased with the age in both the myelinated (healthy) and demyelinated (diseased) state. Some recent studies found that the crucial roles affiliated to CB5R are superoxide production, controlling of

NO levels and the formation of peroxynitrite [134] . Furthermore, from previous studies it can be speculated that calcium toxicity is related to CB5R [12].

CB5R performs important cellular functions such as CoQ reduction, cholesterol synthesis, and fatty acid chain elongation. It is assumed that CB5R may perform similar functions in the myelin sheath. The major function of the oxidoreductases and specifically, CB5R, is to regenerate the NAD⁺ and replenish the pool of pyridine nucleotides, NAD⁺/NADH.

Immunodetection of NQO1 confirmed its presence in myelin membrane. Differential detergent fractionation of myelin and Western blot analysis indicates that NQO1 may be localized in the lipid raft microdomain of myelin membrane. In addition, Western blot analysis confirmed that NQO1 is present in truncated form. This truncated form could be mNQO-like form or degraded product of NQO1. The other protein band appeared with molecular weight ~27kDa could be the NQO2 or a novel NQO1 isoform. In diseased myelin, due to high oxidative stress, the NQO1 expression level was elevated and band appeared at 30kDa (full length) instead of ~13kDa. The fluctuation in the expression level may suggest its role in myelinogenesis, aging, and disease. Thus, it can be concluded that NQO1 associated activity is present in the myelin membrane but at a different level depending on cell function and physiological demands. Furthermore, the NQO1 gene is under the control of ARE promoter, which activates due to the effect of xenobiotics, oxidants, heavy metals and ionizing radiation.

Activity of NQO1 was measured through three associated activities: menadione-mediated cytochrome c reductase, PMS-mediated WST-1 reductase activity and DCPIP reductase activity. Kinetic analysis of the DCPIP reductase activity illustrated that the

enzyme is allosteric in nature. In addition, it is insensitive to dicoumarol, a potent inhibitor of NQO1, but due to several disadvantages of dicoumarol, such as lack of specificity, dicoumarol should be replaced by ES936 in future. The ES936 is more specific and mechanism-based inhibitor of NQO1. The DCPIP reductase activity was inhibited by DMSO, which has been previously used as G1 and M phase inhibitor in cell cultures. With lipid bilayers, DMSO can form pores and denature the protein when these proteins are present in cholesterol-rich domains [106]. As well enzymatic activity can be inhibited by DMSO due to unfolding and denaturation of protein. The reductase measured activities could be due to dehydrogenases or may be due to cyclin-dependent protein kinases or GAP. Moreover, in diseased myelin, DCPIP reductase activity was enhanced as compared to the healthy myelin of the same age, which shows its involvement in disease implication.

The pyridine nucleotide synthesis or ratio reduces due to the alteration of intracellular status. The reduced synthesis of pyridine nucleotide is compensated by reduced metabolism of glucose and fatty acids. The t-PMET may be responsible for maintaining NAD^+/NADH ratios in the myelin membrane. Therefore, in the cells where mitochondria is dysfunctional, t-PMET is elevated [61]. One of the functions of plasmalemmar CB5R enzyme is to produce the NAD^+ (a primary marker of intracellular status). As NADH-dependent enzyme, lactate dehydrogenase (LDH), is responsible for converting the pyruvate into lactate, along with lactate it also regenerates the NAD^+ . In myelin membrane, LDH is present, but by the 120th day of birth in mouse, its activity is less than 8% [135]. Thus, t-PMET can regenerate NAD^+ . This NAD^+ is utilized by other enzymes including sirtuin1 (SIRT 1) and sirtuin2 (SIRT 2) [136]. Sirtuins, which are localized in the plasma membrane and also found in myelin membrane, are NAD^+

dependent deacetylases [136]. Sirtuins expression in the myelin membrane is PLP and DM-20 dependent [61, 136]. Both SIRT1 and SIRT2 proteins perform vital cell functions such as cell cycle regulation, differentiation, chromatin stabilization, deacetylation, and PLP-dependent neuroprotection [136]. The most important role of SIRT2 is the deacetylation of MAG, an integral membrane protein found on the myelin layer closes to the axon. MAG protein inhibits the regeneration of neurons in the CNS [137, 138]. The level of NAD^+/NADH is responsible for sirtuins activation and deactivation. During aging NAD^+/NADH ratios are altered, and thus the activity of sirtuin is modulated. In plasma membrane, NAD^+ which is utilized by sirtuins, is regenerated by CB5R, NQO1, and other oxidoreductases (see Fig 6.1).

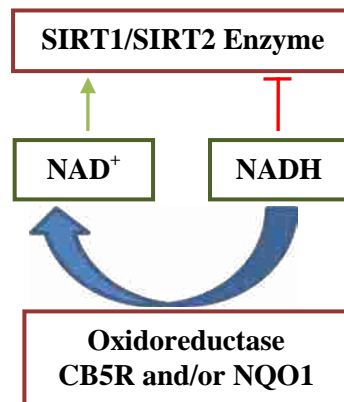


Fig 6.1: Regulatory mechanism of sirt1 by CB5R and other oxidoreductases in plasma membrane. SIRT1 maintains the respiration, deacetylation and cytosolic NAD^+/NADH ratios.

NQO1 is involved in several important functions such as chemo protection, protection of p53 gene and reduction of CoQ. The reduction of CoQ by NQO1 without forming the semiquinone is very crucial for cell survival. CoQ is very important as it electronically links the inner environment of the cell to the external environment of the cell. Within lipid bilayer of the plasma membrane and the myelin membranes, CoQ scavenges

superoxide radical with or without α -tocopherol by breaking the free radical chain reaction [28]. Reduced CoQ is also responsible for avoiding the apoptosis initiated by ceramide signaling. The ratio of CoQ/CoQH₂ is the modulator of sphingomyelinase [139]. Sphingomyelin, a very common and important phospholipid, is present in plasma membrane. This lipid is activated by an enzyme sphingomyelinase and has the ability to induce the apoptosis by initiating the ceramide signaling. CoQH₂ inhibits the activation of sphingomyelinase and protect the cell from unnecessary apoptotic signaling. The oxidized form of CoQ can accumulate the ceramide molecules which may lead to form ceramide-enriched platform. This platform can further initiate the death receptors to cluster in the membrane and can transmit an efficient death signal. The Fas receptors are also called death receptors, and are present on the surface of cells that leads to programmed cell death (apoptosis). It is one of two apoptosis pathways, the other being the mitochondrial pathway. Death receptor ligands characteristically initiate signaling via receptor oligomerization, which in turn results in the recruitment of specialized adaptor proteins and activation of caspase cascades [140, 141]. The mechanism is shown in the Fig 6.2.

In short, the major function of both identified enzymes is to maintain the NAD⁺/NADH ratios and to reduce the CoQ in myelin membrane. CB5R accomplish this task by one electron reductions while NQO1 reduces the CoQ by two electrons reduction and avoids the formation of ROS. The two electron reduction reaction in plasma membrane is also performed by GSH and NQO2 [142]. These two proteins perform almost the same function; it would be interesting to differentiate them on the basis of their similarities and differences (see Table 6.2).

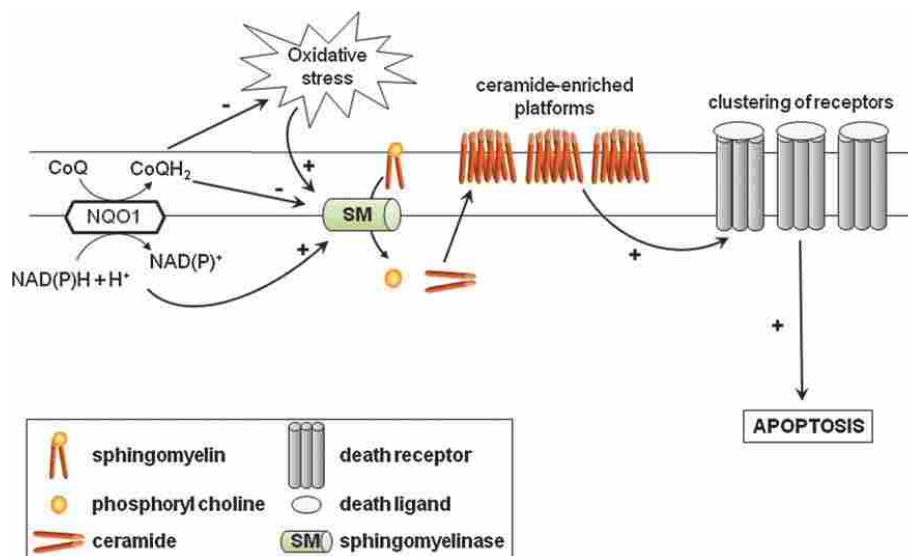


Fig 6.2: Architecture of ceramide signaling generated by NQO1/CoQ. The alteration of CoQ/CoQH₂ ratios can trigger the apoptosis. Once sphingomyelinase activated it can induce the death signal. Fig adapted from reference [139].

Table 6.2: Similarities and differences between CB5R and NQO1. The comparison is done on the basis of structure, function, and catalytic mode.

Based On	Similarities	Differences
Sub-cellular localization	Both proteins have multiple locations in the cell.	<ul style="list-style-type: none"> • CB5R is present in endoplasmic reticulum, Golgi bodies, mitochondria and plasma membrane. • NQO1 is present in cytosol, plasma membrane and nucleus.
Structure	Both proteins have two lobes and $\alpha\beta$ motifs.	<ul style="list-style-type: none"> • In CB5R both lobes are connected by a short hinge but it is monomeric protein. • NQO1 is homodimeric protein.
Prosthetic group	Both protein utilizes FAD as a prosthetic group.	<ul style="list-style-type: none"> • There is only one FAD group in CB5R. • Whereas in NQO1, there is one FAD per monomer.
Catalytic mode of action	Both reduce CoQ.	<ul style="list-style-type: none"> • CB5R catalysis the one electron reduction • NQO1 catalysis the two electron reduction
Enzyme nature	Both are oxidoreductases.	<ul style="list-style-type: none"> • CB5R exhibits the typical "lock and key" model of enzyme, hence follows the Michaelis Menten curve. • NQO1 exhibits the "induced fit" model and allosteric in nature.

In conclusion, taken together, the hypothesis of current research that "t-PMET assisting the myelin membrane" is supported as two components of t-PMET, CB5R and NQO1, were found in the myelin membrane, and another component, VDAC, was previously studied in our lab. The major function of both the identified proteins, CB5R and NQO1, is the regeneration of NAD^+ with the CoQ reduction by one and two electrons, respectively. Fig 6.3 illustrates the presence and function of CB5R and NQO1 in t-PMET.

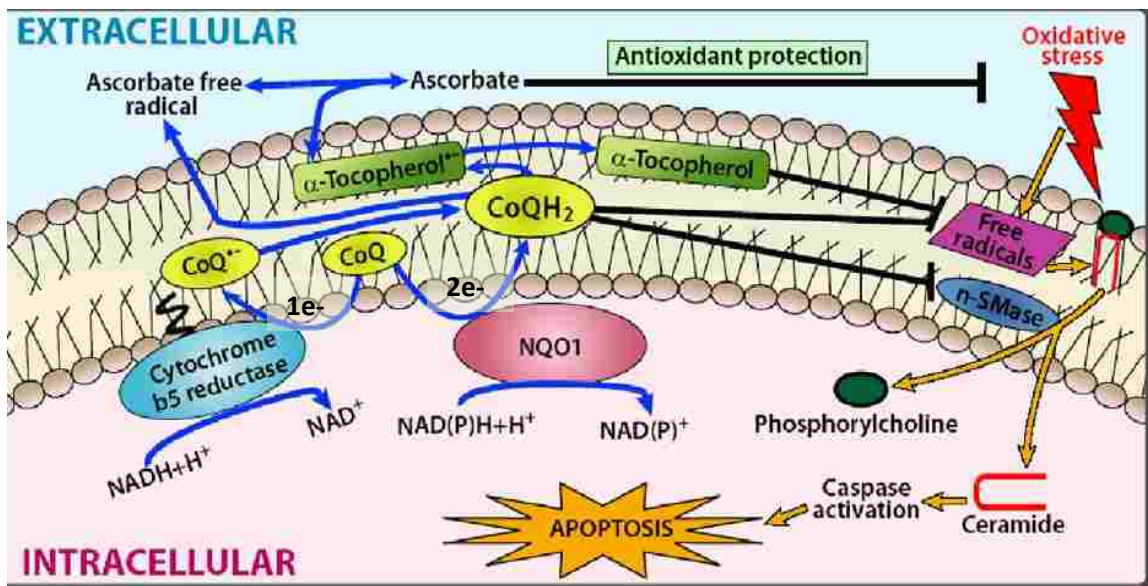


Fig 6.3: CB5R and NQO1 in t-PMET. CB5R catalysis one electron reduction while NQO1 catalysis two electron reduction of CoQ. Figure modified from reference [51].

In light of current research findings and previous studies, it can be concluded that the role of both identified proteins in disease state are interlinked. The overall scenario of both proteins in oxidative stress is depicted in Fig 6.4.

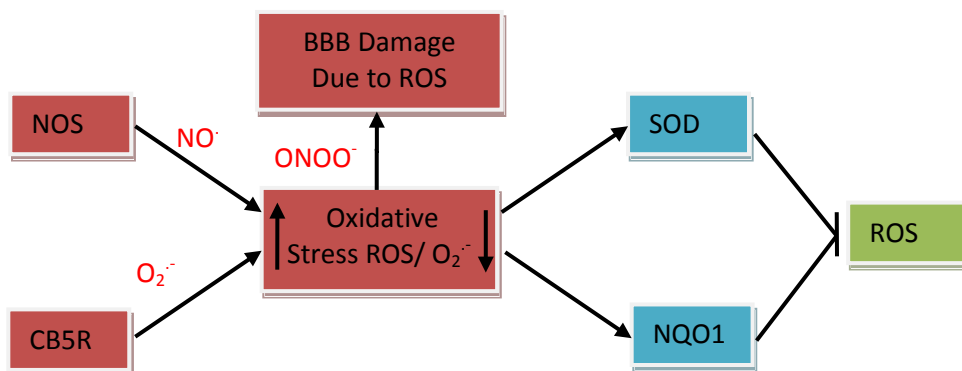


Fig 6.4: Role of NQO1 and CB5R in demyelination. Besides NOX, CB5R is another source of superoxide production and it also controls the release of NO. When function of CB5R is disrupted regardless of the cause, NO release becomes uncontrolled and it can form the peroxynitrite species, studies shows that it has the ability to damage the BBB, the barrier becomes permeable to T-cells, which destroys the myelin sheath. Alternatively, SOD and NQO1 try to dismutate and scavenge the superoxide respectively. But at threshold level oxidative stress is so high that NQO1 and SOD cannot accommodate it and result is the diseased condition or demyelination.

6.2 Future Directions

On the basis of this work, we have identified the following aspects that presented a good avenue for future investigation.

6.2.1 Bioanalytic Separation of Oxidoreductase Activities and the Proteomic Identification

Enzyme activity assay and western blot analysis confirm the presence of cytochrome b5 reductase and NQO1 in myelin membrane. It would be beneficial to separate and purify the enzyme responsible for these activities. For this purpose, a dye-affinity chromatography technique can be employed. Affinity chromatography is a method of separating biochemical mixtures based on a highly specific interaction such as

that between antigen and antibody, enzyme and substrate, or receptor and ligand. Affinity chromatography can be used to purify and concentrate a substance [143].

Blue-sepharose affinity chromatography can be used for enrichment of oxidoreductases from the myelin membrane. Blue-sepharose affinity chromatography uses cibacron blue as the ligand linked to a cellulose-meshwork, such as sepharose. Cibacron blue is a polycyclic dye resembling the structure of NADH. It is thought that resemblance with NADH allows cytochrome b5 reductase and NQO1 to bind with cibacron blue. Since the blue chromophore contains both amino and sulfonate groups, the so called “non-specific” ion-exchange effects would also be expected [144].

Some other future directions related directly or indirectly to current research are as follows:

- Proteomic analysis of all oxidoreductases in the myelin membrane
- Protein sequencing in diseased and healthy myelin should be done to detect any mutation in the enzyme.
- Instead of dicoumarol, inhibitor ES936 should be used for future NQO1 investigations.
- MS is a disease which is prevalent in the countries where the albedo coefficient of UV rays is very high. The effect of UV light on myelin membrane could reveal some interesting facts.
- Role of CB5R in calcium and peroxynitrite toxicity should be unmask.

References

- [1] D. Liewald, R. Miller, N. Logothetis, H.J. Wagner, A. Schuz, Distribution of axon diameters in cortical white matter: an electron-microscopic study on three human brains and a macaque, *Biol. Cybern.* (2014) .
- [2] E.M. Kolb, E.L. Rezende, L. Holness, A. Radtke, S.K. Lee, A. Obenaus, T. Garland Jr, Mice selectively bred for high voluntary wheel running have larger midbrains: support for the mosaic model of brain evolution, *J. Exp. Biol.* 216 (2013) 515-523.
- [3] J.J. Harris, D. Attwell, The energetics of CNS white matter, *J. Neurosci.* 32 (2012) 356-371.
- [4] A.I. Amaral, T.W. Meisingset, M.R. Kotter, U. Sonnewald, Metabolic aspects of neuron-oligodendrocyte-astrocyte interactions, *Front. Endocrinol. (Lausanne)* 4 (2013) 54.
- [5] G. Meinig, H.J. Reulen, C. Magawly, E.J. Zollner, Brain energy metabolism in global brain oedema, *Acta Neurochir. (Wien)* 41 (1978) 273-286.
- [6] M. Simons, J. Trotter, Wrapping it up: the cell biology of myelination, *Curr. Opin. Neurobiol.* 17 (2007) 533-540.
- [7] R.D. Fields, Myelin formation and remodeling, *Cell* 156 (2014) 15-17.
- [8] S. Ravera, M. Bartolucci, G. Barbarito, D. Calzia, I. Panfoli, Electrophoretic separation of purified myelin: a method to improve the protein pattern resolving, *Prep. Biochem. Biotechnol.* 43 (2013) 342-349.

- [9] B.M. Morrison, Y. Lee, J.D. Rothstein, Oligodendroglia: metabolic supporters of axons, *Trends Cell Biol.* 23 (2013) 644-651.
- [10] A.M. Messier, O.A. Bizzozero, Conserved fatty acid composition of proteolipid protein during brain development and in myelin subfractions, *Neurochem. Res.* 25 (2000) 449-455.
- [11] A. Ishii, R. Dutta, G.M. Wark, S.I. Hwang, D.K. Han, B.D. Trapp, S.E. Pfeiffer, R. Bansal, Human myelin proteome and comparative analysis with mouse myelin, *Proc. Natl. Acad. Sci. U. S. A.* 106 (2009) 14605-14610.
- [12] K.A. Nave, Myelination and the trophic support of long axons, *Nat. Rev. Neurosci.* 11 (2010) 275-283.
- [13] F. Zipp, O. Aktas, The brain as a target of inflammation: common pathways link inflammatory and neurodegenerative diseases, *Trends Neurosci.* 29 (2006) 518-527.
- [14] C.J. van den Berg, D. Garfinkel, A stimulation study of brain compartments. Metabolism of glutamate and related substances in mouse brain, *Biochem. J.* 123 (1971) 211-218.
- [15] U. Funfschilling, L.M. Supplie, D. Mahad, S. Boretius, A.S. Saab, J. Edgar, B.G. Brinkmann, C.M. Kassmann, I.D. Tzvetanova, W. Mobius, F. Diaz, D. Meijer, U. Suter, B. Hamprecht, M.W. Sereda, C.T. Moraes, J. Frahm, S. Goebbels, K.A. Nave, Glycolytic oligodendrocytes maintain myelin and long-term axonal integrity, *Nature* 485 (2012) 517-521.

- [16] A.D. de Grey, A hypothesis for the minimal overall structure of the mammalian plasma membrane redox system, *Protoplasma* 221 (2003) 3-9.
- [17] D. Del Principe, L. Avigliano, I. Savini, M.V. Catani, Trans-Plasma Membrane Electron Transport in Mammals: Functional Significance in Health and Disease, *Antioxidants & Redox Signaling* 14 (2011) 2289-2318.
- [18] M.M. VanDuijn, J. Van der Zee, P.J. Van den Broek, The ascorbate-driven reduction of extracellular ascorbate free radical by the erythrocyte is an electrogenic process, *FEBS Lett.* 491 (2001) 67-70.
- [19] D. Marques-da-Silva, A.K. Samhan-Arias, T. Tiago, C. Gutierrez-Merino, L-type calcium channels and cytochrome b5 reductase are components of protein complexes tightly associated with lipid rafts microdomains of the neuronal plasma membrane, *J. Proteomics* 73 (2010) 1502-1510.
- [20] A.T. Dinkova-Kostova, P. Talalay, NAD(P)H:quinone acceptor oxidoreductase 1 (NQO1), a multifunctional antioxidant enzyme and exceptionally versatile cytoprotector, *Arch. Biochem. Biophys.* 501 (2010) 116-123.
- [21] G. Cheng, J.D. Lambeth, Alternative mRNA splice forms of NOXO1: differential tissue expression and regulation of Nox1 and Nox3, *Gene* 356 (2005) 118-126.
- [22] J.L. Turi, X. Wang, A.T. McKie, E. Nozik-Grayck, L.B. Mamo, K. Crissman, C.A. Piantadosi, A.J. Ghio, Duodenal cytochrome b: a novel ferrireductase in airway epithelial cells, *Am. J. Physiol. Lung Cell. Mol. Physiol.* 291 (2006) L272-80.

- [23] S. Villinger, K. Giller, M. Bayrhuber, A. Lange, C. Griesinger, S. Becker, M. Zweckstetter, Nucleotide interactions of the human voltage-dependent anion channel, *J. Biol. Chem.* 289 (2014) 13397-13406.
- [24] F.L. Crane, I.L. Sun, R. Barr, H. Low, Electron and proton transport across the plasma membrane, *J. Bioenerg. Biomembr.* 23 (1991) 773-803.
- [25] J. Rivlin, J. Mendel, S. Rubinstein, N. Etkovitz, H. Breitbart, Role of hydrogen peroxide in sperm capacitation and acrosome reaction, *Biol. Reprod.* 70 (2004) 518-522.
- [26] S.C. Rogers, A. Said, D. Corcuera, D. McLaughlin, P. Kell, A. Doctor, Hypoxia limits antioxidant capacity in red blood cells by altering glycolytic pathway dominance, *FASEB J.* 23 (2009) 3159-3170.
- [27] L.M. Wang, Q.L. Duan, F. Yang, X.H. Yi, Y. Zeng, H.Y. Tian, W. Lv, Y. Jin, Activation of circulated immune cells and inflammatory immune adherence are involved in the whole process of acute venous thrombosis, *Int. J. Clin. Exp. Med.* 7 (2014) 566-572.
- [28] S.F. Martin, C. Gomez-Diaz, R.I. Bello, P. Navas, J.M. Villalba, Inhibition of neutral Mg²⁺-dependent sphingomyelinase by ubiquinol-mediated plasma membrane electron transport, *Protoplasma* 221 (2003) 109-116.
- [29] P.M. Herst, M.V. Berridge, Cell surface oxygen consumption: a major contributor to cellular oxygen consumption in glycolytic cancer cell lines, *Biochim. Biophys. Acta* 1767 (2007) 170-177.

- [30] K. Yagiz, L.Y. Wu, C.P. Kuntz, D. James Morre, D.M. Morre, Mouse embryonic fibroblast cells from transgenic mice overexpressing tNOX exhibit an altered growth and drug response phenotype, *J. Cell. Biochem.* 101 (2007) 295-306.
- [31] R.M. Touyz, E.L. Schiffrin, Increased generation of superoxide by angiotensin II in smooth muscle cells from resistance arteries of hypertensive patients: role of phospholipase D-dependent NAD(P)H oxidase-sensitive pathways, *J. Hypertens.* 19 (2001) 1245-1254.
- [32] A. del Castillo-Olivares, I. Nunez de Castro, M.A. Medina, Dual role of plasma membrane electron transport systems in defense, *Crit. Rev. Biochem. Mol. Biol.* 35 (2000) 197-220.
- [33] D.J. Lane, A. Lawen, Transplasma membrane electron transport comes in two flavors, *Biofactors* 34 (2008) 191-200.
- [34] T. Seno, N. Inoue, D. Gao, M. Okuda, Y. Sumi, K. Matsui, S. Yamada, K.I. Hirata, S. Kawashima, R. Tawa, S. Imajoh-Ohmi, H. Sakurai, M. Yokoyama, Involvement of NADH/NADPH oxidase in human platelet ROS production, *Thromb. Res.* 103 (2001) 399-409.
- [35] T. Kishi, D.M. Morre, D.J. Morre, The plasma membrane NADH oxidase of HeLa cells has hydroquinone oxidase activity, *Biochim. Biophys. Acta* 1412 (1999) 66-77.

- [36] M.C. Bewley, C.C. Marohnic, M.J. Barber, The structure and biochemistry of NADH-dependent cytochrome b5 reductase are now consistent, *Biochemistry* 40 (2001) 13574-13582.
- [37] M. Geiszt, T.L. Leto, The Nox family of NAD(P)H oxidases: host defense and beyond, *J. Biol. Chem.* 279 (2004) 51715-51718.
- [38] Lehninger principles of biochemistry, 4th ed, Scitech Book News 29 (2005) .
- [39] W.T. Norton, Isolation of myelin and its related structures. General principles, *Neurosci. Res. Program Bull.* 9 (1971) 502-504.
- [40] L.J. Pike, Lipid rafts: bringing order to chaos, *J. Lipid Res.* 44 (2003) 655-667.
- [41] L.S. Debruin, G. Harauz, White matter rafting--membrane microdomains in myelin, *Neurochem. Res.* 32 (2007) 213-228.
- [42] J. Karthigasan, B. Kosaras, J. Nguyen, D.A. Kirschner, Protein and lipid composition of radial component-enriched CNS myelin, *J. Neurochem.* 62 (1994) 1203-1213.
- [43] C.M. Taylor, T. Coetzee, S.E. Pfeiffer, Detergent-insoluble glycosphingolipid/cholesterol microdomains of the myelin membrane, *J. Neurochem.* 81 (2002) 993-1004.

- [44] J. Karthigasan, B. Kosaras, J. Nguyen, D.A. Kirschner, Protein and lipid composition of radial component-enriched CNS myelin, *J. Neurochem.* 62 (1994) 1203-1213.
- [45] P. Strittmatter, The reaction sequence in electron transfer in the reduced nicotinamide adenine dinucleotide-cytochrome b5 reductase system, *J. Biol. Chem.* 240 (1965) 4481-4487.
- [46] M. Yamada, T. Tamada, K. Takeda, F. Matsumoto, H. Ohno, M. Kosugi, K. Takaba, Y. Shoyama, S. Kimura, R. Kuroki, K. Miki, Elucidations of the catalytic cycle of NADH-cytochrome b5 reductase by X-ray crystallography: new insights into regulation of efficient electron transfer, *J. Mol. Biol.* 425 (2013) 4295-4306.
- [47] S. Tomatsu, Y. Kobayashi, Y. Fukumaki, T. Yubisui, T. Orii, Y. Sakaki, The organization and the complete nucleotide sequence of the human NADH-cytochrome b5 reductase gene, *Gene* 80 (1989) 353-361.
- [48] J. Ozols, S.A. Carr, P. Strittmatter, Identification of the NH₂-terminal blocking group of NADH-cytochrome b5 reductase as myristic acid and the complete amino acid sequence of the membrane-binding domain, *J. Biol. Chem.* 259 (1984) 13349-13354.
- [49] S. Kimura, M. Kawamura, T. Iyanagi, Role of Thr(66) in porcine NADH-cytochrome b5 reductase in catalysis and control of the rate-limiting step in electron transfer, *J. Biol. Chem.* 278 (2003) 3580-3589.

- [50] S. Kim, M. Suga, K. Ogasahara, T. Ikegami, Y. Minami, T. Yubisui, T. Tsukihara, Structure of *Physarum polycephalum* cytochrome b5 reductase at 1.56 Å resolution, *Acta Crystallogr. Sect. F. Struct. Biol. Cryst. Commun.* 63 (2007) 274-279.
- [51] P. Navas, J.M. Villalba, R. de Cabo, The importance of plasma membrane coenzyme Q in aging and stress responses, *Mitochondrion* 7 Suppl (2007) S34-40.
- [52] S. Bando, T. Takano, T. Yubisui, K. Shirabe, M. Takeshita, A. Nakagawa, Structure of human erythrocyte NADH-cytochrome b5 reductase, *Acta Crystallogr. D Biol. Crystallogr.* 60 (2004) 1929-1934.
- [53] S.R. Keyes, D.L. Cinti, Biochemical properties of cytochrome b5-dependent microsomal fatty acid elongation and identification of products, *J. Biol. Chem.* 255 (1980) 11357-11364.
- [54] J.R. Kurian, S.U. Bajad, J.L. Miller, N.A. Chin, L.A. Trepanier, NADH cytochrome b5 reductase and cytochrome b5 catalyze the microsomal reduction of xenobiotic hydroxylamines and amidoximes in humans, *J. Pharmacol. Exp. Ther.* 311 (2004) 1171-1178.
- [55] D.E. Hultquist, P.G. Passon, Catalysis of methaemoglobin reduction by erythrocyte cytochrome B5 and cytochrome B5 reductase, *Nat. New Biol.* 229 (1971) 252-254.
- [56] A. Bulbarelli, A. Valentini, M. DeSilvestris, M.D. Cappellini, N. Borgese, An erythroid-specific transcript generates the soluble form of NADH-cytochrome b5 reductase in humans, *Blood* 92 (1998) 310-319.

- [57] H.M. Barham, R. Inglis, E.C. Chinje, I.J. Stratford, Development and validation of a spectrophotometric assay for measuring the activity of NADH: cytochrome b5 reductase in human tumour cells, *Br. J. Cancer* 74 (1996) 1188-1193.
- [58] N. Borgese, G. Pietrini, Distribution of the integral membrane protein NADH-cytochrome b5 reductase in rat liver cells, studied with a quantitative radioimmunoblotting assay, *Biochem. J.* 239 (1986) 393-403.
- [59] A.K. Samhan-Arias, M.A. Garcia-Bereguiain, F.J. Martin-Romero, C. Gutierrez-Merino, Clustering of plasma membrane-bound cytochrome b5 reductase within 'lipid raft' microdomains of the neuronal plasma membrane, *Mol. Cell. Neurosci.* 40 (2009) 14-26.
- [60] A.K. Samhan-Arias, C. Gutierrez-Merino, Purified NADH-cytochrome b5 reductase is a novel superoxide anion source inhibited by apocynin: sensitivity to nitric oxide and peroxynitrite, *Free Radic. Biol. Med.* 73 (2014) 174-189.
- [61] R. de Cabo, E. Siendones, R. Minor, P. Navas, CYB5R3: a key player in aerobic metabolism and aging? *Aging (Albany NY)* 2 (2009) 63-68.
- [62] J.M. Villalba, F. Navarro, F. Cordoba, A. Serrano, A. Arroyo, F.L. Crane, P. Navas, Coenzyme Q reductase from liver plasma membrane: purification and role in trans-plasma-membrane electron transport, *Proc. Natl. Acad. Sci. U. S. A.* 92 (1995) 4887-4891.

- [63] E.C. Kennett, P.W. Kuchel, Redox reactions and electron transfer across the red cell membrane, *IUBMB Life* 55 (2003) 375-385.
- [64] K. Shirabe, T. Yubisui, T. Nishino, M. Takeshita, Role of cysteine residues in human NADH-cytochrome b5 reductase studied by site-directed mutagenesis. Cys-273 and Cys-283 are located close to the NADH-binding site but are not catalytically essential, *J. Biol. Chem.* 266 (1991) 7531-7536.
- [65] S.M. Kilbride, S.A. Gluchowska, J.E. Telford, C. O'Sullivan, G.P. Davey, High-level inhibition of mitochondrial complexes III and IV is required to increase glutamate release from the nerve terminal, *Mol. Neurodegener* 6 (2011) 53-1326-6-53.
- [66] F. Navarro, P. Navas, J.R. Burgess, R.I. Bello, R. De Cabo, A. Arroyo, J.M. Villalba, Vitamin E and selenium deficiency induces expression of the ubiquinone-dependent antioxidant system at the plasma membrane, *FASEB J.* 12 (1998) 1665-1673.
- [67] A.K. Jaiswal, Human NAD(P)H:quinone oxidoreductase (NQO1) gene structure and induction by dioxin, *Biochemistry* 30 (1991) 10647-10653.
- [68] R. Li, M.A. Bianchet, P. Talalay, L.M. Amzel, The three-dimensional structure of NAD(P)H:quinone reductase, a flavoprotein involved in cancer chemoprotection and chemotherapy: mechanism of the two-electron reduction, *Proc. Natl. Acad. Sci. U. S. A.* 92 (1995) 8846-8850.
- [69] R.D. Bongard, B.J. Lindemer, G.S. Krenz, M.P. Merker, Preferential utilization of NADPH as the endogenous electron donor for NAD(P)H:quinone oxidoreductase 1

(NQO1) in intact pulmonary arterial endothelial cells, *Free Radic. Biol. Med.* 46 (2009) 25-32.

[70] S.L. Winski, Y. Koutalos, D.L. Bentley, D. Ross, Subcellular localization of NAD(P)H:quinone oxidoreductase 1 in human cancer cells, *Cancer Res.* 62 (2002) 1420-1424.

[71] G. Asher, O. Dym, P. Tsvetkov, J. Adler, Y. Shaul, The crystal structure of NAD(P)H quinone oxidoreductase 1 in complex with its potent inhibitor dicoumarol, *Biochemistry* 45 (2006) 6372-6378.

[72] M.A. Bianchet, M. Faig, L.M. Amzel, Structure and mechanism of NAD[P]H:quinone acceptor oxidoreductases (NQO), *Methods Enzymol.* 382 (2004) 144-174.

[73] M. Faig, M.A. Bianchet, P. Talalay, S. Chen, S. Winski, D. Ross, L.M. Amzel, Structures of recombinant human and mouse NAD(P)H:quinone oxidoreductases: species comparison and structural changes with substrate binding and release, *Proc. Natl. Acad. Sci. U. S. A.* 97 (2000) 3177-3182.

[74] L.M. Nutter, E.O. Ngo, G.R. Fisher, P.L. Gutierrez, DNA strand scission and free radical production in menadione-treated cells. Correlation with cytotoxicity and role of NADPH quinone acceptor oxidoreductase, *J. Biol. Chem.* 267 (1992) 2474-2479.

- [75] D. Siegel, D.L. Gustafson, D.L. Dehn, J.Y. Han, P. Boonchoong, L.J. Berliner, D. Ross, NAD(P)H:quinone oxidoreductase 1: role as a superoxide scavenger, *Mol. Pharmacol.* 65 (2004) 1238-1247.
- [76] D. Siegel, D.L. Gustafson, D.L. Dehn, J.Y. Han, P. Boonchoong, L.J. Berliner, D. Ross, NAD(P)H:quinone oxidoreductase 1: role as a superoxide scavenger, *Mol. Pharmacol.* 65 (2004) 1238-1247.
- [77] A. Tang, N.P. Curthoys, Identification of zeta-crystallin/NADPH:quinone reductase as a renal glutaminase mRNA pH response element-binding protein, *J. Biol. Chem.* 276 (2001) 21375-21380.
- [78] G. Asher, P. Tsvetkov, C. Kahana, Y. Shaul, A mechanism of ubiquitin-independent proteasomal degradation of the tumor suppressors p53 and p73, *Genes Dev.* 19 (2005) 316-321.
- [79] R. De Cabo, R. Cabello, M. Rios, G. Lopez-Lluch, D.K. Ingram, M.A. Lane, P. Navas, Calorie restriction attenuates age-related alterations in the plasma membrane antioxidant system in rat liver, *Exp. Gerontol.* 39 (2004) 297-304.
- [80] A.S. Tan, M.V. Berridge, Superoxide produced by activated neutrophils efficiently reduces the tetrazolium salt, WST-1 to produce a soluble formazan: a simple colorimetric assay for measuring respiratory burst activation and for screening anti-inflammatory agents, *J. Immunol. Methods* 238 (2000) 59-68.

- [81] S.O. Lee, Y.C. Chang, K. Whang, C.H. Kim, I.S. Lee, Role of NAD(P)H:quinone oxidoreductase 1 on tumor necrosis factor- α -induced migration of human vascular smooth muscle cells, *Cardiovasc. Res.* 76 (2007) 331-339.
- [82] A.K. Jaiswal, Regulation of genes encoding NAD(P)H:quinone oxidoreductases, *Free Radic. Biol. Med.* 29 (2000) 254-262.
- [83] T. Cresteil, A.K. Jaiswal, High levels of expression of the NAD(P)H:quinone oxidoreductase (NQO1) gene in tumor cells compared to normal cells of the same origin, *Biochem. Pharmacol.* 42 (1991) 1021-1027.
- [84] D.H. Hyun, J. Kim, C. Moon, C.J. Lim, R. de Cabo, M.P. Mattson, The plasma membrane redox enzyme NQO1 sustains cellular energetics and protects human neuroblastoma cells against metabolic and proteotoxic stress, *Age (Dordr)* 34 (2012) 359-370.
- [85] J. van Horssen, G. Schreibelt, L. Bo, L. Montagne, B. Drukarch, F.L. van Muiswinkel, H.E. de Vries, NAD(P)H:quinone oxidoreductase 1 expression in multiple sclerosis lesions, *Free Radic. Biol. Med.* 41 (2006) 311-317.
- [86] J.L. Stringer, A. Gaikwad, B.N. Gonzales, D.J. Long Jr, L.M. Marks, A.K. Jaiswal, Presence and induction of the enzyme NAD(P)H: quinone oxidoreductase 1 in the central nervous system, *J. Comp. Neurol.* 471 (2004) 289-297.
- [87] A.K. Jaiswal, Human NAD(P)H:quinone oxidoreductase2. Gene structure, activity, and tissue-specific expression, *J. Biol. Chem.* 269 (1994) 14502-14508.

- [88] A.K. Jaiswal, Characterization and partial purification of microsomal NAD(P)H:quinone oxidoreductases, *Arch. Biochem. Biophys.* 375 (2000) 62-68.
- [89] P.Y. Gasdaska, H. Fisher, G. Powis, An alternatively spliced form of NQO1 (DT-diaphorase) messenger RNA lacking the putative quinone substrate binding site is present in human normal and tumor tissues, *Cancer Res.* 55 (1995) 2542-2547.
- [90] S. Chen, K. Wu, R. Knox, Structure-function studies of DT-diaphorase (NQO1) and NRH: quinone oxidoreductase (NQO2), *Free Radic. Biol. Med.* 29 (2000) 276-284.
- [91] H. Sakagami, K. Satoh, Y. Hakeda, M. Kumegawa, Apoptosis-inducing activity of vitamin C and vitamin K, *Cell. Mol. Biol. (Noisy-Le-Grand)* 46 (2000) 129-143.
- [92] A.K. Samhan-Arias, C. Gutierrez-Merino, Purified NADH-cytochrome b5 reductase is a novel superoxide anion source inhibited by apocynin: sensitivity to nitric oxide and peroxynitrite, *Free Radic. Biol. Med.* 73 (2014) 174-189.
- [93] A.I. Boullerne, J.A. Benjamins, Nitric oxide synthase expression and nitric oxide toxicity in oligodendrocytes, *Antioxid. Redox Signal.* 8 (2006) 967-980.
- [94] A.S. Tan, M.V. Berridge, Superoxide produced by activated neutrophils efficiently reduces the tetrazolium salt, WST-1 to produce a soluble formazan: a simple colorimetric assay for measuring respiratory burst activation and for screening anti-inflammatory agents, *J. Immunol. Methods* 238 (2000) 59-68.

- [95] C.M. Cabello, W.B. Bair 3rd, A.S. Bause, G.T. Wondrak, Antimelanoma activity of the redox dye DCPIP (2,6-dichlorophenolindophenol) is antagonized by NQO1, *Biochem. Pharmacol.* 78 (2009) 344-354.
- [96] D.L. Gustafson, D. Siegel, J.C. Rastatter, A.L. Merz, J.C. Parpal, J.K. Kepa, D. Ross, M.E. Long, Kinetics of NAD(P)H:quinone oxidoreductase I (NQO1) inhibition by mitomycin C in vitro and in vivo, *J. Pharmacol. Exp. Ther.* 305 (2003) 1079-1086.
- [97] M.C. Reed, A. Lieb, H.F. Nijhout, The biological significance of substrate inhibition: a mechanism with diverse functions, *Bioessays* 32 (2010) 422-429.
- [98] D.L. Dehn, D. Siegel, E. Swann, C.J. Moody, D. Ross, Biochemical, cytotoxic, and genotoxic effects of ES936, a mechanism-based inhibitor of NAD(P)H:quinone oxidoreductase 1, in cellular systems, *Mol. Pharmacol.* 64 (2003) 714-720.
- [99] P.C. Preusch, D. Siegel, N.W. Gibson, D. Ross, A note on the inhibition of DT-diaphorase by dicoumarol, *Free Radic. Biol. Med.* 11 (1991) 77-80.
- [100] P. Schopfer, E. Heyno, F. Drepper, A. Krieger-Liszkay, Naphthoquinone-dependent generation of superoxide radicals by quinone reductase isolated from the plasma membrane of soybean, *Plant Physiol.* 147 (2008) 864-878.
- [101] C.E. Ganote, J. Worstell, J.P. Kaltenbach, Oxygen-induced enzyme release after irreversible myocardial injury. Effects of cyanide in perfused rat hearts, *Am. J. Pathol.* 84 (1976) 327-350.

- [102] S. Zolnierowicz, M. Zelewski, J. Swierczynski, J. Marszalek, L. Zelewski, Cyanide--an uncompetitive inhibitor of NAD(P)-dependent malic enzyme from human term placental mitochondria, *Biochem. Int.* 17 (1988) 303-309.
- [103] M. Cannon, S. Harford, J. Davies, A comparative study on the inhibitory actions of chloramphenicol, thiamphenicol and some fluorinated derivatives, *J. Antimicrob. Chemother.* 26 (1990) 307-317.
- [104] L.L. Pearce, E. Lopez Manzano, S. Martinez-Bosch, J. Peterson, Antagonism of nitric oxide toward the inhibition of cytochrome c oxidase by carbon monoxide and cyanide, *Chem. Res. Toxicol.* 21 (2008) 2073-2081.
- [105] M. Fiore, R. Zanier, F. Degrassi, Reversible G(1) arrest by dimethyl sulfoxide as a new method to synchronize Chinese hamster cells, *Mutagenesis* 17 (2002) 419-424.
- [106] M.A. de Menorval, L.M. Mir, M.L. Fernandez, R. Reigada, Effects of dimethyl sulfoxide in cholesterol-containing lipid membranes: a comparative study of experiments in silico and with cells, *PLoS One* 7 (2012) e41733.
- [107] R. Zurbriggen, J.L. Dreyer, An NADH-diaphorase is located at the cell plasma membrane in a mouse neuroblastoma cell line NB41A3, *Biochim. Biophys. Acta* 1183 (1994) 513-520.
- [108] J. Tocharus, S. Chongthammakun, P. Govitrapong, Melatonin inhibits amphetamine-induced nitric oxide synthase mRNA overexpression in microglial cell lines, *Neurosci. Lett.* 439 (2008) 134-137.

- [109] K. Wu, R. Knox, X.Z. Sun, P. Joseph, A.K. Jaiswal, D. Zhang, P.S. Deng, S. Chen, Catalytic properties of NAD(P)H:quinone oxidoreductase-2 (NQO2), a dihydronicotinamide riboside dependent oxidoreductase, Arch. Biochem. Biophys. 347 (1997) 221-228.
- [110] F.D. Lublin, S.C. Reingold, Defining the clinical course of multiple sclerosis: results of an international survey. National Multiple Sclerosis Society (USA) Advisory Committee on Clinical Trials of New Agents in Multiple Sclerosis, Neurology 46 (1996) 907-911.
- [111] O. Fernandez, J.C. Alvarez-Cermeno, C. Arnal-Garcia, R. Arroyo-Gonzalez, L. Brieva, M.C. Calles-Hernandez, B. Casanova-Estruch, M. Comabella, J.A. Garcia-Merino, G. Izquierdo, J.E. Meca-Lallana, M.M. Mendibe-Bilbao, D. Munoz-Garcia, J. Olascoaga, P. Oliva-Nacarino, C. Oreja-Guevara, J.M. Prieto, L. Ramio-Torrenta, L. Romero-Pinel, A. Saiz, A. Rodriguez-Antiguedad, G.P. Grupo Post-Ectrimis, Review of the novelties presented at the 29th Congress of the European Committee for Treatment and Research in Multiple Sclerosis (ECTRIMS) (I), Rev. Neurol. 59 (2014) 269-280.
- [112] A.E. Miller, J.S. Wolinsky, L. Kappos, G. Comi, M.S. Freedman, T.P. Olsson, D. Bauer, M. Benamor, P. Truffinet, P.W. O'Connor, for the TOPIC Study Group, Oral teriflunomide for patients with a first clinical episode suggestive of multiple sclerosis (TOPIC): a randomised, double-blind, placebo-controlled, phase 3 trial, Lancet Neurol. (2014) .

- [113] M. Panos, G.P. Christophi, M. Rodriguez, I.A. Scarisbrick, Differential expression of multiple kallikreins in a viral model of multiple sclerosis points to unique roles in the innate and adaptive immune response, *Biol. Chem.* 395 (2014) 1063-1073.
- [114] F.G. Mastronardi, C.A. Ackerley, L. Arsenault, B.I. Roots, M.A. Moscarello, Demyelination in a transgenic mouse: a model for multiple sclerosis, *J. Neurosci. Res.* 36 (1993) 315-324.
- [115] M.A. Baker, A. Krutskikh, B.J. Curry, L. Hetherington, R.J. Aitken, Identification of cytochrome-b5 reductase as the enzyme responsible for NADH-dependent lucigenin chemiluminescence in human spermatozoa, *Biol. Reprod.* 73 (2005) 334-342.
- [116] B.M. Babior, R.S. Kipnes, J.T. Curnutte, Biological defense mechanisms. The production by leukocytes of superoxide, a potential bactericidal agent, *J. Clin. Invest.* 52 (1973) 741-744.
- [117] C. Domenicotti, B. Marengo, D. Verzola, G. Garibotto, N. Traverso, S. Patriarca, G. Maloberti, D. Cottalasso, G. Poli, M. Passalacqua, E. Melloni, M.A. Pronzato, U.M. Marinari, Role of PKC-delta activity in glutathione-depleted neuroblastoma cells, *Free Radic. Biol. Med.* 35 (2003) 504-516.
- [118] G. Lopez-Lluch, M. Rios, M.A. Lane, P. Navas, R. de Cabo, Mouse liver plasma membrane redox system activity is altered by aging and modulated by calorie restriction, *Age (Dordr)* 27 (2005) 153-160.

- [119] A.C. Straub, A.W. Lohman, M. Billaud, S.R. Johnstone, S.T. Dwyer, M.Y. Lee, P.S. Bortz, A.K. Best, L. Columbus, B. Gaston, B.E. Isakson, Endothelial cell expression of haemoglobin alpha regulates nitric oxide signalling, *Nature* 491 (2012) 473-477.
- [120] A.I. Boullerne, J.A. Benjamins, Nitric oxide synthase expression and nitric oxide toxicity in oligodendrocytes, *Antioxid. Redox Signal.* 8 (2006) 967-980.
- [121] F. Torreilles, S. Salman-Tabcheh, M. Guerin, J. Torreilles, Neurodegenerative disorders: the role of peroxynitrite, *Brain Res. Brain Res. Rev.* 30 (1999) 153-163.
- [122] K.H. Tan, S. Harrington, W.M. Purcell, R.D. Hurst, Peroxynitrite mediates nitric oxide-induced blood-brain barrier damage, *Neurochem. Res.* 29 (2004) 579-587.
- [123] P.M. Paez, V. Spreuer, V. Handley, J.M. Feng, C. Campagnoni, A.T. Campagnoni, Increased expression of golli myelin basic proteins enhances calcium influx into oligodendroglial cells, *J. Neurosci.* 27 (2007) 12690-12699.
- [124] S.P. Yu, D.W. Choi, Na(+)-Ca²⁺ exchange currents in cortical neurons: concomitant forward and reverse operation and effect of glutamate, *Eur. J. Neurosci.* 9 (1997) 1273-1281.
- [125] K.A. Nave, Myelination and support of axonal integrity by glia, *Nature* 468 (2010) 244-252.
- [126] A.D. de Grey, A proposed mechanism for the lowering of mitochondrial electron leak by caloric restriction, *Mitochondrion* 1 (2001) 129-139.

- [127] P. Tsvetkov, Y. Adamovich, E. Elliott, Y. Shaul, E3 ligase STUB1/CHIP regulates NAD(P)H:quinone oxidoreductase 1 (NQO1) accumulation in aged brain, a process impaired in certain Alzheimer disease patients, *J. Biol. Chem.* 286 (2011) 8839-8845.
- [128] A. Gaikwad, D.J. Long 2nd, J.L. Stringer, A.K. Jaiswal, In vivo role of NAD(P)H:quinone oxidoreductase 1 (NQO1) in the regulation of intracellular redox state and accumulation of abdominal adipose tissue, *J. Biol. Chem.* 276 (2001) 22559-22564.
- [129] Z. Ungvari, C. Parrado-Fernandez, A. Csiszar, R. de Cabo, Mechanisms underlying caloric restriction and lifespan regulation: implications for vascular aging, *Circ. Res.* 102 (2008) 519-528.
- [130] S. Lee, R. Li, B. Kim, R. Palvolgyi, T. Ho, Q.Z. Yang, J. Xu, W.L. Szeto, H. Honda, J.A. Berliner, Ox-PAPC activation of PMET system increases expression of heme oxygenase-1 in human aortic endothelial cell, *J. Lipid Res.* 50 (2009) 265-274.
- [131] A.K. Jaiswal, Nrf2 signaling in coordinated activation of antioxidant gene expression, *Free Radic. Biol. Med.* 36 (2004) 1199-1207.
- [132] A. Okuda, M. Imagawa, Y. Maeda, M. Sakai, M. Muramatsu, Structural and functional analysis of an enhancer GPEI having a phorbol 12-O-tetradecanoate 13-acetate responsive element-like sequence found in the rat glutathione transferase P gene, *J. Biol. Chem.* 264 (1989) 16919-16926.
- [133] D. Siegel, J.K. Kepa, D. Ross, NAD(P)H:quinone oxidoreductase 1 (NQO1) localizes to the mitotic spindle in human cells, *PLoS One* 7 (2012) e44861.

- [134] F. Elahian, Z. Sepehrizadeh, B. Moghimi, S.A. Mirzaei, Human cytochrome b5 reductase: structure, function, and potential applications, *Crit. Rev. Biotechnol.* 34 (2014) 134-143.
- [135] W. Cammer, D.S. Snyder, T.R. Zimmerman Jr, M. Farooq, W.T. Norton, Glycerol phosphate dehydrogenase, glucose-6-phosphate dehydrogenase, and lactate dehydrogenase: activities in oligodendrocytes, neurons, astrocytes, and myelin isolated from developing rat brains, *J. Neurochem.* 38 (1982) 360-367.
- [136] H.B. Werner, K. Kuhlmann, S. Shen, M. Uecker, A. Schardt, K. Dimova, F. Orfaniotou, A. Dhaunchak, B.G. Brinkmann, W. Mobius, L. Guarente, P. Casaccia-Bonnel, O. Jahn, K.A. Nave, Proteolipid protein is required for transport of sirtuin 2 into CNS myelin, *J. Neurosci.* 27 (2007) 7717-7730.
- [137] H.B. Werner, K. Kuhlmann, S. Shen, M. Uecker, A. Schardt, K. Dimova, F. Orfaniotou, A. Dhaunchak, B.G. Brinkmann, W. Mobius, L. Guarente, P. Casaccia-Bonnel, O. Jahn, K.A. Nave, Proteolipid protein is required for transport of sirtuin 2 into CNS myelin, *J. Neurosci.* 27 (2007) 7717-7730.
- [138] G. Mukhopadhyay, P. Doherty, F.S. Walsh, P.R. Crocker, M.T. Filbin, A novel role for myelin-associated glycoprotein as an inhibitor of axonal regeneration, *Neuron* 13 (1994) 757-767.
- [139] D. Del Principe, L. Avigliano, I. Savini, M.V. Catani, Trans-Plasma Membrane Electron Transport in Mammals: Functional Significance in Health and Disease, *Antioxidants & Redox Signaling* 14 (2011) 2289-2318.

- [140] Y. Xiao, H. Li, J. Zhang, A. Volk, S. Zhang, W. Wei, S. Zhang, P. Breslin, J. Zhang, TNF-alpha/Fas-RIP-1-induced cell death signaling separates murine hematopoietic stem cells/progenitors into 2 distinct populations, *Blood* 118 (2011) 6057-6067.
- [141] S. Wang, W.S. El-Deiry, TRAIL and apoptosis induction by TNF-family death receptors, *Oncogene* 22 (2003) 8628-8633.
- [142] M.S. Dunstan, J. Barnes, M. Humphries, R.C. Whitehead, R.A. Bryce, D. Leys, I.J. Stratford, K.A. Nolan, Novel inhibitors of NRH:quinone oxidoreductase 2 (NQO2): crystal structures, biochemical activity, and intracellular effects of imidazoacridin-6-ones, *J. Med. Chem.* 54 (2011) 6597-6611.
- [143] H. Kim, C. Webster, J.K. Roberts, J. Kositsawat, L.W. Hung, T.C. Terwilliger, C.Y. Kim, Enhancement of crystallization with nucleotide ligands identified by dye-ligand affinity chromatography, *J. Struct. Funct. Genomics* 13 (2012) 71-79.
- [144] I. Lascu, H. Porumb, T. Porumb, I. Abrudan, C. Tarmure, I. Petrescu, E. Presecan, I. Proinov, M. Telia, Ion-exchange properties of Cibacron Blue 3G-A Sepharose (Blue Sepharose) and the interaction of proteins with Cibacron Blue 3G-A, *J. Chromatogr.* 283 (1984) 199-210.